Star-Disc Interaction in Active Galactic Nuclei

Miroslav Šlechta

Astronomical Institute
Faculty of Mathematics and Physics
Charles University Prague

Supervisor: Dr. Vladimír Karas

Prague, 2001

Star-Disc Interaction in Active Galactic Nuclei

Miroslav Šlechta

Thesis submitted to the
Astronomical Institute of the Charles University, Prague,
in fulfilment of the requirements for the degree of Doctor

Prague, 2001

Preface

This work deals with problems of mutual interaction between stars and gaseous material in nuclei of galaxies, especially in active galactic nuclei, where various violent processes occur. The text, which is hereafter presented, contains general introduction to the problem, overview of relevant works of the other authors, and the description of my results regarding several selected topics in this lively field of the astronomical research. Namely, the long-term evolution of the trajectories of stellar-mass bodies is examined under the gravitational influence of the central supermassive nucleus and additional dissipative perturbation due to the disc-like distribution of the accreted matter. The stellar body represents a satellite orbiting around the centre (one of many, as the number density of such orbiters can be as large as 10^6 per cubic parsec in the vicinity of the nucleus). The mass of the galactic centre is dominated by the compact core, and the disc gravity is also considered as a tiny perturbation, which turns out to be essential in some situations.

Star-disc interactions are not of marginal interest only, because they reflect properties of the galactic environment. Various processes of this kind have been explored in order to understand better the structure of the innermost galactic regions. Distribution of stars in nuclear star-clusters must reflect the presence (or the absence, in some cases) of supermassive black holes in galactic cores, which, in turn, have crucial consequences for the history of galaxies and their present-day structure. Different approaches have been developed in order to analyze the problem, and I will describe some of them. The thesis thus concerns with methods rather than individual objects, although the application to real astronomical sources is the final goal of this research.

Nowadays, it appears beyond all reasonable doubts that black holes do exist in active galactic nuclei and also in the nuclei of numerous normal galaxies. However, let us mention that the similar physical mechanisms as those described hereafter can be applied in diverse situations. To mention at least some of the most prominent cases, let us recall that during the recent years we experienced an intense burst of interest in modelling processes of planet formation from circumstellar discs. Many properties of these discs are common to those in galactic nuclei when they are scaled down to stellar masses of the centre, and to appropriate dimensions and time-scales. Indeed, when a protoplanetary body develops within the disc plane, it suffers from the mass accretion and feels external irradiation and gravitational drag forces from the surrounding environment. However, there are important differences, too. The gaseous environment of protoplanetary discs exhibits various differences from the gas in centres of galaxies due to rather different physical conditions, which influence their chemical composition, internal temperature etc. Also here, in the branch of protoplanetary physics, analogously to the case of AGNs, the formation of gaps in the disc depends on parameters of the body and of the accretion flow. As the existence of the gap affects observational properties of the whole system, the problem of the formation of gaps calls for careful discussion.

Furthermore, star-disc collisions have not been studied for their direct influence on the morphological structure of the system and the distribution of trajectories only. It has been discussed in the recent literature that normal stars or giants (rather than a compact object) can be a source of substantial metal enrichment, which has been reported in many quasars. Stellar cores, stripped of their outer envelopes, become intense sources of the disc irradiation when they move along inclined orbits, while bodies embedded in the disc undergo rapid evolution and they can soon produce supernovae. The latter two topics however remain beyond the scope of the present text. The interaction with non-compact objects, e.g. normal stars, appears much more complex than the case of compact satellites, and therefore this field has not been fully understood yet.

Major part of the Thesis was prepared during my fellowship at the Astronomical Institute of the Charles University in Prague in the years 1995–1998, but it was finished only recently, in summer 2001, while I have been at the Astronomical Institute of the Academy of Sciences of the Czech Republic. Therefore, the text does not cover all my scientific work and interests which evolved towards observational astronomy in the course of that long period (at present, we explore mainly the data from HEROS Echelle Spectrograph obtained at the Ondřejov observatory). Preliminary results from the present text were published in conference proceedings [73], while recent results from the other topics have been published in collaborations [25, 41]. I have been involved also in statistical researches of the large-scale distribution of galaxies, which, too, are beyond the scope of the present text [74].

Acknowledgments. I would like to thank my supervisor Dr. Vladimír Karas for numerous consultations, for his patience, and also for critical comments and various textual improvements in the Thesis. I am also grateful to Dr. David Vokrouhlický for valuable discussions about celestial mechanics, to Dr. Attila Mészáros with whom I have collaborated on a contribution dealing with the large-scale structure, and to all other researchers and students at the Astronomical Institute of the Charles University where I experienced pleasant and working environment. Finally, I am grateful to Dr. Petr Hadrava of the Academy of Science for helpful discussions regarding dynamical friction. I am sure that without these colleagues I would have never been able to finish this Thesis, nevertheless, I am aware that it is only the author who is responsible for potential errors in the work. I acknowledge grants GAUK 188/2001 and GACR 205/00/1685 for financial support to my home institution.

Contents

Preface 1
Introduction 5

I Gravity of a Disc 9

1 Preliminaries 9
1.1 Accretion discs . . . 9
1.2 Dynamical friction . . . 16
1.3 Newtonian gravitating discs . . . 18
1.4 Star-disc interaction . . . 19
1.5 A star in the disc plane . . . 20

2 Gravitation of a thin disc 20
2.1 General formulae . . . 20
2.2 Potential in the disc plane . . . 24
2.3 Gradients in z-plane . . . 27
2.4 Potentials and gradients on z-axis . . . 28

II Satellite Motion in the Disc Plane 31

3 Effective cross-section of a transiting star 31
3.1 Effective cross-section of a star in coherent dust . . . 31

4 Effects of mass accretion 34
4.1 Basic considerations . . . 34
4.2 The standard disc . . . 35
4.3 Stellar transit through the disc . . . 38

5 Gravitational friction 44
5.1 Gravitational friction in the homogeneous environment . . . 45
5.2 Gravitational friction in the slab geometry . . . 50

6 Stellar motion in the disc plane 53
6.1 Deceleration force acting on the star . . . 54
6.2 Equations of motion in resistive environment . . . 54

7 Results and discussion 58
7.1 Parameters of the model . . . 58
7.2 Tests of the code . . . 60
7.3 Numerical computations . . . 62

Bibliography 80

III Appendices 83

A Comments on basic accretion modes 83

B Approximations valid near rotation axis 93

C Star trapping in accretion discs 98

Introduction

The subject of active galactic nuclei stays in the focus of the contemporary astrophysics, both theoretical and observational [66, 80]. It has been recognized that most of observational results regarding nuclei of galaxies can be best explained in terms of the model with a supermassive central object (a black hole) which is surrounded by an accretion flow with a disc-like geometry [32, 66]. The observations deal with various, rather independent aspects of the AGN phenomenon: morphology and energetics of the objects, photometric properties, continuum spectra and spectral features, counts of different types of objects and their redshift distribution, and, what is particularly relevant for this work, dynamics of gas and stars near the nucleus [31, 36]. Apart from gaseous environment, individual stars move around the centre along almost free orbits, forming a dense nuclear cluster [53, 72]. Understanding the stellar motion near the compact core appears quite important because it gives dynamical information which provides the most secure evidence about central black holes and gives us the quite accurate estimates of their masses [35]. Although there are other independent ways to determine parameters of astrophysical black holes in AGNs [11, 50, 69] (based on spectral properties and temporal variability of these sources), dynamics of orbital motion remains crucial and will become even more important when the spatial resolution is increased in future. Motivated by the above quoted works and considerations, this Thesis deals with mutual interaction between a normal star or a stellar-mass compact object (a white dwarf, a neutron star, or, with certain approximation, a black hole) and an accretion disc around the massive center.

First, we will briefly discuss successive transitions of the star across the disc plane. Then, since the cumulative drag by gaseous material inclines orbits into the disc plane [64, 82, 83], we will deal with the motion of the star inside the disc. Such an embedded orbit is presumably a result of the long-term evolution, but one should notice that the typical time-scale is 2–3 orders of magnitude less than normal stellar life-time. The effect of star-disc collisions should not thus be ignored. The trajectory of an individual orbiter is determined mainly by gravity of the central mass while periodic transitions through the disc act as tiny perturbations, and we will deal with some aspects of this problem. In other words, the aim of the present work is to contribute to our understanding of several particular processes which occur in AGNs and form, together with other knowledge, our picture of these exciting astronomical objects. The ultimate goal of such research is to understand the fate of a star, transfer of mass and angular momentum between the star and the disc, and also to determine the distribution (in the spatial and in the momentum spaces) of stars within nuclear clusters.

We assume parameters corresponding to stars similar to the Sun (radius $R \approx 1\ R_{\odot}$, mass $M_{*} \approx 1\ M_{\odot}$, where the index "$\odot$" denotes the corresponding solar values), with relatively dense atmospheres (compared to density of the gas in an accretion disc; see below for order-of-magnitude numerical values of relevant quantities). The reason for this choice is partly the simplification of the problem given by the fact that the main-sequence stars, white dwarfs and neutron stars are compact enough and their interaction with gas can be treated, in the first approximation, as interaction of a solid sphere, which is characterized by a fixed value of effective cross-sectional radius. Let us note that in the case of a red giant, such an assumption turns out to be inappropriate: density of the outer atmosphere would be comparable with that of the disc, and so it is possible that the red giant looses its outer atmosphere due to the motion in gaseous environment [21, 33]. Discussion of the problem is then more complex [1], and it leads us, among other complications, to the time dependent effective cross-section of the passing star.

Further, we assume the disc to be geometrically slim (ratio $H(R)/R$ of the semi-thickness of the disc to the corresponding distance from the center is < 1), surrounding a supermassive body with mass $M_{\mathrm{central}} \approx 10^8\ M_{\odot}$. Outer radius of the disc (where density decreases to a negligibly small value) is typically taken to be about $10^3\ R_{\mathrm{G}}$, where $R_{\mathrm{G}} \equiv 2GM_{\mathrm{central}}/c^2$ denotes the gravitational radius of the central body in terms of its mass M_{central}, gravitational constant G and the speed of light c. In this situation it is natural to suppose the ratio of the star to the central body $M_*/M_{\mathrm{central}} \ll 1$. This assumption leads to a simplified model of motion of the star in a resistive environment. Otherwise, for $M_* \gtrsim 10^{-3} M_{\mathrm{central}}$ (and depending also on compactness of the star), we have to admit a possibility that the star opens a gap in the disc which does not close before the star completes one single revolution around the center [71]. Hence the model of resistive force is considerably more complicated and the whole structure of the disc is affected (accretion can be terminated at the gap where accretion rate vanishes). This difficulty appears to be less serious when the flow has non-negligible radial velocity component, as it is in advection dominated flows (where, moreover, the semithickness of the disc is greater than the radius of the star $H > R_*$). In such a case the radial transport of the disc matter helps to close the gap, or the gap downflows with the gas and disappears at some distance.

Furthermore, for $M_* \approx M_{\mathrm{central}}$, even the star outside the disc plane cannot be treated as a point-like test mass in the gravitational field of the central body. Tidal distortion of the stellar body passing near a black hole has been discussed by several authors who show that the star becomes squeezed and heated [19, 46, 65]. Tidal disruption occurs in the case of a close encounter, when the satellite plunges below the tidal radius $R_{\mathrm{t}} \sim 10^9\,(M_{\mathrm{central}}/M_*)^{1/3}\,(R_*/R_{\odot})$ m. On the other hand, distortions of the shape of a compact satellite near a supermassive black hole are negligible and can be ignored.

Finally, as a premise, let us emphasize that in the whole Thesis we adopt classical (Newtonian) description of gravity. Effects of general relativity are not taken into account. This approximation turns out to be adequate in most situations when the star is not too close to the black-hole horizon, i.e. $R \gtrsim 10\ R_{\mathrm{G}}$. Under the given assumption the gravitational potential of the central body is superposed with the potential of the disc, and the star moves in a resistive environment and in combined gravitational fields of the central body and the disc. Some relativistic effects can be still accounted by introducing pseudo-Newtonian gravitational potential for the central mass, and by prescribing sucking-in boundary condition on the surface of the orbiter [56]. Description of the problem within full general relativity is probably too complicated to allow analytical treatment, but we will mention several relevant results which have been obtained numerically.

Plan of sections

This thesis is divided into two main parts and appendices. Part I (starting on page 9) deals with the gravitational potential of a disc. The disc is geometrically thin and described by its surface density $\Sigma = \Sigma(R)$. We present a brief review of relevant formulae, then we give analytical solutions for the potententials (and for corresponding gradients which determine force components) in special cases of the surface-density profile $\Sigma(R)$ gradually decreasing over the disc plane. We also discuss limiting values of potentials and gradients on symmetry axis of the disc (z-axis). These analytical or semi-analytical expressions are further employed in subsequent calculations where they approximate the gravitational field of an accretion disc, and enter into equations of motion of the orbiter. Such approach speeds up computations (in comparison with more realistic models of the gravity of accretion discs which themselves are often given numerically [38]) while preserving important physical features of the model.

Part II (starting on page 31) deals with the stellar motion across the disc and inside it. Due to the resistive environment, energy and angular momentum of the stellar motion are continuously dissipated and the star gradually sinks onto lower orbits. In principle, the orbiter can also gain energy and angular momentum from the gas, but this occurs only under very special and perhaps unrealistic circumstancies, e.g. when the disc rotation is non-Keplerian [76] or when the prescription for star-disc collisions is substantially different from the one adopted hereafter [81]. In terms of Keplerian orbital analysis, the process of energy losses leads to the long-term temporal evolution of parameters of the osculating ellipse: eccentricity decreases to zero, line of apsides precesses with time, inclination of the orbit with respect to the disc decreases [82, 83]. The orbit is eventually inclined into the disc plane, if not captured by the central object before grinding down to the disc.

In order to determine the long-term evolution of the orbit, we first estimate the mass and corresponding momentum which the star meets during its transit through the disc, provided the orbit has non-zero inclination. It can be seen that rather trivial model of a straight-line trajectory across the disc gives adequate results. Such approximation was used in previous works of other authors without detailed checks [82, 83], and it is intuitively substantiated by the assumption about small geometrical thickness of the disc. Subsequent chapters (page 53) concern with stellar orbits in the disc plane (orbits with zero inclination angle) for which we derive equations of motion and solve them numerically. Here, we discuss two models for comparison. In the first model we assume that the disc has negligible gravitational field (considering the resistance of gaseous material only), while in the second model we consider gravitational field of the central body plus gravitational field of the disc. Finally, we examine time dependence of radial distance of the star from the center, and also time dependence of the osculating elements a (semimajor axis), e (eccentricity) and ω (pericenter longitude). We also present estimates of the importance of dynamical friction which has been neglected in all previous works on star-disc collisions. We will see that dynamical friction acts as another effect which causes gradual fall of the orbit.

The work is concluded by discussion of the main results. One should emphasize that this work deals with the motion of a single star. Statistical distribution of mutually interacting stars in the central stellar cluster is not treated in the present work, and it is shown that such neglecting does not lead to considerable errors for the stellar orbit inside the disc. Mutual interaction of the stars must be taken into account, however, when their self-consistent distribution in a galactic cusp is to be studied; cf. [75] and references cited therein.

One can find numerous works on related subjects in current astronomical literature. We refer to relevant contributions at appropriate places in the text. At the end of the work, Appendices contain a more detailed overview of selected results, explicit formulae and some related works.

Part I
Gravity of a Disc

Chapter 1

Preliminaries

In this Chapter we summarize assumptions and basic equations which determine properties of the environment around an accreting core of a galaxy. Then we will proceed to the description of the gravitational field which is the main factor governing the motion of satellites around the core.

Accretion processes are those in which capture of a rarefied matter onto an already formed body occurs [21, 32]. Gravity of the central object plays a major role but microphysics of the accreted material (plasma) is also essential, and it is usually described in terms of hydrodynamical or magnetohydrodynamical equations. As far as the geometry of the accretion flow is concerned, disc-type accretion plays a crucial role in physics of active galactic nuclei.

It has been proposed in the late 60s that the disc accretion onto a massive black hole can explain properties of quasars and similar objects [47, 61]. Original motivations arose mainly from energy considerations (accretion can reach higher efficiency than nuclear burning). Since then, the accretion theory became a well-established field of astrophysical research with direct observational support, although one has to admit that properties of accretion flows in AGNs have been understood much less than it is in the case of accretion in binary stellar systems. In this respect, geometrically thin discs represent far the best-understood approximation which is relevant mainly to objects with almost Keplerian discs at low accretion rates [70]. We will treat the flows (mainly discs with the non-negligible radial inflow) in approximation of vertically integrated quantities, although there are certainly objects for which this approximation is not accurate enough, and the flows appear to be quasi-spherical.

We start this Chapter with a brief review of relevant properties of astrophysical discs and of mutual star-disc interactions. Then we describe basic analytical approaches which have been developed in order to describe gravitational field of discs with various density profiles. Further details can be found in the Appendix.

1.1 Accretion discs

Standard model

Observational evidence suggests that accretion discs are rather common in astronomical objects. Disc-type flows occur when accreting material possesses non-negligible angular momentum. These flows become geometrically thin and form a disc when pressure gradients are small (Keplerian rotation) and accretion rate is restricted. Energy of accreted material is transformed into radiation via viscosity and released from the disc surface. Viscosity mechanisms in astrophysical plasma are poorly known, however. It appears that effective viscosity associated with turbulent motions and small-scale magnetic fields is more important than atomic or molecular viscosity. A widely accepted parametrisation of viscosity has been introduced by Shakura & Sunyaev [70] (see also [21]), leading to the famous standard α model of accretion disc. Here α is a (usually constant) coefficient of proportionality describing the efficiency of the turbulent transport; the kinematic viscosity ν is scaled by the relation

$$\nu = \alpha c_{\mathrm{s}} H \tag{1.1}$$

where c_{s} is speed of sound and H is the semithickness of the disc. The model is characterized by small radial component of the inflow (much less than the azimuthal velocity component) and low (but non-zero) viscosity. Viscosity is also responsible for transporting angular momentum out of the disc due to the differential rotation. Thus the material steadily inflows. Since in the standard model radial velocity of inspiralling motion is negligible in comparison with the orbital velocity, one can write, within the first approximation,

$$v(r) \ll r\Omega(r) \quad ; \quad \Omega(r) \approx \Omega_{\mathrm{K}}(r) \; , \tag{1.2}$$

where $v(r)$ is radial velocity at radius r, $\Omega(r)$ is angular velocity, and $\Omega_{\mathrm{K}}(r)$ is Keplerian angular velocity.

To summarize, the standard model is stationary ($\partial/\partial t = 0$) and axially symmetric ($\partial/\partial\phi = 0$). The flow velocities are steady and they satisfy conditions of the near-to-Keplerian flow with low radial and vertical velocities: $v_{\mathrm{z}} \ll v_r \ll v_\Omega$. The gravitational field of the disc is weak and there is supposed the central potential only. Since the disc is usually adopted to be geometrically thin, it can be described in terms of vertically integrated quantities (over the disc height). Relevant hydrodynamical equations are the continuity equation, conservation equation for the angular momentum and equation for the hydrostatic equilibrium in the z-direction (as there is no vertical flow). Vertically integrated equations acquire a form [21]

$$\begin{aligned}
\frac{\partial}{\partial t}(2\pi r\Delta r\Sigma) &= v_{\mathrm{r}}(r,t)2\pi r\Sigma(r,t) - v_{\mathrm{r}}(r+\Delta r,t)2\pi(r+\Delta r)\Sigma(r+\Delta r,t) \\
&\approx -2\pi\Delta r\frac{\partial}{\partial r}(r\Sigma v_{\mathrm{r}}) \; , && (1.3) \\
\frac{\partial}{\partial t}(2\pi r\Delta r\Sigma r^2\Omega) &= v_{\mathrm{r}}(r,t)2\pi r\Sigma(r,t)r^2\Omega(r) \\
&\quad -v_{\mathrm{r}}(r+\Delta r,t)2\pi(r+\Delta r)\Sigma(r+\Delta r,t)(r+\Delta r)^2\Omega(r+\Delta r) + \\
&\quad +\frac{\partial\mathcal{G}}{\partial r}\Delta r \; . && (1.4) \\
\frac{1}{\rho}\frac{\partial p}{\partial z} &= \frac{GM}{\sqrt{r^2+z^2}} \; . && (1.5)
\end{aligned}$$

Limit $\Delta r \to 0$ and the assumption of stationarity lead to the form (we abbreviate M_{central} to M)

$$\begin{aligned}
\frac{\mathrm{d}}{\mathrm{d}r}(r\Sigma v_{\mathrm{r}}) &= 0 \; , && (1.6) \\
\frac{\mathrm{d}}{\mathrm{d}r}(r\Sigma v_{\mathrm{r}} r^2\Omega) &= \frac{1}{2\pi}\frac{\mathrm{d}\mathcal{G}}{\mathrm{d}r} \; , && (1.7) \\
\frac{1}{\rho}\frac{\mathrm{d}p}{\mathrm{d}z} &= -\frac{GMz}{r^3} \; . && (1.8)
\end{aligned}$$

(we abbreviate $\Sigma(r)$ to Σ, and similarly for other variables). Here $\mathcal{G} = 2\pi r\nu\Sigma r^2\Omega'$ ($' \equiv \mathrm{d}/\mathrm{d}r$) describes the viscous torque. It is possible to find that the presented standard disc model is characterized by three parameters: (i) M – the mass of the central object; (ii) $\mathrm{d}M/\mathrm{d}t$ – the accretion rate; (iii) α – the viscosity parameter [21].

The central object in AGNs is supposed to be a supermassive black hole with a typical mass $M \approx 10^8\ M_\odot$, where $M_\odot = 2\times10^{30}$ kg is the solar mass. The central mass ranges over five orders of magnitude in different types of galaxies, and the existence of supermassive cores in *all* galaxies is subject of much debate. (The mass and compactness of the central object can be roughly determined from the overall luminosity.) The accretion rate $\dot{M}$ is conveniently scaled by the critical accretion inflow $\dot{M}_{\mathrm{crit}}$ at which the total release of the potential energy in the disc $L = \eta\dot{M}c^2$ (η is the efficiency of the process, c is speed of light) is equal to the Eddington luminosity (or Eddington limit), which is defined as the balance of the force of radiation pressure on the completely ionized matter and of the gravitational forces of attraction to the center

$$L_{\mathrm{E}} \equiv \frac{4\pi GMm_{\mathrm{p}}c}{\sigma_{\mathrm{T}}}\,, \tag{1.9}$$

where m_{p} is the proton mass and $\sigma_{\mathrm{T}} = 6.7\times10^{-29}$ m^2 is the Thompson effective cross-section. Notice that, within above approximations, the Eddington limit does not depend on radius. Once the three parameters of the disc are specified, the standard model provides all other astrophysical characteristics of the disc (surface density, pressure, dissipation per unit area per unit time, total disc luminosity, semithickness, temperature, inward mass flux).

Several characteristic time-scales govern processes in standard accretion discs: viscous time t_ν, orbital period t_Ω (dynamical time), and the time t_z during which the hydrostatic equilibrium is established in the vertical (z) direction. One obtains, in terms of the disc height H and sound speed c_{s} [21, 63],

$$t_\nu \propto \frac{r^2}{\nu} \gg t_\Omega \sim t_{\mathrm{z}} = \frac{H}{c_{\mathrm{s}}}\,. \tag{1.10}$$

Let us note that the accretion onto compact objects (white dwarfs, neutron stars and black holes) has several specific properties which follow from the existence of the innermost stable orbit in the case of the black hole. The disc must have an edge near this orbit, below which accretion proceeds along almost free-fall trajectories. Consequently, accretion onto solid surface (ie. for white dwarfs and neutron star) produces a hot boundary region, while in the black-hole case no such boundary layer exists, and the innermost regions radiate less.

Other modes of the accretion flow

Let us remind that disc type accretion represents just one mode of the accretion flow. For example, the spherically symmetric accretion applies to the case of vanishing angular momentum (the spherically symmetric accretion is review in the Appendix and also in [21]).

As another example, the accretion of cold gas onto a moving star possesses axial symmetry (with the axis defined by the relative velocity vector), though it does not form a disc (as the angular momentum of the gas is zero with respect to the inertial system of the moving star; $\boldsymbol{L} = 0$). This type of accretion will be relevant also in our work, when we discuss drag force onto a star crossing the disc plane or the satellite moving inside the disc.

The effective cross-section of the gravitating body m moving in the *cold* medium (Bondi accretion) can be estimated as

$$r_{\rm c} \simeq 2\frac{Gm}{v_\infty^2}\ , \tag{1.11}$$

where v_∞ is relative velocity of the cold environment far from the body. This expression is a slightly different from our own formulae (3.5) and (3.6) (because of different assumptions used in derivations), but actual numerical difference is negligible.

We have not covered the case of an accretion tori (geometrically thick discs in permanent rotation), and we should mention them at least for completeness and possible use in future works [56]. The most interesting properties appear when tori are modelled with effects of general relativity taken into account, because relativistic effects introduce the possibility for the Roche-lobe overflow and set on the runaway instability. These effects are often described with help of pseudo-Newtonian potential $\psi(r)$ (instead of proper general relativity description): $\psi = -\frac{GM}{r-R_{\rm G}}$, $R_{\rm G} = \frac{2GM}{c^2}$. Although the pseudo-Newtonian potential is of very simple form, similar to the Newtonian one, it correctly reproduces both the marginally bound circular orbit at $2R_{\rm G}$ and the last stable circular orbit at $3R_{\rm G}$ [56]. These values agree with the case of exact Schwarzschild metric. Thus the potential is of interest in modelling accretion discs.

The first application of the pseudo-Newtonian solution was given by Paczyński & Wiita in [56], where authors study the thick disc as a counterpart of the standard thin model. They replaced usual assumption of local energy balance with a global conservation requirement and adopted assumption that the local radiated flux is critical.

The angular velocities and the angular momentum per unit mass are in central potential ψ and cylindrical coordinates (r, φ, z)

$$\Omega = \left(\frac{1}{r}\frac{{\rm d}\psi}{{\rm d}r}\right)^{\frac{1}{2}}\ ,\ l = \left(r^3\frac{{\rm d}\psi}{{\rm d}r}\right)^{\frac{1}{2}}\ . \tag{1.12}$$

The total mechanical energy per unit mass is

$$e = \frac{1}{2}v^2 + \psi\ . \tag{1.13}$$

Be z_0 semithickness of the disc. The heat release due to the friction is

$$\epsilon = \left(r\frac{{\rm d}\Omega}{{\rm d}r}\right)^2 \nu \tag{1.14}$$

and the torque at given radius

$$\mathcal{G} = 2\pi r^3 \left(-\frac{{\rm d}\Omega}{{\rm d}r}\right) \int\limits_{-z_0}^{z_0} \nu {\rm d}z\ . \tag{1.15}$$

The total angular momentum flux is

$$\dot{J} = \dot{M}l + \mathcal{G}\ . \tag{1.16}$$

(in the thick disc there is not necessary to suppose that the angular momentum l of the orbiting material is equal to (1.12). They will equal at the inner edge of the disc, where is no torque). Conservation of mass, angular momentum and energy are

$$\frac{\partial}{\partial t}(2\pi r\Sigma) + \frac{\partial \dot{M}}{\partial r} = 0\ , \tag{1.17}$$

$$\frac{\partial}{\partial t}(2\pi r\Sigma l) + \frac{\partial \dot{J}}{\partial r} = 0\ , \tag{1.18}$$

$$\frac{\partial}{\partial t}(2\pi r\Sigma e) + \frac{\partial \dot{E}_{\rm r}}{\partial r} + \frac{\partial \dot{E}_{\rm z}}{\partial r} = 0\ . \tag{1.19}$$

The assumption of stationarity ($\partial_t = 0, \dot{M} = \text{const}$) leads to the

$$\dot{M}\frac{\partial l}{\partial r} + \frac{\partial \mathcal{G}}{\partial r} = 0 \, . \tag{1.20}$$

Equation (1.20) can be integrated to give

$$\mathcal{G} = \mathcal{G}_0 + (-\dot{M})(l - l_0) \tag{1.21}$$

and we have accretion when $\dot{M} < 0$ (the mass of the disc decreases due to the accretion process). Here $\mathcal{G}_0 = \mathcal{G}(r_0) = 0$ is the torque at the inner edge r_0 of the disc.

Let us integrate the viscosity over the semithickness of the disc,

$$S \equiv \int_{-z_0}^{z_0} \nu \mathrm{d}z, \tag{1.22}$$

and thus, with respect to equation (1.15), we obtain

$$S = \frac{\mathcal{G}}{2\pi r^3}\left(\frac{\mathrm{d}\Omega}{\mathrm{d}r}\right)^{-1} = (-\dot{M})\left(\frac{\mathrm{d}\Omega}{\mathrm{d}r}\right)^{-1}(2\pi r^3)^{-1}(l - l_0) \, . \tag{1.23}$$

Equilibrium of the gravitational field and the radiation pressure give the formula for power emitted per unit area,

$$F_{\mathrm{rad}} = \frac{c}{K} g_{\mathrm{eff}} \, , \tag{1.24}$$

where K is the opacity and g_{eff} is the effective acceleration of the gravity, including the centrifugal force. It is obvious that it is normal to the surface of the disc and we have

$$g_{\mathrm{z}} = g_{\mathrm{eff}} \cos\vartheta \, , \tag{1.25}$$

where $g_{\mathrm{z}} = \mathrm{d}\psi_0/\mathrm{d}z$, $\psi_0 = \psi((r^2 + z_0^2)^{1/2})$ and ϑ is the instantaneous angle of the surface and the disc plane:

$$\cos\vartheta = \left[1 + \left(\frac{\mathrm{d}z_0}{\mathrm{d}r}\right)^2\right]^{-1/2} \, . \tag{1.26}$$

Equation (1.24) acquires a form

$$F_{\mathrm{rad}} = \frac{c}{K}\frac{\mathrm{d}\psi_0}{\mathrm{d}z}\left[1 + \left(\frac{\mathrm{d}z_0}{\mathrm{d}r}\right)^2\right]^{1/2} \, . \tag{1.27}$$

To obtain the luminosity of the disc, one has to find the shape of the surface of the disc. Therefore let us define the total potential $\Phi = \psi - \int \Omega^2 r \mathrm{d}r$. The surface of the disc follows the equipotential on which Φ is constant. Thus the total differential of the Φ is

$$\mathrm{d}\Phi = 0 = \left(\frac{\partial\psi}{\partial r} - \Omega^2 r\right)\mathrm{d}r + \left(\frac{\partial\psi}{\partial z}\right)\mathrm{d}z \tag{1.28}$$

or

$$\frac{\mathrm{d}z}{\mathrm{d}r} = \left(\Omega^2 r - \frac{\partial\psi}{\partial r}\right)\left(\frac{\partial\psi}{\partial z}\right)^{-1} \, . \tag{1.29}$$

The solution of this equation is presented in [56] in form $z_0(r) = f(r_0, r_{\mathrm{G}}, l(r), r)$. Remind that r_0 is the inner edge of the disc.

The total luminosity of the disc is expressed as

$$L_{\rm rad} = 2 \int_0^{2\pi} \int_{r_0}^{r_{\rm t}} F_{\rm rad} {\rm d}\sigma \ , \tag{1.30}$$

where we integrate over the surface of the disc. $r_{\rm t}$ is an upper bound of the integration. It represents or the outer edge of the disc or some radius on which the disc passes from the thick to the thin mode – see discussion in Paczyński & Wiita [56].

Substitution of the (1.27) and solution of the $z_0(r)$ leads to the form [56]

$$L_{\rm rad} = \frac{4\pi c G M}{K} I(r_0, r_{\rm t}) \ , \tag{1.31}$$

where $I(r_0, r_{\rm t})$ is dimensionless integral formula. Definition of the critical luminosity (using a Newtonian potential and the spherical symmetry)

$$L_{\rm Edd} = \frac{4\pi c G M}{K} \tag{1.32}$$

one has

$$L_{\rm rad} = L_{\rm Edd} I(r_0, r_{\rm t}) \ . \tag{1.33}$$

The effective gravity at any point on the surface of the disc will be less then the spherical attraction to the central mass at that distance, and thus the critical flux from the disc's surface would be less than that from the spherical surface at the same radius. We can find that our disc can have surface area in excess of such equivalent sphere. Thus there is no reason to require $I(r_0, r_{\rm t}) \leq 1$ and it is not surprising that the total emitted energy from the disc can exceed the Eddington luminosity. For detailed derivation of the relation (1.33) and the discussion on supercritical luminosity see [56] (relation (50) and following).

Accretion near to the axis

Finally, it is instructive to discuss properties of accretion flow near rotation axis. Wolfson [84] finds asymptotic solution assuming the radial velocity $v_{\rm r}^2(\infty) \ll GM/r$, where GM/r is specific infall energy. The gas-dynamics equations of the conservation of momenta (in radial and transversal directions), continuity equation and entropy equation written down in spherical coordinates r, ϑ, ϕ in standard notation are:

$$v_{\rm r}\frac{\partial v_{\rm r}}{\partial r} + \frac{v_\vartheta}{r}\frac{\partial v_{\rm r}}{\partial \vartheta} - \frac{v_\vartheta^2}{r} = -\frac{1}{\rho}\frac{\partial p}{\partial r} - \frac{GM}{r^2} \quad , \tag{1.34}$$

$$v_{\rm r}\frac{\partial v_\vartheta}{\partial r} + \frac{v_\vartheta}{r}\frac{\partial v_\vartheta}{\partial \vartheta} + \frac{v_{\rm r} v_\vartheta}{r} = -\frac{1}{\rho r}\frac{\partial p}{\partial \vartheta} \quad , \tag{1.35}$$

$$\rho\left(\frac{\partial v_{\rm r}}{\partial r} + \frac{2v_{\rm r}}{r} + \frac{1}{r}\frac{\partial v_\vartheta}{\partial \vartheta} + \frac{v_\vartheta}{r}\cot\vartheta\right) + \left(v_{\rm r}\frac{\partial \rho}{\partial r} + \frac{v_\vartheta}{r}\frac{\partial \rho}{\partial \vartheta}\right) = 0 \quad , \tag{1.36}$$

$$v_{\rm r}\frac{\partial p}{\partial r} + \frac{v_\vartheta}{r}\frac{\partial p}{\partial \vartheta} - \gamma\frac{p}{\rho}\left(v_{\rm r}\frac{\partial \rho}{\partial r} + \frac{v_\vartheta}{r}\frac{\partial \rho}{\partial \vartheta}\right) = 0 \quad . \tag{1.37}$$

Their solution is given in form

$$v_{\rm r} = \beta r^{-\frac{1}{2}} x(\vartheta) \ , \tag{1.38}$$

$$v_\vartheta = \beta r^{-\frac{1}{2}} y(\vartheta) \ , \tag{1.39}$$

$$\rho = \alpha r^{-m} f(\vartheta) \ , \tag{1.40}$$

$$p = \alpha\beta^2 r^{-(m+1)} g(\vartheta) \ , \tag{1.41}$$

where

$$\beta \equiv \left(\frac{\gamma-1}{\gamma+1}\right)(2GM)^{\frac{1}{2}} \to GM = \frac{1}{2}\beta^2\left(\frac{\gamma+1}{\gamma-1}\right)^2 . \tag{1.42}$$

γ is the heat-ratio and α is a constant. We supposed $\partial/\partial t \equiv 0$ (stationarity); $v_{\rm r}$ and v_ϑ denote radial and transversal velocities, respectively. Solution is given in Appendix explicitly (see equations (B.1)–(B.4), (B.5)–(B.9)) with approximative solution near to z-axis:

$$x \to x_0 , \tag{1.43}$$

$$y(\vartheta) = a\,\vartheta , \tag{1.44}$$

$$f(\vartheta) = -\frac{A}{a\vartheta^2} , \tag{1.45}$$

$$g(\vartheta) = A\left(\frac{1}{2}x_0 + a\right)\ \ln\vartheta , \tag{1.46}$$

where A is a positive and a is a negative integration constants – see, for example, [84] .

Accretion with rapid radial inflow

Until now we have completely ignored radial transport of matter and all other physical quantities (entropy, heat). Such assumption has simplified relevant hydrodynamical equations and it is also the way in which the subject was developed historically, but it can be inappropriate in many objects where the inflow is non-negligible. Advection dominated accretion flows (abbreviated ADAFs) are defined as those ones with considerable radial motion of the gas (and other quantities; the mass transport is most important for our discussion of collisions and momentum transfer to the satellite). A review of advection dominated discs has been presented in [51, 52] and the bibliography therein, but we remark that it is only radial velocity of material which will enter into our considerations, and which will introduce some differences against the case of standard discs dominated by toroidal motion of matter.

In all cases we will assume an axially symmetric stationary flow. Hence it is possible to write down equations of conservation of the mass, momentum, angular momentum, and energy (integrated over vertical coordinate, z):

$$\frac{\mathrm{d}}{\mathrm{d}r}\left(\rho r H v_{\rm r}\right) = 0 \quad , \tag{1.47}$$

$$v_{\rm r}\frac{\mathrm{d}v_{\rm r}}{\mathrm{d}r} - \Omega^2 r = -\Omega_{\rm K}^2 r - \frac{1}{\rho}\frac{\mathrm{d}}{\mathrm{d}r}\left(\rho c_{\rm s}^2\right) \quad , \tag{1.48}$$

$$v_{\rm r}\frac{\mathrm{d}(\Omega r^2)}{\mathrm{d}r} = \frac{1}{\rho r H}\frac{\mathrm{d}}{\mathrm{d}r}\left(\nu\rho r^3 H\frac{\mathrm{d}\Omega}{\mathrm{d}r}\right) \quad , \tag{1.49}$$

$$\rho v_{\rm r} T\frac{\mathrm{d}s}{\mathrm{d}r} = q^+ - q^- = \rho\nu r^2\left(\frac{\mathrm{d}\Omega}{\mathrm{d}r}\right)^2 - q^- \equiv_{\rm r} f\nu\rho r^2\left(\frac{\mathrm{d}\Omega}{\mathrm{d}r}\right)^2 \quad , \tag{1.50}$$

where ρ is the density of the gas, r radial distance from the center, H is vertical scale, $c_{\rm s}$ isothermal speed of sound, T temperature, s specific entropy, q^+ is a heat produced by viscosity per unit of the volume and q^- is a radiative cooling per unit of the volume. Notice that the two qs can differ due to radial transport and conduction; this is in contrast to thin-disc models where all heat is radiated away at the very same radius where it was liberated by viscosity.

Left-hand-side terms in eq. (1.50) describe the rate of the accretion per unit volume. Thus, f is ratio of internal energy with respect to the produced heat, and it represents the rate of efficiency of the advection process. Coefficient of the kinematic viscosity ν is rewritten as

$$\nu = \alpha c_{\mathrm{s}} H = \alpha \frac{c_{\mathrm{s}}^2}{\Omega_{\mathrm{K}}} \ . \tag{1.51}$$

It is commonly supposed that the α-parameter is independent on r.

Assuming classical Newtonian angular velocity

$$\Omega_{\mathrm{K}}^2 = \frac{GM_{\mathrm{BH}}}{r^3} \tag{1.52}$$

and $f \neq f(r)$, one can find solution of eqs. (1.47)–(1.50),

$$\begin{aligned} v_{\mathrm{r}}(r) &= -\frac{(5+2\epsilon')}{3\alpha^2} g(\alpha,\epsilon') \alpha v_{\mathrm{ff}} & (1.53)\\ \Omega(r) &= \left[\frac{2\epsilon'(5+2\epsilon')}{9\alpha^2} g(\alpha,\epsilon')\right]^{\frac{1}{2}} \frac{v_{\mathrm{ff}}}{r} \ , & (1.54)\\ c_{\mathrm{s}}^2(r) &= \frac{2(5+2\epsilon')}{9\alpha^2} g(\alpha,\epsilon') v_{\mathrm{ff}} \ , & (1.55) \end{aligned}$$

where

$$\begin{aligned} v_{\mathrm{ff}} &\equiv \left(\frac{GM}{r}\right)^{\frac{1}{2}} \ , & (1.56)\\ \epsilon' &\equiv \frac{\epsilon}{f} = \frac{1}{f}\left(\frac{5/3-\gamma}{\gamma-1}\right) \ , & (1.57)\\ g(\alpha,\epsilon') &\equiv \left[1+\frac{18\alpha^2}{(5+2\epsilon')^2}\right]^{\frac{1}{2}} - 1 \ . & (1.58) \end{aligned}$$

Here $\gamma \in (4/3,\ 5/3)$ and $\epsilon \in (0,\ 1)$. Simplification $f = 1$ and $\alpha < 1$ (typically it is equal $\alpha \approx 0.1$) leads to – see [22, 51, 52]

$$\begin{aligned} \frac{v}{v_{\mathrm{ff}}} &\simeq \left(\frac{\gamma-1}{\gamma-5/9}\right) \alpha \ , & (1.59)\\ \frac{\Omega}{\Omega_{\mathrm{K}}} &\simeq \left[\frac{2}{3}\,\frac{5/3-\gamma}{\gamma-5/9}\right]^{\frac{1}{2}} \ , & (1.60)\\ \frac{c_{\mathrm{s}}^2}{v_{\mathrm{ff}}^2} &\simeq \frac{2}{3}\left(\frac{\gamma-1}{\gamma-5/9}\right) \ . & (1.61) \end{aligned}$$

As it is seen out of presented solutions,

- the radial velocity is comparable with the free fall velocity. Thus the radial accretion is relatively very fast;
- the angular velocity is less then the Keplerian one. In an extreme model of $\gamma \to 5/3$ the angular velocity decreases to the zero.

1.2 Dynamical friction

Now we turn to one of the effects, which is directly related to the presence of gaseous environment and influences motion of the satellite around the central mass. Various such effects have been taken into account by other authors who examined star-disc collisions: direct accretion and hydrodynamical effects of turbulences appear as the most important ones [72, 86]; effects of general relativity have been considered [81] (motion in the black-hole spacetime, gravitational radiation losses of the satellite orbital energy) as well as the gravity of the disc [82, 83]. The latter two effects turn out to be important on very long time scales. As another effect that should be considered along the way to more realistic description of the problem, we include dynamical friction acting on the orbiter due to the surrounding gaseous disc. The above-mentioned works and our own numerical simulations described in Chapter 7 show that the gravitational field of the disc and velocity variation of the effective cross-section of the star are not significant on short and medium time-scales, likewise the pseudo-Newtonian correction. On the other hand gravitational dynamical friction can play, in general, considerable role in the evolution of orbital parameters.

We start with a brief exposition of the problem of dynamical friction which has numerous applications in astronomy under different contexts. Rephaeli & Salpeter [68] discuss gravitational interaction between a massive object and a gaseous cloud. They find expressions for the drag forces on the body moving through coherent (collisionless) dust in two limits of either the subsonic or the supersonic speed. The gravitational drag on a supersonic object is

$$-\frac{\mathrm{d}E}{\mathrm{d}t} = 4\pi\frac{G^2M^2\rho}{v}\ln\left(\frac{b_{\rm max}}{b_{\rm min}}\right) , \tag{1.62}$$

where $\mathrm{d}E/\mathrm{d}t$ denotes energy losses; $b_{\rm max}$ and $b_{\rm min}$ indicate the boundary which is taken into account of the drag. Deceleration is given by $(\mathrm{d}E/\mathrm{d}t)/Mv$, which turns out to be identical to our expression for the gravitational drag in the homogeneous environment given below.

Broad discussion of the dynamical friction can be found in [6] where the authors derive analytical expressions for gravitational drag in homogeneous coherent environment, namely (per one collision with the test particle m),

$$\begin{aligned} \mid \Delta v_{\star\,\perp} \mid &= \frac{2mv_0}{G(M+m^2)}bv_0^2\left[1+\frac{b^2v_0^4}{G^2(M+m)^2}\right]^{-1} , & (1.63)\\ \mid \Delta v_{\star\,\|} \mid &= \frac{2mv_0}{M+m}\left[1+\frac{b^2v_0^4}{G^2(M+m)^2}\right]^{-1} . & (1.64)\end{aligned}$$

Here v_0 is relative velocity of the test particle at infinity, b is impact parameter, m is the mass of the test particle, M mass of the body, $\Delta v_{\star\,\perp}$ determines change the velocity of the mass M in direction perpendicular to $\boldsymbol{v_0}$ due to gravitational friction of the mass m; $\Delta v_{\star\,\|}$ is velocity change of the mass M in direction parallel to the $\boldsymbol{v_0}$.

Assuming that environment can be treated as homogeneous far from the body, one finds an analytical solution of dynamical deceleration in the form

$$\left.\frac{\mathrm{d}\boldsymbol{v_\star}}{\mathrm{d}t}\right|_{v_\star} = 2\pi\ln\left(1+\Lambda^2\right)G^2m(M+m)f(v_{\rm m})\frac{\boldsymbol{v_{\rm m}}-\boldsymbol{v_\star}}{\mid \boldsymbol{v_{\rm m}}-\boldsymbol{v_\star}\mid^3}\ \mathrm{d}^3\,\boldsymbol{v_{\rm m}} . \tag{1.65}$$

Here $f(v_{\rm m})$ is the velocity distribution function of bodies m and

$$\Lambda = \frac{b_{\rm max}v_0^2}{G(M+m)} . \tag{1.66}$$

These formulae can be directly compared with [6] eqs. (7.10-a)–(7.10-b) and (7.13-a)–(7.13-b) in [6].

Let us remark that the classical problem of dynamical friction has recently gained a new important application in astronomy. This regards the problem of planet formation when a protoplanetary body is first created in a circumstellar disc, and then, the newly formed object moves with the disc, interacting with the remaining material [44]. The planet is formed by rapid accretion when its core mass increases above a critical mass [7]. Also in this situation, two main effects are induced in the background disc: (i) tidal perturbation of a jupiter-size planet leads to the gap formation near its orbit and thereby limits the accretion flow; (ii) outgoing and ingoing density waves are excited and they carry angular momentum to distant regions of the disc. These waves are eventually dissipated at some location in the disc where their angular momentum is deposited [43]. Torque exerted on the disc has the same magnitude and opposite sign as backreaction acting onto the planet. Relevant expression for the torque has been derived in by Goldreich & Tremaine [24] in terms of infinite series. Gap formation has been treated independently in ref. [34]. Different aspects of dynamical friction in astronomy have been discussed by Hoffer [26] (a particle in a stellar background) and Ostriker [55] (linearized theory for a massive perturber in gaseous medium).

1.3 Newtonian gravitating discs

Gravitational potential and corresponding gravitational field of thin discs has been studied by numerous authors. Inspirative models of thin discs have been described in [28, 30, 82, 83]. These authors derive expressions for potentials of thin discs and they give an analytical solution in some special situations. Their expressions start from well known approaches: they suppose infinitely thin axially symmetric disc with outer radius a, the surface-density profile $\Sigma = \Sigma(R)$. We mention the model here because we found these results conveniently formulated for the purposes of the present work (they offer compact formulae for potentials and gradients which can be easily evaluated numerically; see the next part of this thesis). At first, ref. [28] deals with a light (weakly gravitating) thin disc: $M \gg M_{\rm disc}$. Exact analytical solution of potentials and gradients (as functions of elliptic integrals E and K) are obtained for several special density profiles $\Sigma(R) \propto R^{-n}$, $n = (0; 1; 3)$. General relativistic treatment has been also presented there as an extension of ref. [5]. The spacetime of the solution [5] is locally identical to the Kerr black-hole metric outside the horizon. Authors show that the material of the disc has both transversal and radial pressure.

Other types of Newtonian potentials of discs with some specific surface-density profiles can be found in Lemaitre & Dubru [42] and Brada & Milgrom in [8].

The relevant references for the potential of discs are Binney & Tremaine [6] and Evans & de Zeeuw [20]. These authors study infinite thin discs with particular emphasis to applications in galactic dynamics (a model of the flat component of galaxies).

Evans & de Zeeuw take the following approach: they examine infinite amount of concentric ellipsoids with constant rates of semiaxes, $a : b : c$, for all ellipsoids, and with varying density ρ. Then they project the resulting thin infinite three-dimensional disc onto the $z = 0$-plane and obtain an infinite two-dimensional disc as a model of the flat component of a galaxy. Notice that Evans & de Zeeuw study also other, more general types of discs. A detailed discussion of three-axial potentials has been given in refs. [17, 18, 20].

In the following paragraphs we refer to also Toomre's disc (with surface density $\Sigma \propto R^{-m}$; m is a positive real) as one special case of the Evans & de Zeeuw models [6, 20]. The reason why we refer to Toomre's disc is mainly that it is particularly simple and can be readily studied with analytical approaches. We will use a similar surface density profile $\Sigma(R)$ of this model farther in Part I of the thesis. For special cases of circular discs ($a = b$) the potential $V_n(R, z)$ of the Toomre's disc is

$$V_n(R, z = 0) = \frac{\pi G a^2 \Sigma_0}{2^{n-1} B(n, n) \left(\frac{1}{2} - n\right)} \int_0^\infty \frac{(a^2 + u)^{n-\frac{3}{2}} u^{n-1}}{(\lambda + u)^{n-\frac{1}{2}} u^{n-\frac{1}{2}}} \mathrm{d}u \,, \tag{1.67}$$

where n is an integer and $B(n, n)$ is the beta function

$$B(i, j) = \frac{\Gamma(i)\Gamma(j)}{\Gamma(i + j)} \tag{1.68}$$

where Γ is the gamma-function, i, j are integers and $\lambda = a^2 + R^2$.

For the special case of $n = 1$ (which corresponds to surface density varying as $\Sigma = \Sigma_0 (1 + R)^{-2}$) we obtain

$$V_1(R, z = 0) = -2\pi G \Sigma_0 \frac{a^2}{\sqrt{a^2 + R^2}} K \left(\frac{R}{\sqrt{a^2 + R^2}} \right) \,. \tag{1.69}$$

Here K is the elliptic integral of the second order (see (2.3)). The potential of this Toomre's disc is thus similar to the potential expressed by Karas & Vokrouhlický [28, 30, 82, 83]. For more details see [20], and also page 26.

1.4 Star-disc interaction

Let us now consider a body orbiting in the disc plane ($z = 0$) around the center of the disc. The stellar orbit is not necessarily circular (or even elliptical) due to the interaction with material of the disc (but it is close to such orbits because the disc acts as tiny perturbation only). Stellar motion is supersonic, with a speed $v > \mathcal{M}$ (in terms of the Mach number), [21, 51]. It has been generally adopted, both on theoretical grounds and observationally, that there is relatively large number of stars orbiting close to the core and forming a dense cluster in the central part of a galaxy [49, 57]. Typical number density is $\approx 10^6\,\mathrm{pc}^{-3}$ and total number of stars $\approx 10^8$, and, therefore, star-disc collision are not a rare event.

Zurek, Siemiginowska & Colgate [86] estimate the importance of star-disc collisions in the AGN model for a star passing through the disc at some non-zero inclination angle. They assume that the gaseous tail behind the passing star contributes to the formation of the broad-line region (BLR) clouds, origin of which remains an open question yet. These authors estimate the amount of matter which the transiting star tears out of the disc, showing that it can exceed 10^2–10^3 times the amount of material which the transiting star accretes directly by its effective gravitational cross-section. Uncertainties of the estimate stem from the lack of a consistent hydrodynamical models of such fast motion of the spherical body through the resistive environment, and hence the results may be somewhat in error [86]. It is relevant to emphasize that the amount of matter which the passing star meets along its way through the disc and, possibly, tears out of the disc will change orbital parameters of the star itself [82, 83]. Orbital parameters evolve in a manner self-consistent with the hydrodynamical drag acting against the stellar motion. Hence a model of stellar transit is important for celestial mechanics or galactic dynamics near the core – see [6].

1.5 A star in the disc plane

A star orbiting around the center inside the disc plane, $z = 0$, moves in the resistive environment for its whole trajectory. Gaseous material of the disc is accreted and redistributed and hence a gap in the disc may be opened. It depends on parameters of specific situation whether the star is able to open a permanent gap in the disc or, quite on the contrary, whether the gap behind the star closes in time shorter then orbital period of the star.

Syer & Clarke [71] derive several estimates regarding the stellar motion inside a thin accretion disc. They adopt standard Shakura & Sunyaev thin disc with Newtonian potential of the central body and Keplerian rotation law of the gas. In their Section 2, authors look for conditions that must be satisfied in order to open a gap in the disc. Indeed, under certain circumstances it is possible that the star orbiting in the disc plane creates the gap within originally smooth gaseous slab of the disc as a consequence of the tidal interaction of the body with the gas. Mainly the existence of the gap depends on the ratio of the gap width to the vertical height of the disc: it is said that the gap can exist if the width of the gap exceed the semithickness of the disc. Of course, the shape of the gap depends on the viscosity of the disc (the α-parameter). We have already mentioned at several occasions in the text above that a moving body exerts viscous and tidal torques on the gas and induces transport of the angular momenta and the matter. This tidal transport pushes material away from the body, the effect which enhances opening of the gap [44]. Notice that accretion onto a protoplanet is possible even after gap formation. The process continues due to (so called) horseshoe-type orbits [34]. Accretion rate again depends on semithickness of the disc — the thicker is the disc, the larger accretion rate.

Chapter 2

Gravitation of a thin disc

This Chapter deals with gravitational field of an infinitesimally thin disc. First, I briefly review gravitational potentials and corresponding gradients of thin discs (see also refs. [6, 28, 82, 83]), comparing them with one another. These expressions will be used in the second part of thesis to study orbital motion.

2.1 General formulae

Let us define polar coordinates (r, φ, z). We will consider an axially symmetric homogeneous disc with the surface density $\Sigma_0 = \text{const}$; so the potential is function of r and z only $V = V(r, z)$. There are two well-known methods to obtain the potential formula. Lass & Blitzer [39] write:

$$V(r,z) = 2G\Sigma_0 \left[\pi|z| - B_a\, E(k_a) - \frac{a^2 - r^2}{B_a} K(k_a) - \frac{a-r}{a+r}\,\frac{z^2}{B_a}\Pi(n_a^2, k_a)\right] \;, \tag{2.1}$$

where a is the outer radius of the disc and

$$E(k_a) = \int_0^{\pi/2} \sqrt{1 - k_a^2 \sin^2\psi}\, \mathrm{d}\psi \;, \tag{2.2}$$

$$K(k_a) = \int_0^{\pi/2} \frac{\mathrm{d}\,\psi}{\sqrt{1 - k_a^2 \sin^2\psi}} \;, \tag{2.3}$$

$$\Pi(n_a^2, k_a) = \int_0^{\pi/2} \frac{\mathrm{d}\,\psi}{(1 - n_a^2 \sin^2\psi)\sqrt{1 - k_a^2 \sin^2\psi}} \tag{2.4}$$

are elliptic integrals with

$$k_a^2 = \frac{4ar}{B_a^2} \;, \tag{2.5}$$

$$n_a^2 = \frac{4ar}{(a+r)^2} \tag{2.6}$$

and

$$B_a = \sqrt{z^2 + (a+r)^2} \;. \tag{2.7}$$

The same result can be found in textbooks, e.g., in [6], but the above form appears to be more compact and useful for practical purposes. It is not the only method to obtain the potential of a thin disc. Various approaches giving general and compact formulae can be found in the literature [28, 82]. In the latter works the potential is derived for variable surface density $\Sigma = \Sigma(R)$, where $R \in <\varepsilon,\ a>$ is the radial coordinate in the disc plane $z = 0$, requiring axial symmetry only. (Here, ε and a stand for inner and outer disc radius, respectively.)

We can choose Cartesian coordinate system so that the coordinates (expressed in terms of spherical coordinates r, θ, ϕ) of the point (1) at which we look for the potential V are $(r\sin\theta, 0, r\cos\theta)$, and coordinates of the point (2) are $(\rho\cos\phi, \rho\sin\phi, 0)$ (see Figure 2.1). Let r be the distance of the point (1) and ρ be the distance of the point (2) from the zero point. Vector $\boldsymbol{\rho}$ lies in the $z = 0$ plane.

$$\boldsymbol{r}_1 = (r\sin\theta, 0, r\cos\theta), \tag{2.8}$$

$$\boldsymbol{r}_2 = (\rho\cos\phi, \rho\sin\phi, 0) \;, \tag{2.9}$$

$$\boldsymbol{r}_{12} = \boldsymbol{r}_1 - \boldsymbol{r}_2 = (r\sin\theta - \rho\cos\phi, -\rho\sin\phi, r\cos\theta) \;. \tag{2.10}$$

The distance of points 1 and 2 is

$$|\boldsymbol{r}_{12}| = \sqrt{r^2 + \rho^2 - 2r\rho\sin\theta\cos\phi} \tag{2.11}$$

and the potential V

$$V = -G \int_{\text{(disc)}} \frac{\Sigma(\rho)}{|\boldsymbol{r}_{12}|}\, \mathrm{d}S = -G \int_{\text{(disc)}} \frac{\Sigma(\rho)\rho}{\sqrt{r^2 + \rho^2 - 2r\rho\sin\theta\cos\phi}} \mathrm{d}\rho\, \mathrm{d}\phi \tag{2.12}$$

$$= -2G \int_0^a \Sigma(\rho)\rho\, \mathrm{d}\rho \int_0^\pi \frac{\mathrm{d}\phi}{\sqrt{r^2 + \rho^2 - 2r\rho\sin\theta\cos\phi}} \;. \tag{2.13}$$

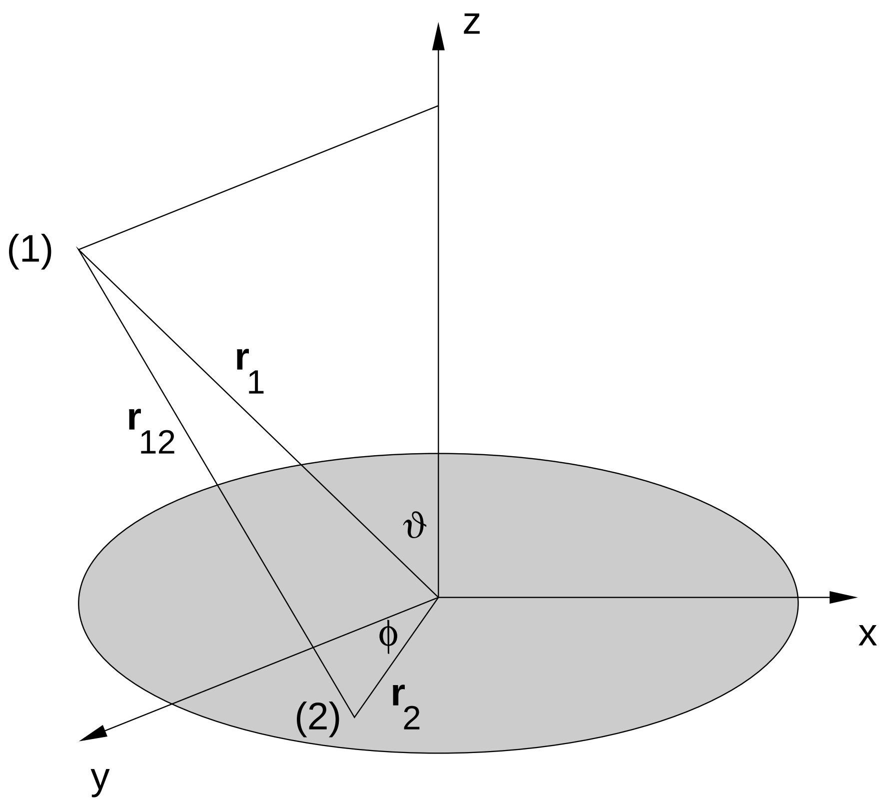

Figure 2.1: Geometry used when deriving the disc potential.

Substitution

$$\xi = \tan\frac{\phi}{2}\ , \tag{2.14}$$

$$\mathrm{d}\phi = \frac{2\ \mathrm{d}\xi}{1+\xi^2}\ , \tag{2.15}$$

$$\cos\phi = \frac{1-\xi^2}{1+\xi^2} \tag{2.16}$$

gives:

$$V = -2G\int\limits_0^a \Sigma(\rho)\rho\ \mathrm{d}\rho\ \int\limits_0^\infty \frac{\frac{2\ \mathrm{d}\xi}{\sqrt{1+\xi^2}}}{\left[(r^2+\rho^2)(1+\xi^2)-2r\rho(1-\xi^2)\sin\theta\right]^{1/2}} \tag{2.17}$$

$$= -4G\int\limits_0^a \Sigma(\rho)\rho\ \mathrm{d}\rho\ \int\limits_0^\infty \frac{\mathrm{d}\xi}{\left[(1+\xi^2)(A^2+B^2\xi^2)\right]^{1/2}} \tag{2.18}$$

$$= -4G\int\limits_0^a \frac{\Sigma(\rho)\rho\ \mathrm{d}\rho}{B}\int\limits_0^\infty \frac{\mathrm{d}\xi}{\sqrt{\left(1+\xi^2\right)\left(\frac{A^2}{B^2}+\xi^2\right)}} \tag{2.19}$$

$$= -4G\int\limits_0^a \frac{\Sigma(\rho)\rho}{B}K(k)\ \mathrm{d}\rho\ \ . \tag{2.20}$$

Here

$$A^2 = r^2 + \rho^2 - 2r\rho\sin\theta \ , \tag{2.21}$$
$$B^2 = r^2 + \rho^2 + 2r\rho\sin\theta \ , \tag{2.22}$$
$$k^2 = \frac{4r\rho\sin\theta}{B^2} \ . \tag{2.23}$$

So, we have the result

$$V = -4G\int_0^a \frac{\Sigma(\rho)\rho}{B} K(k)\ \mathrm{d}\rho \ . \tag{2.24}$$

This is the relation for the potential of the thin disc written in form of spherical coordinates (r, ϑ, φ). It is reasonable to express the formula in terms of cylindrical coordinates (r', φ, z). Variables r, r' and z are in relation $r^2 = r'^2 + z^2$; $r' = r\sin\vartheta$. Density ρ is evaluated in the disc-plane and has the same value in both of coordinates systems. Thus it is possible to rewrite (2.21) and (2.22) to the form

$$A^2 = z^2 + (r' - \rho)^2 \ , \tag{2.25}$$
$$B^2 = z^2 + (r' + \rho)^2 \ . \tag{2.26}$$

To prevent a confusion (for example the ρ may define both the coordinate of the point in the disc plane and the density) it is reasonable to redefine polar coordinates $\rho \to R$ and $r' \to r$ and to write down relations (2.21), (2.22), (2.23), (2.25), (2.26) in form

$$B(R) = \sqrt{z^2 + (R+r)^2} \ , \tag{2.27}$$
$$A(R) = \sqrt{z^2 + (R-r)^2} \ , \tag{2.28}$$
$$k^2(R) = \frac{4Rr}{B^2(R)} \ . \tag{2.29}$$

and rewrite (2.24) onto form

$$V(r,z) = -4G\int_0^a \frac{\Sigma(R)R}{B(R)}\ K(k(R))\ \mathrm{d}R \ . \tag{2.30}$$

We look for the potential at the point with polar coordinates (r, φ, z), $R \in (0, a)$ is the integration variable. Formula (2.30) can be found in Karas [28] and Vokrouhlický & Karas [82].

It is useful to remark that the gradient of the potential, given by Lass & Blitzer [39] in eq. (2.1), is in agreement with ref. (2.30), though written in very different form;

$$\frac{\partial V(r,z)}{\partial r} = -2\frac{G}{r}\int_0^a \frac{\Sigma(R)R}{B(R)}\Big[E(k)\frac{R^2 - r^2 + z^2}{z^2 + (r-R)^2} - K(k)\Big]\ \mathrm{d}R \ , \tag{2.31}$$

$$\frac{\partial V(r,z)}{\partial z} = -4Gz\int_0^a \frac{\Sigma(R)R}{A^2(R)B(R)}E(k)\ \mathrm{d}R. \tag{2.32}$$

$$\frac{\partial V(r,z)}{\partial r} = -2\frac{G\Sigma_0}{rB_a}\left[B_a^2 E(k_a) - \left(z^2 + a^2 + r^2\right)K(k_a)\right] \ , \tag{2.33}$$

$$\frac{\partial V(r,z)}{\partial z} = 2G\Sigma_0\left[\pm\pi - \frac{z}{B_a}\left(K(k_a) + \frac{a-r}{a+r}\Pi(n_a^2, k_a)\right)\right] \ . \tag{2.34}$$

Gradients (2.33) and (2.34) are expressed in simple form (no further integration is needed). On the other hand, the form of gradients (2.31) and (2.32) appears considerably more general.

2.2 Potential in the disc plane

Expression (2.30) describes the potential of a disc with a general profile of surface density, $\Sigma \equiv \Sigma(R)$. General form of (2.30) can be simplified in the case of a special relation $\Sigma(R)$ in the disc plane, $z = 0$. Here one encounters a difficulty, however. Looking for the potential at a point $r < a$, the integrand exhibits discontinuity when $r = R$. Naturally, this is not a physical divergence and the problem can be avoided; Let us write $\Sigma(R) = [\Sigma(R) - \Sigma(r)] + \Sigma(r)$, where we should integrate with respect to R and look for the potential in the point $r < a$. Thus we obtain from eq. (2.30)

$$V(r,z) = -4G \int_0^\infty \frac{[\Sigma(R) - \Sigma(r)]\ R}{B(R)} K(k(R))\mathrm{d}R + V_\mathrm{u}(r,z)\ , \tag{2.35}$$

where $V_\mathrm{u}(r,z)$ is the potential of a referential *homogeneous* disc with constant surface density $\Sigma_\mathrm{constant} = \Sigma(r)$ (see, for example, [28, 82]). One can see that potential (2.35) has no divergence for $R = r$.

Potential outside of the disc: $r > a$

Now we will solve the problem in the outer part of the disc, i.e., for $r > a$. Let us consider (see eq. (2.30))

$$V = -4G \int_0^a \frac{\Sigma(R)R}{r+R}\ K(k(R))\ \mathrm{d}R\ , \tag{2.36}$$

where

$$k^2(R) = \frac{4Rr}{(r+R)^2}\ . \tag{2.37}$$

The surface density be $\Sigma \propto R^{-n}$; $n \geq 0$ is real. We can put

$$k_2 \equiv \frac{R}{r} < 1\ . \tag{2.38}$$

and

$$k^2 = \frac{4k_2}{(1+k_2)^2}\ . \tag{2.39}$$

It is convenient to use the Gauss' transformation (see [13], p. 39). It gives

$$K(k) = (1+k_2)K(k_2)\ , \tag{2.40}$$

where

$$k_2 \equiv \frac{1-k'}{1+k'}\ . \tag{2.41}$$

The parameter $k' \equiv \sqrt{1-k^2}$. Using eqs. (2.38) and (2.40),

$$V = -4Gr \int_{\frac{\varepsilon}{r}}^{\frac{a}{r}} \Sigma(rk_2)k_2 K(k_2)\ \mathrm{d}k_2\ . \tag{2.42}$$

Since the surface density in most of models increases with decreasing radial coordinate, we are not allowed to integrate from 0. Instead, we carry integration from ε which represents the inner edge of the disc. Expression (2.42) can be solved for some special shapes of $\Sigma(R)$, obtaining (R_0 is a scale factor)

- $\Sigma = \Sigma_0 = \text{const}$. Now we have

$$V_{[0]} = -4Gr\Sigma_0 \left[E\left(\frac{a}{r}\right) - K\left(\frac{a}{r}\right) + \left(\frac{a}{r}\right)^2 K\left(\frac{a}{r}\right) \right] . \tag{2.43}$$

- $\Sigma = \Sigma_0(R_0/R) = \Sigma_0 R_0/(rk_2)$: Potential is given by a sum:

$$V_{[-1]} = -2\pi G\Sigma_0 R_0 \left[k_2 \left(1 + \sum_{n=1}^{\infty} \frac{\left[(2n)!\right]^2 k_2^{2n}}{(2n+1)2^{4n}(n!)^4} \right) \right]_{k_2=\varepsilon/r}^{a/r} . \tag{2.44}$$

- $\Sigma = \Sigma_0(R_0/R)^2 = \Sigma_0 R_0^2/(r^2k_2^2)$: This solution cannot be expressed analytically, however.
- $\Sigma = \Sigma_0(R_0/R)^3 = \Sigma_0 R_0^3/(r^3k_2^3)$:

$$V_{[-3]} = +4G\frac{\Sigma_0 R_0^3}{r} \left[\frac{E\left(\frac{a}{r}\right)}{a} - \frac{E\left(\frac{\varepsilon}{r}\right)}{\varepsilon} \right] . \tag{2.45}$$

Potential below the inner edge: $r < \varepsilon$

By a similar approach we can obtain the potential inside the disc, $r < \varepsilon$. Then we use substitution

$$k_2 \equiv \frac{r}{R} < 1 . \tag{2.46}$$

Using of the Gauss transformation gives a general result

$$V = 4Gr \int_{\frac{r}{\varepsilon}}^{\frac{r}{a}} \Sigma\left(\frac{r}{k_2}\right) \frac{1}{k_2^2} K\left(k_2\right) \mathrm{d}k_2 \tag{2.47}$$

and for special cases we can have:

- $\Sigma = \Sigma_0$:

$$V_{[0]} = -4G\Sigma_0 \left[aE\left(\frac{r}{a}\right) - \varepsilon E\left(\frac{r}{\varepsilon}\right) \right] . \tag{2.48}$$

- $\Sigma = \Sigma_0(R_0/R) = \Sigma_0 R_0 k_2/r$: Solution is not analytically available.
- $\Sigma = \Sigma_0(R_0/R)^2 = \Sigma_0 R_0^2 k_2^2/r^2$:

$$V_{[-2]} = 2\pi G\frac{\Sigma_0 R_0^2}{r} \left[k_2 \left(1 + \sum_{n=1}^{\infty} \frac{\left[(2n)!\right]^2 k_2^{2n}}{(2n+1)2^{4n}(n!)^4} \right) \right]_{k_2=r/\varepsilon}^{r/a} . \tag{2.49}$$

- $\Sigma = \Sigma_0(R_0/R)^3 = \Sigma_0 R_0^3 k_2^3/r^3$:

$$V_{[-3]} = 4G\frac{\Sigma_0 R_0^3}{r^2} \left[E\left(k_2\right) - K\left(k_2\right) + k_2^2 K\left(k_2\right) \right]_{k_2=r/\varepsilon}^{r/a} \tag{2.50}$$

Potential inside the body of the disc: $\varepsilon < r < a$

To obtain the potential inside the body of the disc ($\varepsilon < r < a$), we can again use a trick. Let us divide the disc into two parts: the "lower" part ($r > R$) and the "upper" part ($r < R$), respectively. For the first part of the disc we use the substitution (2.38), and for the second one (2.46). In equation (2.42) we integrate from ε/r to 1 and in equation (2.47) from 1 to

r/a. Having these two parts, we can add them and obtain potential of the complete disc. Of course, for $R = r$ both of our potentials diverge but these divergences have opposite signs and so we can subtract them.

We obtain for special cases these results:

- $\Sigma = \Sigma_0$:
$$V_{[0]} = -4G\Sigma_0 aE\left(\frac{r}{a}\right) , \tag{2.51}$$
which is much more compact then Lass' & Blitzer's formula, as given in [39]. The same result gives also Karas in [28] and Karas & Vokrouhlický in [82].

- $\Sigma = \Sigma_0(R_0/R)^3$:
$$V_{[-3]} = 4G\frac{\Sigma_0 R_0^3}{r^2}\left[E\left(\frac{r}{a}\right) - \left(1 - \frac{r^2}{a^2}\right)K\left(\frac{r}{a}\right) - \frac{r}{\varepsilon}E\left(\frac{\varepsilon}{r}\right)\right] . \tag{2.52}$$

Evans' models of Toomre's discs

Inspirative models of thin discs are given by Evans & de Zeeuw [20]. Among others, they derive Toomre's disc with a polynomial variation of surface density.

Supposing an infinite number of concentric ellipsoids with constant rates of semiaxes $a : b : c$ for all ellipsoids and with different density ρ (see Section 1.3) they model the infinite elliptical disc with the polynomially variable density

$$\rho = \frac{\rho_0}{(1+m^2)^p} , \tag{2.53}$$

where (in Cartesian coordinates x, y, z)

$$m^2 = \frac{x^2}{a^2} + \frac{y^2}{b^2} + \frac{z^2}{c^2} , \tag{2.54}$$

(p is a real). Limit $c \to 0$ gives the model of the thin infinite disc with the surface density

$$\Sigma = \frac{\Sigma_0}{(1+\tilde{m}^2)^q} , \tag{2.55}$$

where

$$\tilde{m}^2 = \frac{x^2}{a^2} + \frac{y^2}{b^2} \tag{2.56}$$

and $p = q + \frac{1}{2}$. Since this discussion concerns infinite discs, constants a, b and c represent scale factors only, not final dimensions of ellipsoids or discs, respectively.

Having these results, one obtains potentials of circular thin discs in z-plane as limit $a = b$. Thus one obtains the potential of the infinite disc with circular variability of the surface density

$$\Sigma = \frac{\Sigma_0}{\left(1+\frac{r^2}{a^2}\right)^q} , \tag{2.57}$$

where $r^2 = x^2 + y^2$. For the special case $q = 1$ one has (1.69), which can be rewritten into form

$$V_1(r, z=0) = -2\pi G a^2 \Sigma_0 R_F(0, a^2, a^2 + r^2) , \tag{2.58}$$

where

$$R_F(k,l,m) \equiv \int\limits_0^\infty \frac{\mathrm{d}t}{\sqrt{(t+k)(t+l)(t+m)}} \ , \tag{2.59}$$

k, l m are real numbers [14, 20].

We can compare this formula with the equivalent expression (2.36). Having, we obtain

$$V(r,0) = -G\Sigma_0 \int\limits_0^\infty \frac{R}{r+R} \frac{1}{1+R^2} K(k)\ \mathrm{d}R \tag{2.60}$$

Since we suppose an infinite disc, we integrate to infinity. We should set $k^2 = 4Rr/(r+R)^2$ but this expression is equal to 1 for $R=r$ and hence elliptic integral $K(k)$ diverges. We have two ways to avoid this problem. At first, we can introduce ε as a very small z-component and write

$$k^2 = \frac{4Rr}{\varepsilon + (r+R)^2} < 1 \quad \forall\ R; r \ . \tag{2.61}$$

At second, we write $\Sigma(R) = [\Sigma(R) - \Sigma(r)] + \Sigma(r)$ (see discussion in previous Chapter and (2.35)). Both these methods give acceptable coincidence with Evans's expression (1.69).

2.3 Gradients in z-plane

It is straightforward (though tedious in some cases) to obtain gradients in the disc plane. General formulae are:

- Outside of the disc:

$$\frac{\partial V}{\partial r} = 4G \int\limits_{\frac{\varepsilon}{r}}^{\frac{a}{r}} \Sigma\left(rk_2\right) \frac{k_2}{1-k_2^2} E\left(k_2\right) \mathrm{d}k_2 \ . \tag{2.62}$$

- Fully inside the disc (bellow the inner edge of the disc):

$$\frac{\partial V}{\partial r} = 4G \left[\frac{1}{k_2}\Sigma\left(\frac{r}{k_2}\right) K\left(k_2\right)\right]_{k_2=r/\varepsilon}^{r/a} - 4G \int\limits_{\frac{r}{\varepsilon}}^{\frac{r}{a}} K\left(k_2\right) \frac{\mathrm{d}}{\mathrm{d}k_2} \left[\frac{1}{k_2}\Sigma\left(\frac{r}{k_2}\right)\right] \mathrm{d}k_2 \ . \tag{2.63}$$

In special cases outside the disc we obtain:

- $\Sigma = \Sigma_0$:

$$\left.\frac{\partial V}{\partial r}\right|_{[0]} = 4G\Sigma_0 \left[K\left(\frac{a}{r}\right) - E\left(\frac{a}{r}\right)\right] \ . \tag{2.64}$$

- $\Sigma = \Sigma_0(R_0/R)$:

$$\left.\frac{\partial V}{\partial r}\right|_{[-1]} = 4G\frac{\Sigma_0 R_0}{r^2} \left[aK\left(\frac{a}{r}\right) - \varepsilon K\left(\frac{\varepsilon}{r}\right)\right] \ . \tag{2.65}$$

- $\Sigma = \Sigma_0(R_0/R)^2$: Analytical solution is not available.
- $\Sigma = \Sigma_0(R_0/R)^3$: Analytical solution is not available.

Gradients fully inside discs (bellow inner edges of discs) are:

- $\Sigma = \Sigma_0$:
$$\left.\frac{\partial V}{\partial r}\right|_{[0]} = 4G\frac{\Sigma_0}{r}\left[aK\left(\frac{r}{a}\right) + \varepsilon E\left(\frac{r}{\varepsilon}\right) - aE\left(\frac{r}{a}\right) - \varepsilon K\left(\frac{r}{\varepsilon}\right)\right] . \tag{2.66}$$

- $\Sigma = \Sigma_0(R_0/R)$:
$$\left.\frac{\partial V}{\partial r}\right|_{[-1]} = 4G\frac{\Sigma_0}{r}\left[K\left(\frac{r}{a}\right) - K\left(\frac{r}{\varepsilon}\right)\right] . \tag{2.67}$$

Gradients of potentials inside bodies of discs are:

- $\Sigma = \Sigma_0$:
$$\left.\frac{\partial V}{\partial r}\right|_{[0]} = 4G\Sigma_0\frac{a}{r}\left[K\left(\frac{r}{a}\right) - E\left(\frac{r}{a}\right)\right] \tag{2.68}$$

- $\Sigma = \Sigma_0(R_0/R)$:
$$\left.\frac{\partial V}{\partial r}\right|_{[-1]} = 4G\frac{\Sigma_0}{r}\left[K\left(\frac{r}{a}\right) - \frac{\varepsilon}{r}K\left(\frac{\varepsilon}{r}\right)\right] \tag{2.69}$$

Gradients of potentials are not available when $\Sigma \propto R^{-2}$ and $\Sigma \propto R^{-3}$ by this way. Fortunately in the second case we have the potential $V_{[-3]}$ and hence we are able to derive this potential and obtain the gradient.

This hint gives for $r > a$:

$$\left.\frac{\partial V}{\partial r}\right|_{[-3]} = -4G\frac{\Sigma_0 R_0^3}{r^2}\left[2\frac{E\left(\frac{a}{r}\right)}{a} - 2\frac{E\left(\frac{\varepsilon}{r}\right)}{\varepsilon} - \frac{K\left(\frac{a}{r}\right)}{a} + \frac{K\left(\frac{\varepsilon}{r}\right)}{\varepsilon}\right] \tag{2.70}$$

and for $\varepsilon < r < a$ (see (2.52)):

$$\left.\frac{\partial V}{\partial r}\right|_{[-3]} = -4G\frac{\Sigma_0 R_0^3}{r^3}\left[2E\left(\frac{r}{a}\right) - 2K\left(\frac{r}{a}\right) - 2\frac{r}{\varepsilon}E\left(\frac{\varepsilon}{r}\right) + \frac{r^2}{a^2}K\left(\frac{r}{a}\right) + \frac{r}{\varepsilon}K\left(\frac{\varepsilon}{r}\right)\right] . \tag{2.71}$$

2.4 Potentials and gradients on z-axis

Although we deal with some problems on the motion in the disc plane in this thesis, we give also a short review of potentials and their gradients on z-axis for completeness.

It is very easy to find potentials and their gradients in z-axis ($r \equiv 0$). Really, having formula for the axial symmetric potential in z-axis:

$$V = -G\int_{\varepsilon}^{a}\int_{0}^{2\pi}\frac{\Sigma(R)R\,\mathrm{d}R\,\mathrm{d}\varphi}{\sqrt{R^2+z^2}} = -2\pi G\int_{\varepsilon}^{a}\frac{\Sigma(R)R\,\mathrm{d}R}{\sqrt{R^2+z^2}} , \tag{2.72}$$

we can find potentials and then their gradients:

- $\Sigma = \Sigma_0$: homogeneous disc. In this case we can integrate from 0:

$$V = -2\pi G\Sigma_0\left[\sqrt{a^2+z^2} - z\right] , \tag{2.73}$$
$$\left.\frac{\mathrm{d}V}{\mathrm{d}z}\right|_{[0]} = -2\pi G\Sigma_0 z\left[\frac{1}{\sqrt{a^2+z^2}} - \frac{1}{z}\right] . \tag{2.74}$$

For more details see [6].

- $\Sigma = \Sigma_0 R^{-1}$:

$$
\begin{aligned}
V &= -2\pi G \Sigma_0 \ln \left| \frac{a + \sqrt{a^2 + z^2}}{\varepsilon + \sqrt{\varepsilon^2 + z^2}} \right| , & (2.75) \\
\left.\frac{\mathrm{d}V}{\mathrm{d}z}\right|_{[-1]} &= \frac{-2\pi G \Sigma_0 z \left(\varepsilon\sqrt{\varepsilon^2 + z^2} - a\sqrt{a^2 + z^2} + \varepsilon^2 - a^2\right)}{\left(a + \sqrt{a^2 + z^2}\right)\left(\varepsilon + \sqrt{\varepsilon^2 + z^2}\right)\sqrt{a^2 + z^2}\sqrt{\varepsilon^2 + z^2}} & (2.76)
\end{aligned}
$$

- $\Sigma = \Sigma_0 R^{-3}$:

$$
\begin{aligned}
V &= -2\pi G \Sigma_0 \left[\frac{\sqrt{\varepsilon^2 + z^2}}{z^2 \varepsilon} - \frac{\sqrt{a^2 + z^2}}{z^2 a} \right] , & (2.77) \\
\left.\frac{\mathrm{d}V}{\mathrm{d}z}\right|_{[-3]} &= -2\pi G \Sigma_0 \left[\frac{z^2 + 2a^2}{a z^3 \sqrt{a^2 + z^2}} - \frac{z^2 + 2\varepsilon^2}{\varepsilon z^3 \sqrt{\varepsilon^2 + z^2}} \right] . & (2.78)
\end{aligned}
$$

One can easily verify that for large z ($z \gg a$) all of these gradients decrease as

$$
\frac{\mathrm{d}V}{\mathrm{d}z} \propto -2\pi G \Sigma_0 \frac{1}{z^2} \to 0 \ . \tag{2.79}
$$

For $z \to 0$ the gradient $\left.\frac{\mathrm{d}V}{\mathrm{d}z}\right|_{[-1]} \to 0$ while $\left.\frac{\mathrm{d}V}{\mathrm{d}z}\right|_{[-3]}$ increases to infinity.

Part II
Satellite Motion in the Disc Plane

Chapter 3

Effective cross-section of a transiting star

The main aim of this part is to estimate effects acting on a star moving inside the gas described by density, temperature and pressure typical for accretion discs (see, e.g. [21]). We find, numerically, the deceleration force and we integrate stellar motion. There are two main processes which decelerate or accelerate the star: the accretion of matter on the surface of the star, and gravitational (called also dynamical) friction. Thus the basic step needed in modelling stellar motion through the environment is to recognize both of processes and estimated them. The accretion process affects the star close to its path, up to some finite limited distance from where all matter downflows to the body. Outside this region, gravitational friction dominates the friction with theoretically infinite outer range. In the other words, it is necessary to find an effective cross-section of the transiting star (which can be generally different from the geometrical one) – and this is the topic of this Chapter. We derive a formula which is more general then the corresponding relation given in [16]. Next, we apply it to the problem of motion through the thin disc, generally consisting of (gas) continuum.

Having the formula, we explore motion inside the disc. First of all we derive some formulae for the mass which the star meets along its path through the disc. Having the potential of the central mass and the potential of the disc, we compare stellar orbits in the resistive environment (and in gravitational field of the central body) with and without the gravitational field of the disc taken into account.

3.1 Effective cross-section of a star in coherent dust

It is well known that a spherical star has the same external gravitational field as a point mass. We can thus suppose the mass point M_*, which represents the star, and a disc-like target with the radius R_d around the center which represents a geometrical cross section of the star. The situation is illustrated at the picture 3.2 with a general position of the disc-like target and the initial position of the test particle. Asking for the special model of the accretion at the star, the disc-like target has to be perpendicular to the direction of the motion. We suppose that the target moves through an infinite test particle field and ask for the amount of the matter which hits it. It means that we look for the radius of a tube from which all

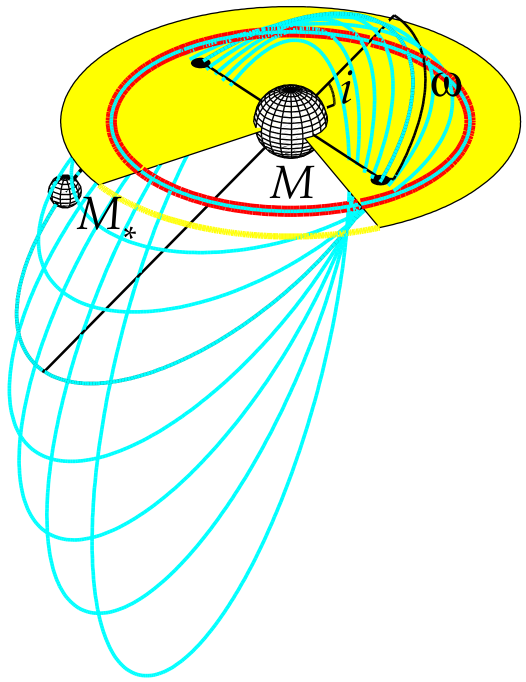

Figure 3.1: Geometry of star-disc collisions. This simplified sketch illustrates how orbital elements of the satellite (mass M_*) undergo the long-term evolution due to hydrodynamical drag of the disc material. Two phases of the orbital evolution must be distinguished.

First, the shape of the orbit is described by eccentricity; orientation of the orbit is determined by its inclination i and argument of pericenter ω. These parameters are gradually changed as functions of time: An initially elongated and inclined orbit becomes circular and embedded in the disc plane.

Once the satellite star is embedded in the disc, further evolution proceeds via hydrodynamical interaction with the surrounding medium. Hereafter, we will consider effects of direct accretion onto the stellar body and of gravitational friction.

matter encounters the target.

Let us consider expression (see Figure 3.2 for the explanation of variables):

$$\frac{1}{R_{\rm d}} = \frac{GM_*}{r^2v^2\sin^2\xi}\left(1-\cos\psi\right) + \frac{1}{r}\left(\cos\psi + \cot\xi\sin\psi\right) \ . \tag{3.1}$$

We look for parameters $(\xi, \xi_*, \beta, \boldsymbol{v}, r)$ defining hyperbolical orbits of the material which touch the target just on the edge $R_{\rm d}$ at the nearest point to the initial position $\boldsymbol{r}$ (see Fig 3.2). Hence one can see that $\xi = \beta$, the vector $\boldsymbol{v}$ has to be parallel to the z-axis and $\boldsymbol{e_{\rm z}} = -\boldsymbol{e_{\rm v}}$ (where $\boldsymbol{e_{\rm z}}$ is the unit vector in z-axis and $\boldsymbol{e_{\rm v}}$ is the unit vector in the velocity $\boldsymbol{v} = v\boldsymbol{e_{\rm v}}$). Also

$$\psi = \frac{\pi}{2} - \beta \quad \Rightarrow \quad \cos\psi = \sin\beta \ ,$$
$$\sin\psi = \cos\beta \ .$$

Then we obtain

$$\frac{1}{R_{\rm d}} = \frac{GM_*}{r^2v^2\sin^2\xi}\left(1-\sin\xi\right) + \frac{1}{r}\left(\sin\xi + \frac{\cos^2\xi}{\sin\xi}\right) \ . \tag{3.2}$$

This expression can be converted to the quadratic equation

$$0 = \sin^2\xi + \frac{R_{\rm d}}{r}\left(\frac{GM_*}{rv^2} - 1\right)\sin\xi - \frac{R_{\rm d}}{r}\frac{GM_*}{rv^2} \ , \tag{3.3}$$

whose solution we will find. The discriminant of the quadratic equation (3.3) is never negative and thus the solution of (3.3) is always real. The first root of the quadratic equation is never negative while the second one is never positive. Since we look for the effective cross-section of the star, we will take the positive root only. It corresponds to the positive angle ξ (supposing that $\xi < \frac{\pi}{2}$).

Let us define variable h as the distance of the particle from z-axis. Thus one has immediately $h = r\sin\beta$. As $\xi = \beta$, h is given by $h/r = \sin\xi$, and we find

$$h = \frac{1}{2}R_{\rm d}\left(1 - \frac{GM_*}{rv^2}\right) + \frac{1}{2}\sqrt{R_{\rm d}^2\left(\frac{GM_*}{rv^2} - 1\right)^2 + 4R_{\rm d}\frac{GM_*}{v^2}}. \tag{3.4}$$

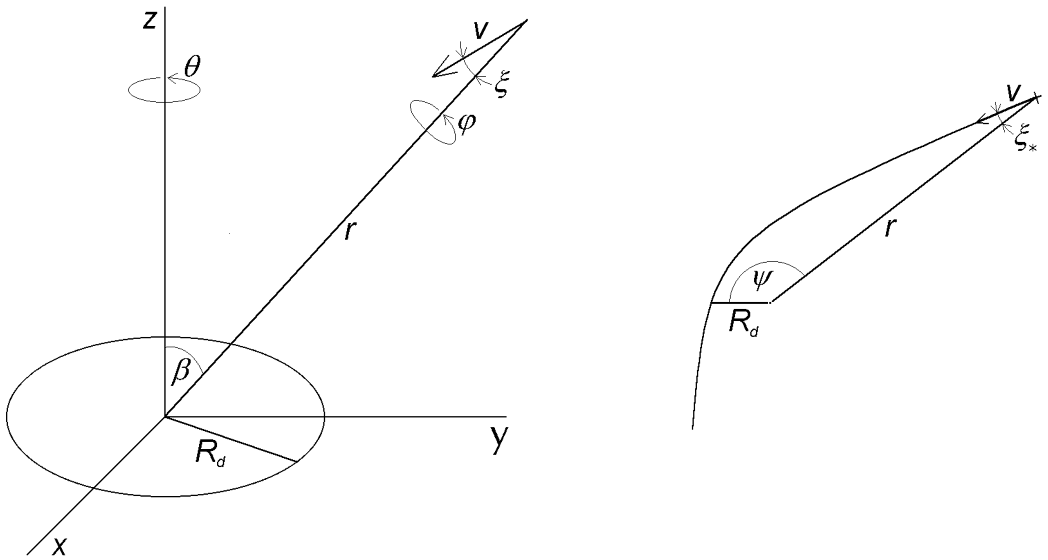

Figure 3.2: Path of a test particle in the gravitational field of a massive body (a star). Here $\boldsymbol{v}$ is velocity of the particle at large distances $|\boldsymbol{r}|$ from the center. R_d is radius of some target; we interpret R_d as the geometrical cross-section of the central star. Right-hand side picture introduces the angle ψ: the trajectory of the particle touches the target at a point of maximum distance.

We can see that

$$\lim_{v\to\infty} h = R_\mathrm{d} \; . \tag{3.5}$$

We supposed a model in which the star is at rest and the gas migrates against it with the velocity $\boldsymbol{v}$. It means that $\boldsymbol{v}$ must be parallel to the axis of motion (see $\xi = \beta$ and the upper text). It is equivalent to the limit $r \to \infty$. Therefore, we need to perform this limit to obtain the required effective radius of the star $\mathcal{R}$. We obtain

$$\mathcal{R} = \lim_{r\to\infty} h = \frac{1}{2}R_\mathrm{d} + \frac{1}{2}\sqrt{R_\mathrm{d}^2 + 4R_\mathrm{d}\frac{GM_*}{v^2}} \; . \tag{3.6}$$

Let us define the rate of accretion $A \equiv \frac{\mathrm{d}M_*}{\mathrm{d}t} = \dot{M}_* = \pi\mathcal{R}^2\rho v$

$$A = \frac{1}{2}\pi R_\mathrm{d}^2\rho\left[v + 2\frac{GM_*}{R_\mathrm{d}v} + \sqrt{v^2 + 4\frac{GM_*}{R_\mathrm{d}}}\right] \; . \tag{3.7}$$

(Of course, various expressions for the accretion rate are given in literature; other published expression see, e.g., [16]). Supposing

$$4\frac{GM_*}{R_\mathrm{d}v^2} \equiv \varepsilon \ll 1 \; , \tag{3.8}$$

we can set $\sqrt{1+\varepsilon} \approx 1 + \frac{1}{2}\epsilon$ in eq (3.7) and obtain

$$A = \pi R_\mathrm{d}^2\rho\left[v + 2\frac{GM_*}{R_\mathrm{d}v}\right] \; , \tag{3.9}$$

which is the expression given in [16]. From the (3.9) one can get the expression for Danby's effective cross-section. For a solar-type body

$$R_\mathrm{d} \;=\; R_\odot \;=\; 6.96\times10^8 \text{ m} \; , \quad M_* = M_\odot \;=\; 1.99\times10^{30} \text{ kg} \; , \tag{3.10}$$

the comparison of the formula given by the expression (3.7) and (3.9) gives

$$\frac{R_{\text{our}}}{R_{\text{Danby}}} = \frac{1}{2}\left(1 + \sqrt{\frac{1 + 4\frac{GM_*}{v^2 R_{\text{d}}}}{1 + 2\frac{GM_*}{v^2 R_{\text{d}}}}}\right) \tag{3.11}$$

For the Sun we have $(R_{\text{our}}/R_{\text{Danby}})_\odot \doteq 1.04$ for $v \approx 1.4 \cdot 10^6 \text{m s}^{-1}$.

Chapter 4

Effects of mass accretion

The deceleration force due to the accreted material is determined mainly by the amount of matter which the star meets on its path through the gaseous disc, which we approximate as a thin planparallel slab with density ρ depending generally both on radial and z-coordinate.

We will explore a set of possible stellar trajectories through the disc in this Chapter. At first, we suppose circular orbits; length of arc embedded in the disc is negligible in comparison with the path outside it, and hence the curvature of the trajectory in the disc is negligible. Thus it is possible to approximate the path as a straight line with inclination angle $\alpha \approx \pi/2$. Of course, on a highly inclined orbit (with inclination angle near zero) this approximation is incorrect and one has to consider circular or generally elliptical orbit (parabolical or hyperbolical orbits are outside our interests in this thesis, as we consider only satellites bound to the centre).

We believe that this Chapter will give some ideas useful, for example, to the discussion on the stellar capture by an accretion disc; see also [75, 82, 83]. Authors of these papers use a simple model of a transit across a thin disc, while the present Chapter offers some ways to possible generalizations of their assumptions in future investigations.

4.1 Basic considerations

At the beginning, in order to obtain the order of magnitude estimates of relevant quantities, we summarize a very simple scheme: The star crosses *perpendicularly* through the disc of density profile

$$\rho(R) = \rho_0 R^{-n}\, e^{-\kappa|z|} \quad , \quad R \in < \varepsilon, a > , \tag{4.1}$$

where $\rho_0 = \rho_c R_0^{+n}$, R_0 is the scale factor, ε and a are inner and outer edges of the disc, ρ_c is the disc density at its inner edge at $z = 0$ and $\kappa \propto 1/H$ is a constant. We will use this notation also in the remaining Sections of this Chapter.

We can immediately notice that

$$\lim_{R \to 0} \rho = \infty \ , \tag{4.2}$$

but the problem with divergence can be avoided by setting the power law in the form

$$\rho = \rho_0(\varepsilon + R)^{-n} e^{-\kappa|z|} \ , \tag{4.3}$$

where ε is much lesser then R. Notice that we are not particularly interested in the effects very near to the center, and we do not use limit $R \to 0$ anywhere in the discussion; hence we can neglect ε without considerable errors.

If H is geometrical semi-thickness of the disc and $\pi\mathcal{R}^2$ is the effective cross-section of the star – see (3.6) then the amount of the gas which the star meets on its transit through the disc is

$$\begin{aligned} M &= \pi\mathcal{R}^2 \int_{-H}^{H} \rho(R,z)\mathrm{d}z = \\ &= \pi\mathcal{R}^2 \int_{-H}^{H} \rho_0 R^{-n} e^{-\kappa|z|}\mathrm{d}z = \\ &= 2\pi\mathcal{R}^2\rho_0 R^{-n}\,\frac{1}{\kappa}\left(1 - e^{-\kappa H}\right) \ . \end{aligned}$$

Supposing

$$\frac{H}{R} \equiv \xi \approx 10^{-3} \ll 1 \ , \tag{4.4}$$

[21] we can write:

$$H = \xi R \ . \tag{4.5}$$

$$M = \frac{2}{\kappa}\pi\mathcal{R}^2\rho_0 R^{-n}(1 - e^{-\kappa\xi R}) \ . \tag{4.6}$$

Let us remark that we admitted a variable disc density, changing with the distance from the central object, but we neglected this variation on the typical stellar cross-section dimension scale. This appears to be an acceptable approximation. We estimate that the central body has a typical mass about $10^8\ M_\odot$, so its gravitational radius is about 3×10^8 km. Typical stellar radius is 7×10^5 km. The star transits through the disc at the typical distance about 1000 $R_\mathrm{G} = 3 \times 10^{11}$ km from the center, the ratio of stellar radius to its distance is 2.3×10^{-6} and hence this approximation gives negligible errors.

4.2 The standard disc

A perpendicular transit

Similarly to the previous basic model we now assume the star transiting perpendicularly through the thin planparallel disc, for which we adopt the standard model [21, 63] with density profile

$$\rho = \rho_0\ R^{-n}\ e^{-\kappa z^2} \ , \tag{4.7}$$

where $\kappa \propto H^{-2}$, or, in an special form (see [21]),

$$\kappa = \frac{1}{2H^2} \ . \tag{4.8}$$

Then:

$$\begin{aligned} M &= \pi\mathcal{R}^2 \int\limits_{-H}^{H} \rho(R,z)\mathrm{d}z = \\ &= 2\pi\mathcal{R}^2 \int\limits_{0}^{H} \rho(R,z)\mathrm{d}z = \\ &= 2\pi\mathcal{R}^2 \rho_0 R^{-n} \int\limits_{0}^{H} e^{-\kappa z^2}\mathrm{d}z \ . \end{aligned}$$

Substitution:

$$\sqrt{\kappa}\, z = t \Rightarrow \sqrt{\kappa}\mathrm{d}z = \mathrm{d}t \ . \tag{4.9}$$

gives:

$$M = \frac{\pi}{\sqrt{\kappa}}\mathcal{R}^2 \rho_0 R^{-n} \int\limits_{0}^{H\sqrt{\kappa}} e^{-t^2}\mathrm{d}t \ . \tag{4.10}$$

This is Laplace-Gauss' integral, belonging to the group of Fresnel's integrals. They satisfy

$$\int_0^x e^{-t^2}\ \mathrm{d}t = x - \frac{x^3}{3\times 1!} + \frac{x^5}{5\times 2!} - \frac{x^7}{7\times 3!}\cdots \tag{4.11}$$

Thus we obtain

$$M = 2\sqrt{2}H\pi\mathcal{R}^2\rho_0 R^{-n}\left[\left(\frac{1}{2}\right)^{\frac{1}{2}} - \frac{\left(\frac{1}{2}\right)^{\frac{3}{2}}}{3\times 1!} + \frac{\left(\frac{1}{2}\right)^{\frac{5}{2}}}{5\times 2!} - \frac{\left(\frac{1}{2}\right)^{\frac{7}{2}}}{7\times 3!}\cdots\right] \ . \tag{4.12}$$

We used $\kappa = 1/(2H^2)$. The expression can be rewritten into form:

$$M \doteq 1.71125\pi H\mathcal{R}^2\rho_0 R^{-n} \ . \tag{4.13}$$

One can integrate over the interval $\langle -\infty; +\infty\rangle$. The error will not be considerable due to the exponentially decreasing of the density.

An inclined transit of a star through the disc

The perpendicular transit of the body through the disc is a rough approximation, generally far from the reality. One should admit the path of the star with the inclination angle different from $\pi/2$. Since the star enters in the disc at the distance different from that where it exits, one should take into account that, generally, also density varies along the path, $\rho = \rho(R)$. Therefore, this Section is divided into two parts. At the first one we suppose the order estimation that the disc density is approximatively independent on the radial distance R along the path of the star – see 4.15. At the second one we revise this restriction and we suppose $\rho = \rho(R,z)$ – see (4.25).

A simplified model: $\rho = \rho(z)$

Let us consider the standard model (4.7) again:

$$\rho = \rho_0 R^{-n} e^{-\kappa z^2} \ , \tag{4.14}$$

with assumption

$$\rho_0 R^{-n} = \text{const} . \tag{4.15}$$

Since the cross-section of the star is a circle and the star transits through the disc with the declination angle α, the section of the tubs (defined by the stellar path through the disc) is elliptical on the planparallel disc, where

$$\mathcal{R}' = \frac{\mathcal{R}}{\sin\alpha} \tag{4.16}$$

is the semimajor axis of the ellipse. The area of ellipse is

$$S_* = \pi\mathcal{R}\mathcal{R}' = \pi\frac{\mathcal{R}^2}{\sin\alpha} . \tag{4.17}$$

The mass inside the tube is then

$$M = \int\limits_{(\mathrm{V})} \rho \,\mathrm{d}V = \rho_0 R^{-n}\pi\frac{\mathcal{R}^2}{\sin\alpha}\int\limits_{-H}^{H} e^{-\kappa z^2}\,\mathrm{d}z . \tag{4.18}$$

In particular, for the integration from $-\infty$ to $+\infty$ one has

$$M = \rho_0\frac{\pi\mathcal{R}^2}{\sin\alpha}R^{-n}\sqrt{\frac{\pi}{\kappa}} . \tag{4.19}$$

Considering the fact that $\kappa = 1/(2H^2)$ we can write

$$M = \rho_0\frac{\pi\mathcal{R}^2}{\sin\alpha}R^{-n}H\sqrt{2\pi} . \tag{4.20}$$

We remind that this is not fully correct because we assumed a thin disc and integrated vertical coordinate z from $-\infty$ to $+\infty$. On the other hand we can reasonably suppose a strongly decreasing density which rapidly decays with $|z|$ increasing, and so the error which we introduce in this way turns out to be negligible.

A model with $\rho = \rho(R, z)$

We adopt the straight line model of the stellar path now, similarly to the previous paragraph, but the more realistic assumption is that the density varies with the actual distance from the center R.

We can find surfaces of the constant density as a function $R = R(z)$: Be R_0 the impact parameter of the straight-line trajectory (the minimum distance of the stellar path to the massive center). The star enters into the disc at the point $\boldsymbol{R}_{\mathbf{in}}$, and leaves it out at $\boldsymbol{R}_{\mathbf{out}}$. We define the angle ψ_{in} as $\angle(R_{\mathrm{in}},\ \text{center},\ R_0)$, and ψ_{out} as $\angle(R_0,\ \text{center},\ R_{\mathrm{out}})$. Due to the axial symmetry (with the line center – R_0 as an axis of the symmetry) it is $\psi_{\mathrm{in}} = \psi_{\mathrm{out}} \equiv \psi_0$ and $|\boldsymbol{R}_{\mathbf{in}}| = |\boldsymbol{R}_{\mathbf{out}}|$.

The star migrates through the disc both in vertical (from $-H$ to the $+H$) and horizontal (from the point $\boldsymbol{R}_{\mathbf{in}}$ to the $\boldsymbol{R}_{\mathbf{out}}$) directions. Thus one should integrate over both coordinates. We define new variable y along the horizontal projection of the stellar path to the disc, and we express it as a function of z: $y = y(z)$, integrating along the z only. It is then give by

$$y = z\cot\alpha , \tag{4.21}$$

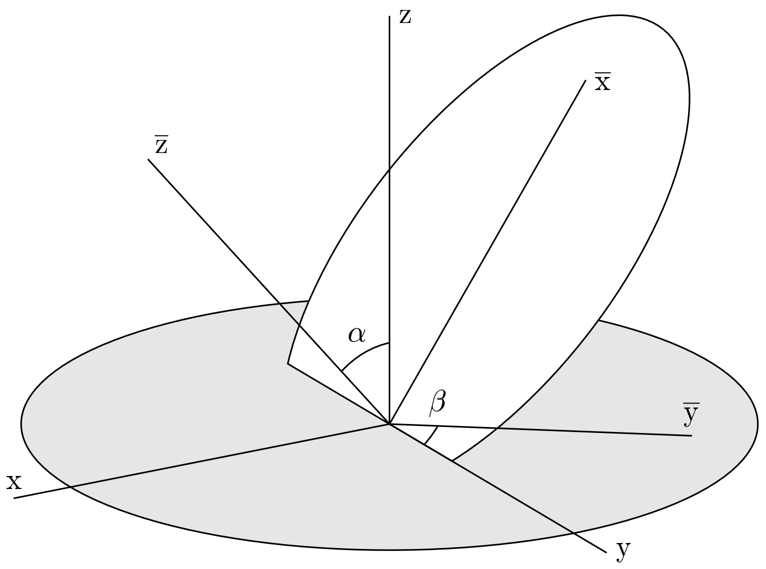

Figure 4.1: Three-dimensional scheme of a general transit of the star through the disc.

where α is the inclination of the stellar path.

Thus one has:

$$\begin{aligned} y &= z \cot \alpha \ , & (4.22) \\ R^2 &= R_0^2 + y^2 \ . & (4.23) \end{aligned}$$

This relation can be substituted into the integral

$$M = \frac{\pi \mathcal{R}^2}{\sin \alpha} \rho_0 \int\limits_{-H}^{H} R^{-n} e^{-\kappa z^2} \mathrm{d}z \tag{4.24}$$

to obtain

$$M = 2 \frac{\pi \mathcal{R}^2}{\sin \alpha} \rho_0 \int\limits_{0}^{H} \left[R_0^2 + (Bz)^2 \right]^{-\frac{n}{2}} e^{-\kappa z^2} \mathrm{d}z \ , \tag{4.25}$$

where

$$B \equiv \cot \alpha \ . \tag{4.26}$$

4.3 Stellar transit through the disc

The estimation of the amount of matter which the star meets along its path becomes very complicated when the inclination angle decreases to zero. The path inside the disc is considerably curved and thus the assumption of the straight trajectory is violated; A more realistic description needs to be accepted. The star passing through the disc moves on an elliptical (or circular, in special case) orbit whose declination angle to the disc plane is α.

Let use introduce two types of coordinates. The first type we define in the disc plane and denote them $(x,\ y,\ z)$. The second type is situated in the orbital plane and denoted $(\tilde{x},\ \tilde{y},\ \tilde{z})$. Of course in the orbital plane $\tilde{z} = 0$. Equation of ellipse is written in the form

$$\frac{\tilde{x}^2}{a^2} + \frac{\tilde{y}^2}{b^2} = 1 \ , \tag{4.27}$$

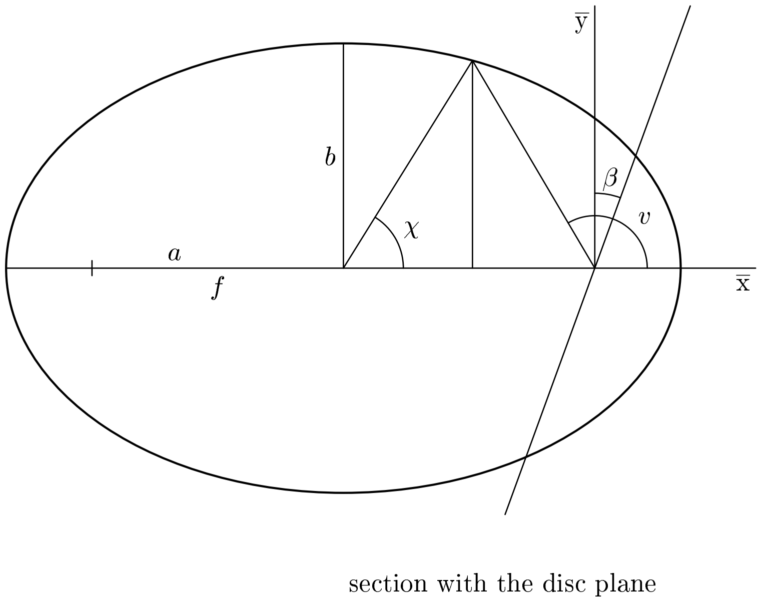

Figure 4.2: Schematic geometry a general transit of the star through the disc.

where $a \geq b$ are semimajor axes of ellipse. We denote

$$f = \sqrt{a^2 - b^2}\ . \tag{4.28}$$

Since

$$\tan\chi = \frac{\tilde{\tilde{y}}}{\tilde{\tilde{x}}}\ , \tag{4.29}$$

we obtain (see Figs. 4.1–4.2)

$$|\tilde{\tilde{x}}| = \frac{ab}{\sqrt{b^2 + a^2\tan^2\chi}}\ , \tag{4.30}$$

$$|\tilde{\tilde{y}}| = \frac{ab\tan\chi}{\sqrt{b^2 + a^2\tan^2\chi}}\ , \tag{4.31}$$

$$\tilde{\tilde{z}} = \tilde{z} = 0\ . \tag{4.32}$$

It is useful to remind the reader that the zero point $[0, 0]$ in the definition of the elliptical trajectory, eq. (4.27), is situated in the center of the ellipse. Transformation to the coordinate system with zero point in the focus of the ellipse can be written down as:

$$\tilde{\tilde{x}} \longrightarrow \tilde{x} - f\ ;\ \tilde{\tilde{y}} = \tilde{y}\ ‘. \tag{4.33}$$

Thus one meets the same situation as shown in Figures 4.1 and 4.2, corresponding to

$$|\tilde{x}| = \frac{ab}{\sqrt{b^2 + a^2\tan^2\chi}} - f\ , \tag{4.34}$$

$$|\tilde{y}| = \frac{ab\tan\chi}{\sqrt{b^2 + a^2\tan^2\chi}}\ , \tag{4.35}$$

$$\tilde{z} = 0\ . \tag{4.36}$$

Without any loss of generality we define that y-axis lies in the section of the orbital and the disc planes. Let us rotate $\tilde{x}\ \tilde{y}$-plane around $\tilde{z}$-axis to reach $y = \tilde{y}$ (angle of rotation is denoted β). The matrix of the rotation is

$$\mathbf{M}_1 = \begin{pmatrix} \cos\beta & \sin\beta & 0 \\ -\sin\beta & \cos\beta & 0 \\ 0 & 0 & 1 \end{pmatrix} . \tag{4.37}$$

Rotating around $y = \tilde{y}$ we reach $x \to \tilde{x}$, $z \to \tilde{z}$. The angle is α and the matrix of rotation is

$$\mathbf{M}_2 = \begin{pmatrix} \cos\alpha & 0 & -\sin\alpha \\ 0 & 1 & 0 \\ \sin\alpha & 0 & \cos\alpha \end{pmatrix} . \tag{4.38}$$

Hence the transformation matrix $\mathbf{M} = \mathbf{M}_2 \times \mathbf{M}_1$ is

$$\mathbf{M} = \begin{pmatrix} \cos\alpha\cos\beta & \cos\alpha\sin\beta & -\sin\alpha \\ -\sin\beta & \cos\beta & 0 \\ \sin\alpha\cos\beta & \sin\alpha\sin\beta & \cos\alpha \end{pmatrix} , \tag{4.39}$$

and it gives the transformation

$$\begin{pmatrix} x \\ y \\ z \end{pmatrix} = \mathbf{M} \begin{pmatrix} \tilde{x} \\ \tilde{y} \\ 0 \end{pmatrix} . \tag{4.40}$$

So the transformation relations are

$$x = (\tilde{x}\cos\beta + \tilde{y}\sin\beta)\cos\alpha \, , \tag{4.41}$$
$$y = -\tilde{x}\sin\beta + \tilde{y}\cos\beta \, , \tag{4.42}$$
$$z = (\tilde{x}\cos\beta + \tilde{y}\sin\beta)\sin\alpha \, . \tag{4.43}$$

The element of the elliptical path is

$$\mathrm{d}l = \sqrt{\left(\frac{\mathrm{d}x}{\mathrm{d}\chi}\right)^2 + \left(\frac{\mathrm{d}y}{\mathrm{d}\chi}\right)^2 + \left(\frac{\mathrm{d}z}{\mathrm{d}\chi}\right)^2}\,\mathrm{d}\chi \, . \tag{4.44}$$

Equations (4.41) $\div$ (4.43) lead to

$$\begin{aligned} \mathrm{d}x &= (\mathrm{d}\tilde{x}\cos\beta + \mathrm{d}\tilde{y}\sin\beta)\cos\alpha \, , \\ \mathrm{d}y &= -\mathrm{d}\tilde{x}\sin\beta + \mathrm{d}\tilde{y}\cos\beta \, , \\ \mathrm{d}z &= (\mathrm{d}\tilde{x}\cos\beta + \mathrm{d}\tilde{y}\sin\beta)\sin\alpha \end{aligned}$$

and from (4.34) $\div$ (4.36) we have

$$\begin{aligned} \frac{\mathrm{d}\tilde{x}}{\mathrm{d}\chi} &= \pm\frac{a^3 b\tan\chi(1+\tan^2\chi)}{(b^2 + a^2\tan^2\chi)^{\frac{3}{2}}} \, , \\ \frac{\mathrm{d}\tilde{y}}{\mathrm{d}\chi} &= \mp\frac{ab^3(1+\tan^2\chi)}{(b^2 + a^2\tan^2\chi)^{\frac{3}{2}}} \, . \end{aligned}$$

We can see that

$$\frac{\mathrm{d}\tilde{y}}{\mathrm{d}\chi} = -\frac{b^2}{a^2}\frac{1}{\tan\chi}\frac{\mathrm{d}\tilde{x}}{\mathrm{d}\chi} \, . \tag{4.45}$$

This relation can written in the form (4.44) to obtain

$$
\begin{aligned}
\mathrm{d}l &= \sqrt{\left(\frac{\mathrm{d}x}{\mathrm{d}\chi}\right)^2 + \left(\frac{\mathrm{d}y}{\mathrm{d}\chi}\right)^2 + \left(\frac{\mathrm{d}z}{\mathrm{d}\chi}\right)^2}\,\mathrm{d}\chi = \\
&= \mathrm{d}\chi \left(\frac{\mathrm{d}\tilde{y}}{\mathrm{d}\chi}\right) \left[\cos^2\alpha \left(\sin\beta - \frac{a^2}{b^2}\cos\beta\tan\chi\right)^2 \right. \\
&\quad \left. + \left(\cos\beta + \frac{a^2}{b^2}\sin\beta\tan\chi\right)^2 + \sin^2\alpha\left(\sin\beta - \frac{a^2}{b^2}\cos\beta\tan\chi\right)^2\right]^{\frac{1}{2}} = \\
&= \mathrm{d}\chi \left(\frac{\mathrm{d}\tilde{y}}{\mathrm{d}\chi}\right) \left[\left(\sin\beta - \frac{a^2}{b^2}\cos\beta\tan\chi\right)^2 (\sin^2\alpha + \cos^2\alpha) \right. \\
&\quad \left. + \left(\cos\beta + \frac{a^2}{b^2}\sin\beta\tan\chi\right)^2\right]^{\frac{1}{2}} = \\
&= \mathrm{d}\chi \left(\frac{\mathrm{d}\tilde{y}}{\mathrm{d}\chi}\right) \left[\left(\sin\beta - \frac{a^2}{b^2}\cos\beta\tan\chi\right)^2 + \left(\cos\beta + \frac{a^2}{b^2}\sin\beta\tan\chi\right)^2\right]^{\frac{1}{2}} = \\
&= \mathrm{d}\chi \left(\frac{\mathrm{d}\tilde{y}}{\mathrm{d}\chi}\right) \left[1 + \frac{a^4}{b^4}\tan^2\chi\right]^{\frac{1}{2}} .
\end{aligned}
$$

Hence

$$
\mathrm{d}l = \mp \frac{ab^3}{\cos^2\chi\,(b^2 + a^2\tan^2\chi)^{\frac{3}{2}}} \left[1 + \frac{a^4}{b^4}\tan^2\chi\right]^{\frac{1}{2}} \mathrm{d}\chi\,. \tag{4.46}
$$

Relation (4.46) describes an element of ellipse. With respect to this one we will integrate. Therefore we look for the integrand now. We suppose that α is small, which means that the orbital plane is near to disc plane. This is a reasonable approximation: If α is large, for example $\alpha \approx \frac{\pi}{2}$, we can approximate the stellar orbit by a straight line, as it was discussed in previous Sections, and it is not necessary to accept this way of solution.

For α small, one needs to set $\beta = 0$ to be able to continue with the analytical solution (in the limit situation $\alpha = 0$ the angle β is not well defined). Let us set $\alpha \neq 0 \cup \beta = 0$. The matrix of transformation $\mathbf{M}$ (see eq. (4.39)) is

$$
\mathbf{M} = \begin{pmatrix} \cos\alpha & 0 & -\sin\alpha \\ 0 & 1 & 0 \\ \sin\alpha & 0 & \cos\alpha \end{pmatrix} \tag{4.47}
$$

and

$$
\begin{aligned}
x &= \tilde{x}\cos\alpha\,, \\
y &= \tilde{y}\,, \\
z &= \tilde{x}\sin\alpha\,.
\end{aligned}
$$

Distance from the center is

$$
\begin{aligned}
R &= \sqrt{\tilde{y}^2 + \tilde{x}^2\cos^2\alpha}\,, \\
\tilde{z} &= \tilde{x}\sin\alpha\,.
\end{aligned}
$$

Since we have (4.34) $\div$ (4.36) and suppose:

$$\rho = \rho_0 R^{-n} e^{-\kappa z^2} \, , \tag{4.48}$$

we obtain

$$\begin{aligned} \rho &= \rho_0 \left[\left(\frac{\pm ab}{\sqrt{b^2 + a^2 \tan^2 \chi}} - \sqrt{a^2 - b^2} \right)^2 \cos^2 \alpha \right. \\ &\quad \left. + \frac{a^2 b^2 \tan^2 \chi}{b^2 + a^2 \tan^2 \chi} \right]^{-\frac{n}{2}} e^{-\kappa \left(\frac{\pm ab}{\sqrt{b^2 + a^2 \tan^2 \chi}} - \sqrt{a^2 - b^2} \right)^2 \sin^2 \alpha} \, . \end{aligned} \tag{4.49}$$

The amount of the matter which the star meets on its path through the disc is, immediately, given by

$$\begin{aligned} M &= S_* \rho_0 \int \left[\left(\frac{\pm ab}{\sqrt{b^2 + a^2 \tan^2 \chi}} - \sqrt{a^2 - b^2} \right)^2 \cos^2 \alpha \right. \\ &\quad \left. + \frac{a^2 b^2 \tan^2 \chi}{b^2 + a^2 \tan^2 \chi} \right]^{-\frac{n}{2}} e^{-\kappa \left(\frac{\pm ab}{\sqrt{b^2 + a^2 \tan^2 \chi}} - \sqrt{a^2 - b^2} \right)^2 \sin^2 \alpha} \\ &\quad \times \frac{ab^3 \left[1 + \frac{a^4}{b^4} \tan^2 \chi \right]^{\frac{1}{2}}}{\cos^2 \chi \, (b^2 + a^2 \tan^2 \chi)^{\frac{3}{2}}} \, \mathrm{d}\chi \, . \end{aligned} \tag{4.50}$$

The integral can be solved only in the special case of the circular orbit (and moreover under another special condition which is discussed below). In the case of a circular orbit, $a = b$, and the star goes through the disc in $\chi \approx \frac{\pi}{2}$. (When $\chi > \frac{\pi}{2}$ or $\chi < \frac{\pi}{2}$, then the star is either above or under of the disc plane.)

Thus for density ρ we have

$$\rho = \rho_0 \left[\frac{a^2 \tan^2 \chi}{1 + \tan^2 \chi} + \cos^2 \alpha \frac{a^2}{1 + \tan^2 \chi} \right]^{-\frac{n}{2}} e^{-\kappa \frac{a^2}{1 + \tan^2 \chi} \sin^2 \alpha} \, . \tag{4.51}$$

Goniometric relations

$$\begin{aligned} \frac{1}{1 + \tan^2 \chi} &= \cos^2 \chi \, , \\ \frac{\tan^2 \chi}{1 + \tan^2 \chi} &= \sin^2 \chi \end{aligned}$$

lead to

$$\rho = \rho_0 a^{-n} \left(\sin^2 \chi + \cos^2 \chi \cos^2 \alpha \right)^{-\frac{n}{2}} e^{-\kappa a^2 \sin^2 \alpha \cos^2 \chi} \, . \tag{4.52}$$

$$\chi \approx \frac{\pi}{2} \Rightarrow \left| \chi - \frac{\pi}{2} \right| \ll \frac{\pi}{2} \tag{4.53}$$

and

$$\sin \chi \approx 1 + \frac{1}{2} \left(\chi - \frac{\pi}{2} \right) + \frac{1}{2^4} \left(\chi - \frac{\pi}{2} \right)^4 \ldots \, , \tag{4.54}$$

$$\cos \chi \approx - \left(\chi - \frac{\pi}{2} \right) + \frac{1}{6} \left(\chi - \frac{\pi}{2} \right)^3 \ldots \, . \tag{4.55}$$

$$\begin{aligned}
\rho &\approx \rho_0 a^{-n}\left[\left(1-\frac{1}{2}\left(\chi-\frac{\pi}{2}\right)^2\right)^2+\cos^2\alpha\left(\chi-\frac{\pi}{2}\right)^2\right]^{-\frac{n}{2}} e^{-\kappa a^2\sin^2\alpha\left(\chi-\frac{\pi}{2}\right)^2} \\
&\approx \rho_0 a^{-n}\left[\left(1-\frac{1}{2}\left(\chi-\frac{\pi}{2}\right)^2\right)^2+\cos^2\alpha\left(\chi-\frac{\pi}{2}\right)^2\right]^{-\frac{n}{2}} \\
&\quad\times\left[1-\kappa a^2\sin^2\alpha\left(\chi-\frac{\pi}{2}\right)^2\right] .
\end{aligned}$$

Due to (4.53) one has

$$\left(\chi-\frac{\pi}{2}\right) \ll \left[1-\frac{1}{2}\left(\chi-\frac{\pi}{2}\right)^2\right] \tag{4.56}$$

and

$$\begin{aligned}
\rho &= \rho_0 a^{-n}\left[1-\frac{1}{2}\left(\chi-\frac{\pi}{2}\right)^2\right]^{-n}\left[1-\kappa a^2\sin^2\left(\chi-\frac{\pi}{2}\right)^2\right] \\
&\approx \rho_0 a^{-n}\left[1+\frac{n}{2}\left(\chi-\frac{\pi}{2}\right)^2\right]\left[1-\kappa a^2\sin^2\alpha\left(\chi-\frac{\pi}{2}\right)^2\right] \\
&\approx \rho_0 a^{-n}\left[1+\left(\chi-\frac{\pi}{2}\right)^2\left(\frac{n}{2}-\kappa a^2\sin^2\alpha\right)\right] .
\end{aligned}$$

Now we set $a = b$ to the expression (4.46), and integrate analytically. We obtain

$$\mathrm{d}l = \frac{ab^3}{\cos^2\chi(b^2+a^2\tan^2\chi)^{\frac{3}{2}}}\left[1+\frac{a^4}{b^4}\tan^2\chi\right]\mathrm{d}\chi = a\ \mathrm{d}\chi\ ; \tag{4.57}$$

$$\mathrm{d}l = a\ \mathrm{d}\chi\ . \tag{4.58}$$

The mass accreted onto the star is integrated over two arcs of the orbit: $\langle\pi/2-\varepsilon;\pi/2+\varepsilon\rangle$ and $\langle 3\pi/2-\varepsilon;3\pi/2+\varepsilon\rangle$. Due to assumption of a circular orbit, $a = b$, we have a symmetry of these two parts and hence it is possible to multiply the mass by the factor of two:

$$\begin{aligned}
M &= 2\rho_0 a^{-n} S_* \int_{\frac{\pi}{2}-\varepsilon}^{\frac{\pi}{2}+\varepsilon}\left[1+\left(\chi-\frac{\pi}{2}\right)^2\left(\frac{n}{2}-\kappa a^2\sin^2\alpha\right)\right] a\ \mathrm{d}\chi \\
&= 2\rho_0 a^{1-n} S_* \int_{-\varepsilon}^{\varepsilon}\left[1+\wp x^2\right]\mathrm{d}x = 2\rho_0 a^{1-n} S_*\left[x+\frac{\wp}{3}x^3\right]_{-\varepsilon}^{\varepsilon} .
\end{aligned}$$

$$M = 2\rho_0 a^{1-n} S_*\left[x+\frac{\wp}{3}x^3\right]_{-\varepsilon}^{\varepsilon} . \tag{4.59}$$

Here we denoted $\wp \equiv \frac{n}{2} - \kappa a^2\sin^2\alpha$.

Equation (4.59) gives the result we looked for. However, it can still be a problem to estimate ε. The disc density is supposed to be $\rho \propto e^{-\kappa z^2}$ and so the disc has no well defined bounds in the vertical direction. We thus introduce the approximation of $\rho < \frac{1}{e}\rho_0$ (neglecting a part of the disc) and we integrate that part of the disc in which $\rho > \frac{1}{e}\rho_0$. We find

$$\exp\{-\kappa a^2\sin^2\alpha\cos^2\chi\}\ . \tag{4.60}$$

Hence we can estimate

$$\frac{1}{\sqrt{\kappa}} = a\varepsilon \sin\alpha \Rightarrow \varepsilon = \frac{1}{a\sqrt{\kappa}\sin\alpha} \tag{4.61}$$

and obtain

$$M = 4\rho_0 a^{1-n}\varepsilon\left(1 + \frac{\wp}{3}\varepsilon^2\right) . \tag{4.62}$$

Considering eq. (4.61) we have the final result

$$M = 4\rho_0 \frac{1}{a^n\sqrt{\kappa}\sin\alpha}\left(1 + \frac{\frac{n}{2} - \kappa a^2 \sin^2\alpha}{3a^2\kappa\sin^2\alpha}\right) . \tag{4.63}$$

Here one can notice a difficulty if $\alpha = 0$. Then the stellar orbit is just embedded in the disc plane, and we have to integrate with $\varepsilon = \frac{\pi}{2}$ (star meets material along the complete circle). We expect

$$M = 2\pi a^{1-n}\rho_0 S_* , \tag{4.64}$$

but we obtain (see (4.59))

$$M = 2\pi a^{1-n}\rho_0 S_*\left(1 + \frac{\pi^2}{24}n\right) . \tag{4.65}$$

The fundament of the problem is of course born in our approximations. Although we supposed that α is a small angle, we used the approximation of very thin disc and hence we supposed (4.53) in our solution. Admitting the motion in the disc plane, we have to adopt χ arbitrary (the stellar orbit is fully embedded inside the disc and $\chi \in < 0, 2\pi >$) and hence we are not allowed to adopt approximations (4.54) and (4.55).

The presented results can be useful, as mentioned at the start of the Chapter, to the future discussion on stellar capture. Vokrouhlický, Vokrouhlický & Karas and Šubr adopt, in their papers [75, 82, 83], a simple model of transit of a star through the disc with a given surface density; here, their assumptions were rewritten in eqs. (4.7) and, correspondingly, in (4.12) and (4.13), while remaining paragraphs of this Chapter enable some generalisation. In this way it is possible to obtain more exact estimations of stellar paths in terms of integrations with varying density during each transit.

Chapter 5

Gravitational friction

Independently of the direct accretion onto a stellar surface, one should take into account at least one another effect which can play a considerable role in the evolution of stellar orbits. Namely, the star is affected by gravitational attraction of the disc material even if it does not

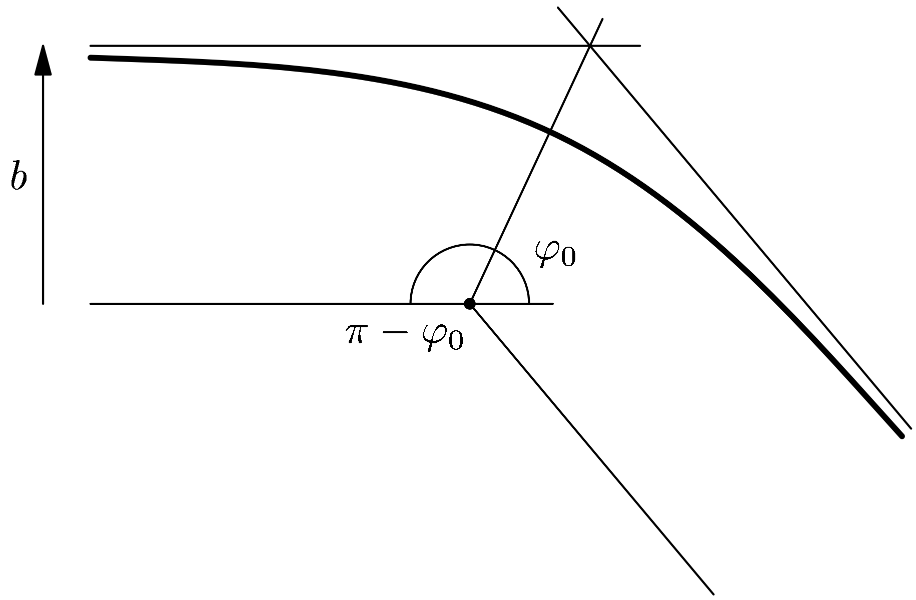

Figure 4.3: Path of a test particle near to the star: geometry and variables used in the discussion of gravitational friction.

fall onto the surface. The gravitational (called also *dynamical*) friction exhibits influence up to the outer boundary of the gas environment which, in practice, may be enormously far.

Thus one should find both the inner boundary of the medium, and the outer one. Naturally, the inner boundary is just equal to the effective cross-section, which is estimated in relations (3.6) and (3.7). Thus the direct accretion inflow decelerating the star (presented in the previous Chapter) is integrated from zero to the radius given by (3.6), while the gravitational friction should be integrated from (3.6) to the outer bound of the disc or another limit.

This Chapter is divided into two parts. In the first one we recall relations relevant for the gravitational friction [6] and we give an example for the gravitational friction in the homogeneous isotropic environment – (see eq. (5.22)). In the second part we estimate the gravitational friction in a flat disc-like environment – see expression (5.44). At the end we expand the relation (5.44) to the Taylor series in order to estimate the behavior of the gravitational friction close to the star (5.53).

5.1 Gravitational friction in the homogeneous environment

Let us suppose a star with the mass M moving through homogeneous and coherent environment. Velocity of the star is $\boldsymbol{v}_{\mathrm{M}}$. A test particle of the mass m is supposed to be situated on impact distance (impact parameter) b. The total mass of the two body problem is thus $\mathcal{M} = M + m$ and the test particle's reduced mass is

$$\mu = \frac{mM}{\mathcal{M}} \,. \tag{5.1}$$

In the case of the homogeneous environment, it is not necessary to reduce the mass because each test particle at one side of the star has its counterpart test particle at the opposite side (axial symmetry with respect to the direction of motion). One can suppose $m \ll M$ only and estimate the gravitational drag. This assumption, however, fails in an inhomogeneous

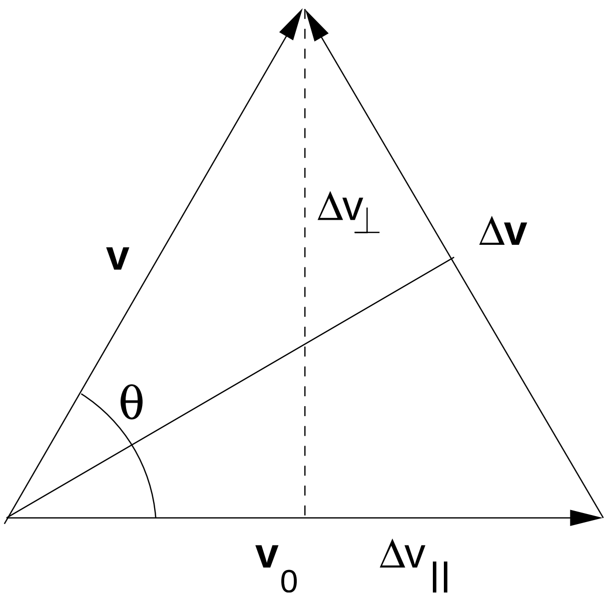

Figure 4.4: A vector triangle of velocities.

environment (for example thin disc-mode environment with $\Sigma = \Sigma(R)$), and thus we use the reduced masses in all Sections of this Chapter.

Let $\boldsymbol{v_0}$ be initial relative velocity of the particle μ with respect to the $\mathcal{M}$ (unperturbed velocity at $-\infty$) and $\boldsymbol{v}$ the final relative velocity (unperturbed velocity at $+\infty$). Then $\Delta\boldsymbol{v} = \boldsymbol{v} - \boldsymbol{v_0}$ is the final change of the initial velocity and it is possible to find (see also Fig. 4.4)

$$\Delta v = 2v_0 \sin\frac{\vartheta}{2} , \tag{5.2}$$

$$\Delta v_{||} = v_0(1-\cos\vartheta) , \tag{5.3}$$

$$\Delta v_{\perp} = v_0 \cos\vartheta , \tag{5.4}$$

where ϑ is deflection of $\boldsymbol{v}$ with respect to the $\boldsymbol{v_0}$. $\Delta\boldsymbol{v} = (\Delta v_{||} \ , \ \Delta v_{\perp})$, where $\Delta\boldsymbol{v}_{||} \parallel \boldsymbol{v_0}$ and $\Delta\boldsymbol{v}_{\perp} \perp \boldsymbol{v_0}$. See also [6].

The instantaneous deceleration force is

$$\boldsymbol{F} = \frac{\mathrm{d}\boldsymbol{p}}{\mathrm{d}t} \tag{5.5}$$

which gives the change of momentum

$$\begin{aligned}
|\Delta\boldsymbol{p}| &= \int\limits_{-\infty}^{+\infty} \boldsymbol{F}\cdot\boldsymbol{s}\mathrm{d}t \\
&= \int\limits_{-\infty}^{+\infty} F\cos\varphi\mathrm{d}t \\
&= 2\int_0^{\frac{\pi+\vartheta}{2}} F\cos\varphi\frac{r^2}{L}\,\mathrm{d}\varphi \\
&= 2\int_0^{\frac{\pi+\vartheta}{2}} \frac{G\mu\mathcal{M}}{r^2}\,\frac{r^2}{bv_0}\cos\varphi\,\mathrm{d}\varphi \\
\Delta p &= \mu\Delta v = 2\frac{G\mu\mathcal{M}}{bv_0}\sin\left(\frac{\pi+\vartheta}{2}\right) \ .
\end{aligned} \tag{5.6}$$

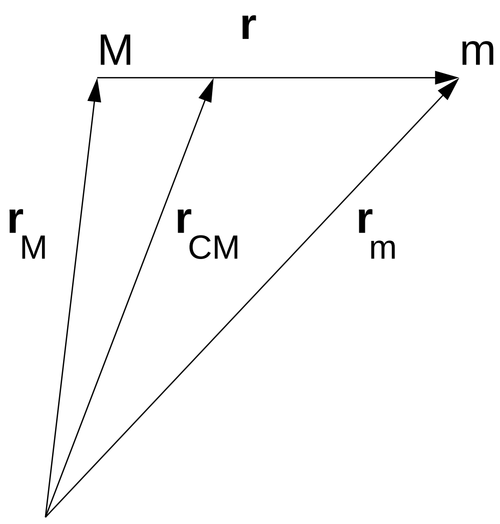

Figure 5.1: Position vectors of the main body (mass M) and the test particle (mass m).

Here $\boldsymbol{s}$ is the unit vector parallel to the vector Δv. The angular momentum is $L = r^2\dot{\varphi} = bv_0 = \text{const}$ and $\mathrm{d}t = r^2/L\mathrm{d}\varphi$. We integrate time from $-\infty$ to $+\infty$ (as the particle moves from and to infinite distance); $t = 0$ is the moment of the closest approach of the particle to the central mass. Thus the gravitational interaction covers an infinite time interval. This expression leads easily to the formula for ϑ. Indeed, comparison of (5.2) and (5.6) gives

$$\tan\frac{\vartheta}{2} = \frac{G\mathcal{M}}{bv_0} \, . \tag{5.7}$$

Due to symmetry of the problem we obtain

$$\sum v_\perp = 0 \, . \tag{5.8}$$

The geometrical formula

$$1 - \cos\vartheta = \frac{2}{1 + \tan^{-2}\frac{\vartheta}{2}} \tag{5.9}$$

and equation (5.3) give

$$\Delta v_{||} = 2v_0 \, \frac{1}{1 + \left(\frac{bv_0^2}{G\mathcal{M}}\right)^2} \, . \tag{5.10}$$

This relation concerns the body of reduced mass μ while we ask for the corresponding expression for the body of mass m. It means that we need relation $v_\mathrm{M} = v_\mathrm{M}(v_{||})$. Let $\boldsymbol{r}_\mathbf{m}$ and $\boldsymbol{r}_\mathbf{M}$ be position vectors of the test particle m and the star M, respectively, $\boldsymbol{r}_\mathbf{CM}$ be center of mass – see Fig. 5.1.

Then relations

$$\boldsymbol{r} = \boldsymbol{r}_\mathbf{m} - \boldsymbol{r}_\mathbf{M} \, , \tag{5.11}$$

$$\boldsymbol{r}_\mathbf{M} = \boldsymbol{r}_\mathbf{CM} - \frac{m}{M+m}\boldsymbol{r} \qquad \Big/ \frac{\mathrm{d}}{\mathrm{d}t} \, , \tag{5.12}$$

$$\boldsymbol{v}_\mathbf{M} = \boldsymbol{v}_\mathbf{CM} - \frac{m}{M+m}\boldsymbol{v} \tag{5.13}$$

give

$$\Delta \boldsymbol{v}_\mathbf{M} = -\frac{m}{M+m}\Delta\boldsymbol{v} \, . \tag{5.14}$$

Thus one has

$$\left(\Delta v_{\mathrm{M}\,||}\right)_0 \equiv \left|\Delta \boldsymbol{v}_{\mathbf{M}\,||}\right| = 2\,\frac{m}{M+m}\,v_0\,\frac{1}{1+\left(\frac{bv_0^2}{G\mathcal{M}}\right)^2}\ . \tag{5.15}$$

This gives the final change of the parallel velocity of the star under the influence of a single particle. To obtain the gravitational friction formula, it is necessary to integrate the relation (5.15) over all impact parameters and, generally, over the velocity distribution (see eq. (5.34) for the result).

Homogeneous coherent environment

Considering relation (5.15), one needs to express the frequency of collisions and to estimate the gravitational friction under prescription of a homogeneous coherent environment. Let us remark that the environment may be also isotropic but due to one prominent direction (defined by the velocity vector of the moving mass) we do not express it explicitly. Be N the particle density. The star meets

$$\nu = 2\pi b\,\mathrm{d}b\,v_0 N \tag{5.16}$$

particles per unit time. The drag exerted by particles with impact parameter $b \in (b,\ b+\mathrm{d}b)$ is

$$\left.\frac{\mathrm{d}v_{\mathrm{M}}}{\mathrm{d}t}\right|_{\mathrm{b}} = \left(\Delta v_{||}\right) 2\pi b \mathrm{d}b v_0 N\ , \tag{5.17}$$

which gives (after the integration over all impact parameters):

$$\left|\frac{\mathrm{d}v_{\mathrm{M}}}{\mathrm{d}t}\right| = 4\pi v_0^2 \frac{mN}{M+m}\int\limits_{b_{\min}}^{b_{\max}} \frac{b}{1+\left(\frac{bv_0^2}{G(m+M)}\right)^2}\mathrm{d}b\ . \tag{5.18}$$

A trivial substitution

$$y \equiv \frac{bv_0^2}{G(m+M)} \tag{5.19}$$

gives

$$\left|\frac{\mathrm{d}v_{\mathrm{M}}}{\mathrm{d}t}\right| = 2\pi\frac{G^2 m(m+M)N}{v_0^2}\left[\ln(1+y^2)\right]_{y_{\min}}^{y_{\max}}\ . \tag{5.20}$$

It is obviously adopted $y \gg 1$ and thus $\ln(1+y^2) \approx 2\ln y$. Hence

$$\left[\ln(1+y^2)\right]_{y_{\min}}^{y_{\max}} = 2\ln\left(\frac{b_{\max}}{b_{\min}}\right)\ . \tag{5.21}$$

The transcription into dimensionless variables[1] reads

$$\frac{\mathrm{d}v^*}{\mathrm{d}t^*} = 8\pi 10^{-7}\frac{\xi}{v^{2\,*}}\ln\left(\frac{b_{\max}}{b_{\min}}\right) \tag{5.22}$$

where $\xi = \rho/(1\mathrm{kg.m}^{-3})$.

[1]Dimensionless variables are defined by relations (6.12) $\div$ (6.14).

Chandrasekhar's formula for the dynamical friction

Let us turn back to the relation (5.15). Generally, it is not necessary to think of the coherent environment as cold, with all particles being fixed and moving only with macroscopic velocity against the body, as considered in the previous Section 5.1. On the contrary, we can take test particles with appropriate velocity distribution function $f(\boldsymbol{v}_{\rm m})$ and find the gravitational friction under this scheme.

The necessary step is to express frequency of collisions.

$$\nu_{\rm coll} = 2\pi b \; {\rm d}b \; v_0 f(v_{\rm m}) {\rm d}v_{\rm m} \; . \tag{5.23}$$

The change of velocity of the star due to a single collision is

$$\left.\frac{{\rm d}\boldsymbol{v}_{\bf M}}{{\rm d}t}\right|_{v_{\rm m}\, b} = \left(\Delta v_{{\rm M}\,\|}\right)_0 2\pi b \; {\rm d}b \; \boldsymbol{v}_{\bf 0} f(v_{\rm m}) {\rm d}v_{\rm m} \; . \tag{5.24}$$

Integration over all acceptable b gives

$$\begin{aligned} \frac{{\rm d}\boldsymbol{v}_{\bf M}}{{\rm d}t} &= \frac{4\pi m v_0}{M+m} \boldsymbol{v}_{\bf 0} f(v_{\rm m}) {\rm d}v_{\rm m} \int\limits_0^{b_{\rm max}} \frac{b \; {\rm d}b}{1+\left(\frac{b v_0^2}{G\mathcal{M}}\right)^2} \\ &= \frac{4\pi m v_0 \boldsymbol{v}_{\bf 0}}{M+m} \frac{1}{2} \frac{G^2\mathcal{M}^2}{v_0^4} f(v_{\rm m}) {\rm d}v_{\rm m} \ln\left[1+\left(\frac{b_{\rm max} v_0^2}{G\mathcal{M}}\right)^2\right] \; . \end{aligned}$$

The Coulomb logarithm Λ is defined as

$$\Lambda^2 \equiv \left(\frac{b_{\rm max} v_0^2}{G\mathcal{M}}\right)^2 \tag{5.25}$$

which leads to the expression

$$\frac{{\rm d}\boldsymbol{v}_{\bf M}}{{\rm d}t} = 2\pi m(M+m) G^2 f(v_{\rm m}) {\rm d}v_{\rm m} \frac{\boldsymbol{v}_{\bf 0}}{v_0^3} \ln\left(1+\Lambda^2\right) \; . \tag{5.26}$$

Approximation $\ln(1+\Lambda^2) \approx 2\ln\Lambda$ leads to the

$$\frac{{\rm d}\boldsymbol{v}_{\bf M}}{{\rm d}t} = 4\pi m(M+m) G^2 f(v_{\rm m}) {\rm d}v_{\rm m} \frac{\boldsymbol{v}_{\bf 0}}{v_0^3} \ln\Lambda \; . \tag{5.27}$$

Now, it is necessary to integrate the expression (5.27) over all acceptable velocities in the velocity distribution function $f(v_{\rm m})$. It means that we ask for the integral

$$\frac{{\rm d}\boldsymbol{v}_{\bf M}}{{\rm d}t} = 4\pi m(M+m) G^2 \ln\Lambda \int\limits_{(v_{\rm m})} f(v_{\rm m}) \frac{\boldsymbol{v}_{\bf m} - \boldsymbol{v}_{\bf M}}{|\boldsymbol{v}_{\bf m} - \boldsymbol{v}_{\bf M}|^3} \; {\rm d}v_{\rm m} \; . \tag{5.28}$$

One can use a trick to find solution of the integral (5.28): Gravitational force in the classical Newtonian transcription is rewritten in the form

$$\boldsymbol{F}(\boldsymbol{r}_{\bf 1}) = G \int\limits_{(\boldsymbol{r}_{\bf 2})} \rho(\boldsymbol{r}_{\bf 2}) \; \frac{\boldsymbol{r}_{\bf 1} - \boldsymbol{r}_{\bf 2}}{|\boldsymbol{r}_{\bf 1} - \boldsymbol{r}_{\bf 2}|^3} {\rm d}\boldsymbol{r}_{\bf 2} \tag{5.29}$$

and one looks for the force acting at the point $\boldsymbol{r}_{\bf 1}$ (while $\boldsymbol{r}_{\bf 2}$ is integration variable) which is very similar to the expression (5.28). We consider a spherically symmetric distribution of the matter, and therefore the gravitational force is determined by matter residing inside the corresponding sphere. Applying this well known fact to the integral (5.28), assuming that the distribution of velocities is isotropic and defining the function

$$\rho(v_{\rm m}) = 4\pi m(M+m)Gf(v_{\rm m})\ln\Lambda; \tag{5.30}$$

we obtain

$$\frac{\mathrm{d}\boldsymbol{v}_{\mathbf{M}}}{\mathrm{d}t} = G\int\limits_{(v_{\rm m})} \rho(v_{\rm m})\frac{\boldsymbol{v}_{\mathbf{m}}-\boldsymbol{v}_{\mathbf{M}}}{|\boldsymbol{v}_{\mathbf{m}}-\boldsymbol{v}_{\mathbf{M}}|^3}\,\mathrm{d}v_{\rm m}\ . \tag{5.31}$$

In the Newton gravitational law,

$$\boldsymbol{F} = -\frac{GM(r)}{r^3}\boldsymbol{r} \quad ; \quad M(r) = \int\limits_0^r 4\pi r^2\rho(r)\mathrm{d}r\ . \tag{5.32}$$

Analogously to this we can formally introduce "mass in the space of velocities"

$$M(v) \equiv \int\limits_0^v \rho(v_{\rm m})4\pi v_{\rm m}^2\mathrm{d}v_{\rm m} \tag{5.33}$$

and thus we obtain

$$\frac{\mathrm{d}\boldsymbol{v}_{\mathbf{M}}}{\mathrm{d}t} = -\frac{16\pi^2 m(M+m)G^2\ln\Lambda}{v_{\rm M}^3}\int\limits_0^v f(v_{\rm m})v_{\rm m}^2\boldsymbol{v}_{\mathbf{M}}\mathrm{d}v_{\rm m}\ . \tag{5.34}$$

The expression (5.34) is the Chandrasekhar formula for the dynamical friction.

5.2 Gravitational friction in the slab geometry

The relative velocity of the star with respect to the disc is supposed – see Fig. 5.2

$$\boldsymbol{v_0(x)} = \boldsymbol{v(x)} - \boldsymbol{v_*} \tag{5.35}$$

and the impact parameter b is

$$b = (x-x_0)\sin\alpha = x\,\frac{v_{\rm t0}(x)}{v_0(x)} = x\,\frac{v_{\rm t}(x)-v_{\rm t\,*}}{\sqrt{(v_{\rm t}(x)-v_{\rm t\,*})^2+(v_{\rm r}(x)-v_{\rm r\,*})^2}} \tag{5.36}$$

The expression for dynamical friction is (see, e.g. (1.63), (1.64), or ref. [6])

$$\Delta v_{*\,\parallel} = 2\,\frac{m}{M+m}\,v_0\,\frac{1}{1+\left(\frac{bv_0^2}{G\mathcal{M}}\right)^2}\,, \tag{5.37}$$

$$\Delta v_{*\,\perp} = 2\,\frac{m}{G(M+m)^2}\,bv_0^3\,\frac{1}{1+\left(\frac{bv_0^2}{G\mathcal{M}}\right)^2}\,. \tag{5.38}$$

These expressions can be written down in the matrix form as

$$\begin{pmatrix} \Delta v_{*\,\parallel} \\ \Delta v_{*\,\perp} \end{pmatrix} = 2\,\frac{m}{\mathcal{M}}\,v_0\,\frac{1}{1+\left(\frac{bv_0^2}{G\mathcal{M}}\right)^2}\begin{pmatrix} 1 \\ \frac{bv_0^2}{G\mathcal{M}} \end{pmatrix}\,. \tag{5.39}$$

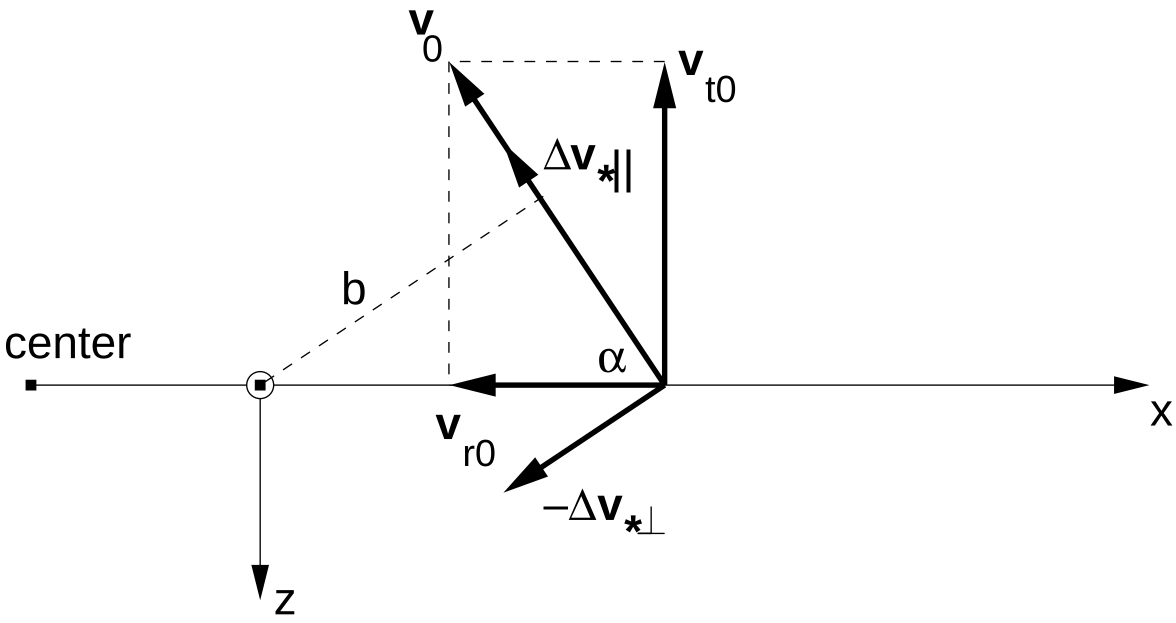

Figure 5.2: A schematic model of the gravitational friction in the thin disc. The massive center of the disc is on the left. Position of the star is denoted with $\odot$ $(x = x_0)$; a test particle is located at the cross-section of vectors; v_0 is relative velocity of the test particle and the star, v_{t0} and v_{r0} are radial and transversal velocities, respectively. $\Delta v_{\star\perp}$ and $\Delta v_{\star\|}$ denote how the star will change its velocity in perpendicular and parallel directions, respectively, via interaction with the test particle.

We remind that $\mathcal{M} = M + m$. The general rotation matrix is

$$\mathbf{M} = \begin{pmatrix} \cos\xi & \sin\xi \\ -\sin\xi & \cos\xi \end{pmatrix} \tag{5.40}$$

while we need to perform rotation around the zero point to transform $(v_\perp; v_\|) \to (v_\mathrm{r}; v_\mathrm{t})$ – see Fig. 5.2. Thus we have

$$\begin{pmatrix} \Delta v_{*\mathrm{t}} \\ \Delta v_{*\mathrm{r}} \end{pmatrix} = \begin{pmatrix} \sin\alpha & -\cos\alpha \\ \cos\alpha & \sin\alpha \end{pmatrix} \begin{pmatrix} \Delta v_{*\,\|} \\ \Delta v_{*\,\perp} \end{pmatrix} \tag{5.41}$$

In our model of the dynamical friction, one considers

$$\begin{pmatrix} \mathrm{d}v_{*\mathrm{t}}/\mathrm{d}t \\ \mathrm{d}v_{*\mathrm{r}}/\mathrm{d}t \end{pmatrix} = \int\limits_{x_0-X}^{x_0+X} \frac{2m}{\mathcal{M}} \frac{v_0(x)}{1+\left(\frac{bv_0^2}{G\mathcal{M}}\right)^2} \begin{pmatrix} \sin\alpha - \frac{bv_0^2}{G\mathcal{M}}\cos\alpha \\ \cos\alpha + \frac{bv_0^2}{G\mathcal{M}}\sin\alpha \end{pmatrix} \nu(x)\mathrm{d}x\ , \tag{5.42}$$

where ν is the frequency of collisions and $x_0 \pm X$ indicate the boundary of integration. It may be supposed

$$\nu(x) = v_0(x)\sin\alpha\,\sigma(x)\ , \tag{5.43}$$

where σ is the particle surface density, x_0 is the instantaneous distance of the star to the center (position of the star is denoted by $\odot$ in Fig. 5.2). Therefore the dynamical friction in the flat disc-like environment may be approximated as

$$\begin{pmatrix} \mathrm{d}v_{*\mathrm{t}}/\mathrm{d}t \\ \mathrm{d}v_{*\mathrm{r}}/\mathrm{d}t \end{pmatrix} = \int\limits_{x_0-X}^{x_0+X} \frac{2m}{M} \frac{v_0(x)}{1+\left(\frac{bv_0^2}{G\mathcal{M}}\right)^2} \begin{pmatrix} \sin\alpha - \frac{bv_0^2}{G\mathcal{M}}\cos\alpha \\ \cos\alpha + \frac{bv_0^2}{G\mathcal{M}}\sin\alpha \end{pmatrix} v_0(x)\sin\alpha\,\sigma(x)\mathrm{d}x\ . \tag{5.44}$$

One should remark that m represents in fact the mass of some virtual test particle. In a realistic situation it is an element of the disc medium which defines the flow at each given place. Of course, such an element is necessarily deformed by differential rotation, nevertheless the adopted view represents a common and widely used approximation: the disc is often modelled as an object composed from many ($\gtrsim 10^3$) coherent (pseudo)-particles (for example, [34, 44]).

Taylor expansion of the integral (5.44)

The integral (5.44) must be solved numerically, nevertheless it is possible to estimate its behavior near to the star (one can put zero point of local Cartesian coordinates (x, y)) – see Figure 5.2 – to $[0,0]$ without any loss of generality).

Taylor's expansion of the velocity v_0 to the first order adopts the form

$$\begin{aligned} v_0(x) &= \sqrt{(v_{\mathrm{t}*}-v_{\mathrm{t}}(x))^2+(v_{\mathrm{r}*}-v_{\mathrm{r}}(x))^2} = \sqrt{(v_{\mathrm{t}*}-v_{\mathrm{t}}(0))^2+(v_{\mathrm{r}*}-v_{\mathrm{r}}(0))^2} \\ &\quad + x\frac{(v_{\mathrm{t}*}-v_{\mathrm{t}}(0))(-v_{\mathrm{t}}^{'}(0))+(v_{\mathrm{r}*}-v_{\mathrm{r}}(0))(-v_{\mathrm{r}}^{'}(0))}{\sqrt{(v_{\mathrm{t}*}-v_{\mathrm{t}}(0))^2+(v_{\mathrm{r}*}-v_{\mathrm{r}}(0))^2}} + \mathcal{O}(2) \\ &= v_0(0) + x\frac{v_0^{'}(0)}{v_0(0)} + \mathcal{O}(2) \ , \end{aligned} \tag{5.45}$$

where $v_0^{'}(0) \equiv -(v_{\mathrm{t}*}-v_{\mathrm{t}}(0))v_{\mathrm{t}}^{'} - (v_{\mathrm{r}*}-v_{\mathrm{r}}(0))v_{\mathrm{r}}^{'}$, and $' \equiv \mathrm{d}/\mathrm{d}x$ Similarly to the (5.45) one can find Taylor's expansion for other variables in the integral (5.44):

$$v_0^2(x) = v_0^2(0) + 2xv_0^{'}(0) \ , \tag{5.46}$$

$$\sin\alpha(x) = \sin\alpha(0) + x\left[-\frac{v_{\mathrm{t}}^{'}(0)}{v_0(0)} - \sin\alpha(0)\frac{-v_0^{'}(0)}{v_0^2(0)}\right] \ , \tag{5.47}$$

$$\sin^2\alpha(x) = \sin\alpha^2(0) + 2x\sin\alpha(0)\left[-\frac{v_{\mathrm{t}}^{'}(0)}{v_0(0)} - \sin\alpha(0)\frac{-v_0^{'}(0)}{v_0^2(0)}\right] \ , \tag{5.48}$$

$$\cos\alpha(x) = \cos\alpha(0) + x\left[-\frac{v_{\mathrm{t}}^{'}(0)}{v_0(0)} - \cos\alpha(0)\frac{-v_0^{'}(0)}{v_0^2(0)}\right] \ , \tag{5.49}$$

$$\Sigma(x) = \Sigma(0) + x\Sigma^{'}(0) \ , \tag{5.50}$$

where

$$\sin\alpha(x) \equiv \frac{v_{\mathrm{t}0}}{v_0(x)} \ , \quad \cos\alpha(x) \equiv \frac{v_{\mathrm{r}0}}{v_0(x)} \ . \tag{5.51}$$

Indices t and r denote transversal and radial coordinates, respectively. Moreover, supposing

$$1 + \left(\frac{bv_0^2}{G\mathcal{M}}\right)^2 \approx \left(\frac{bv_0^2}{G\mathcal{M}}\right)^2 \ , \tag{5.52}$$

the Taylor expansion of the whole integral (5.44) leads to the expression

$$\frac{\mathrm{d}v_{\mathrm{i}*}}{\mathrm{d}t} = 2G^2M^2\int\frac{\xi_{\mathrm{i}}+x\eta_{\mathrm{i}}}{x^2}\mathrm{d}x \ , \tag{5.53}$$

$$\xi_{\mathrm{i}} = \xi_{\mathrm{i}}(v_0(0), v_{\mathrm{t}}(0), v_{\mathrm{r}}(0), \sin\alpha(0), \cos\alpha(0), \Sigma(0)) \ , \tag{5.54}$$

$$\eta_{\mathrm{i}} = \eta_{\mathrm{i}}(v_0(0), v_{\mathrm{t}}(0), v_{\mathrm{r}}(0), \sin\alpha(0), \cos\alpha(0), \Sigma(0)) \ . \tag{5.55}$$

Here index i denotes t and r. ξ and η are constants which can be found from zero terms of Taylor's expansions.

Thus it is apparent that the expression for the gravitational friction is dominated by two terms in the thin disc. The first mode decreases as $\propto 1/x$, while the second one represents well-known Coulombian logarithm $\ln x$. The presence of the logarithmical term evokes a problem with the estimation of the upper integration boundary. A reasonable estimation of this term is possible when it appears in the galactic dynamics problems, but it comes out somewhat more complicated in thin disc-type applications. The gravitational friction of the star migrating through the cluster is described by the frictional drag integrated up to the characteristic radius of the cluster – see [6]. In the present context, one could integrate (5.44) over the whole disc, but this is not possible since assumptions of the model are fulfilled nearby the star only. The curvature of orbits (both of the star and of particles) is small in close neighbourhood where the stellar orbit almost touches paths of test particles. The particles at considerably lower orbits have their orbits diverging quickly away from the stellar one, while those at considerably higher orbits have almost straight-line orbits and the stellar orbit is now too deformed with respect to them, and hence the approximation is invalid as well. Thus we are lead to a compromise: to integrate over a part of the disc and stay close to the initial location.

Chapter 6

Stellar motion in the disc plane

There are three main effects which act on the motion of a body (i.e. a star) embedded in the accretion disc (the orbit of the body is in the plane $z = 0$): the gravitational field, accretion process onto the body, and the gravitational drag. The gravitational field is dominated by the central mass while the gravitational field of the disc is supposed to be a small perturbation. The direct accretion inflow of the gaseous material onto stellar surface should be integrated up to some distance which we have estimated in relation (3.6). Outside this limiting distance one should take into account the gravitational friction. In this Chapter we deal with the dragging of the body embedded in a disc, supposing that $R \ll z \ll r$; the radius R of the body is much smaller then the semithickness of the disc z; the disc is thin with respect to the distance to the center r.

In the first Section we will discuss the deceleration force acting on the star moving through a resistive environment. The problem consists especially in the choice of the resistive coefficient (usually called Γ) because, generally, it depends on physical conditions of the environment — the density of the disc, velocity of the star etc. It is important to say, that the star moves with a supersonic speed – see [21, 51]. It is not easy to find a model of such process and hence all arguments are given with some uncertainty and not as a strict mathematical solution.

The second Section deals with equations of motion of the star in the disc. We write down Lagrangian of the motion and obtain two ordinary differential equations of the second order and then we rewrite them to four equations of the first order. We solve them by the

Runge-Kutta method (Runge – Kutta – Fehlberg 45) or by the Bulirsch – Stoer method. The solution of these equations (6.8) $\div$ (6.11) gives as a result $(r^*, \varphi, r^{*\,\prime}, \varphi')$ (for explanation of variables see (6.12) $\div$ (6.14)). We rewrite these variables into usual variables of celestial mechanics, (a^*, e, ω) – semimajor axis, eccentricity and pericenter longitude, respectively.

In the third Section of this Chapter we discuss various modifications of the model of the disc (disc with the homogeneous and inhomogeneous surface densities and non-Keplerian motion of the material around the center etc.).

6.1 Deceleration force acting on the star

In most cases (either the case of an advection disc, or the case of an extremely eccentric satellite orbit moving in a circular Keplerian disc), the stellar velocity inside the disc is hypersonic (at least at some area of the parameter space; see, e.g., [21, 51]). The resistive force acting on the star is then

$$\boldsymbol{F}_{\rm res} = -\Gamma S \rho v^2 \boldsymbol{e}_{\rm v} \; , \tag{6.1}$$

where ρ is the gas density, S is the (effective) cross-section of the body (see, e.g., [3, 12, 23, 37]). Let v is the absolute value of the relative velocity $\boldsymbol{v} = v\boldsymbol{e}_{\rm v}$ and $\boldsymbol{e}_{\rm v}$ is the unit vector. Γ is a resistive coefficient discussed bellow.

Zurek et al. [86] studied an analogous problem in the case of the oblique passage of the body through the disc. They also estimated the total mass which the body meets along its path in the course of an oblique passage of the body through the disc, and they looked for the mass of the tail which the star tears out of the disc. They find that the mass of the tail is about thousand times greater than the amount of the material which the star accretes. Uncertainties in their estimate follow from the lack of a consistent hydrodynamical model of a hypersonic motion, for which Zurek et al. suppose that turbulent processes behind the star creating a tail of matter. (We recall that we have a hypersonic process and also that the star has a spherical shape so that it is highly 'non-aerodynamical' body. For such combination there is no fully consistent description available.)

Hence it is appropriate to admit also another approach [3, 23, 37], namely, to consider the transit of the star through the disc and the creation of turbulent vortices behind the supersonic star being two quite independent processes. At first, the transiting star creates a tunnel in the gas. The radius of the tunnel is given by the effective cross-section of the passing star. The motion of the star is fast enough that the surrounding gas is not able to react. The second process is a closing of the tunnel due to the viscosity or the pressure gradient (as described in [71]) which creates turbulent vortices and shock waves.

This description leads to a conclusion that the coefficient Γ should be independent of the shape and even velocity of the passing star, and this fact is often admitted in meteoritics (see [12]), leading to reasonable results in that field. Hence we also adopt the above as the first approximation: $\Gamma \approx 1$.

6.2 Equations of motion in resistive environment

The Lagrangian equations of the motion with a non-gravitational deceleration are:

$$\frac{\mathrm{d}}{\mathrm{d}t}\frac{\partial L}{\partial \dot{q}_j} - \frac{\partial L}{\partial q_j} + \frac{\partial R}{\partial \dot{q}_j} = 0 \; , \tag{6.2}$$

where $q_1 = r$ and $q_2 = \varphi$ are radial and transversal components, respectively. The velocity of the star is $v_*^2 = \dot{r}^2 + r^2\dot{\varphi}^2$. The Lagrangian L in the (6.2) reads

$$L = \frac{1}{2}M_* v_*^2 + M_* \tilde{V}(r) \; ; \tag{6.3}$$

where the potential $\tilde{V}(r)$ is the sum of the potential of the central mass and a small perturbation due to the gravitation of the disc (see eqs.$\tilde{(}$6.33) in Sec. 6.2) and R is the Rayleigh dissipative function describing the non-gravitational force. R can be expressed as

$$-\frac{\partial R}{\partial \dot{q}_j} = F_{\mathrm{res}\;,j} \; . \tag{6.4}$$

The Rayleigh dissipative function, introduced by (6.4), acquires the form

$$R = \frac{1}{3}\Gamma S\rho \left[(\dot{r} - \dot{r}_{\mathrm{d}})^2 + r^2\,(\dot{\varphi} - \dot{\varphi}_{\mathrm{d}})^2\right]^{\frac{3}{2}} \tag{6.5}$$

where $\left[(\dot{r} - \dot{r}_{\mathrm{d}})^2 + r^2\,(\dot{\varphi} - \dot{\varphi}_{\mathrm{d}})^2\right]$ indicates the relative velocity of the star and the medium. It is usually denoted v.

The (6.4), (6.5) together with (6.2) & (6.3) gives the resistive deceleration force (6.1). Then, equations (6.1), (6.2) and (6.5) give

$$\ddot{r} \;=\; r\dot{\varphi}^2 - \left.\frac{\partial \tilde{V}}{\partial r}\right|_* - \frac{\Gamma S\rho}{M_*}\sqrt{(\dot{r} - \dot{r}_{\mathrm{d}})^2 + r^2\,(\dot{\varphi} - \dot{\varphi}_{\mathrm{d}})^2}\;(\dot{r} - \dot{r}_{\mathrm{d}}) \; , \tag{6.6}$$

$$\ddot{\varphi} \;=\; -2\frac{\dot{r}\dot{\varphi}}{r} - \frac{\Gamma S\rho}{M_*}\sqrt{(\dot{r} - \dot{r}_{\mathrm{d}})^2 + r^2\,(\dot{\varphi} - \dot{\varphi}_{\mathrm{d}})^2}\;(\dot{\varphi} - \dot{\varphi}_{\mathrm{d}}) \; . \tag{6.7}$$

Here M_* is the mass of the test particle (a star).

Two equations (6.6)–(6.7) of the second order can be converted to four equations of the first order as follows:

$$\dot{r} \;=\; \alpha \; , \tag{6.8}$$

$$\dot{\varphi} \;=\; \beta \; , \tag{6.9}$$

$$\dot{\alpha} \;=\; r\beta^2 - \frac{GM}{r^2} - \frac{\Gamma S\rho}{M_*}\sqrt{(\alpha - \alpha_{\mathrm{d}})^2 + r^2\,(\beta - \beta_{\mathrm{d}})^2}\;(\alpha - \alpha_{\mathrm{d}}) - \left.\frac{\partial V}{\partial r}\right|_* , \tag{6.10}$$

$$\dot{\beta} \;=\; -2\frac{\alpha\beta}{r} - \frac{\Gamma S\rho}{M_*}\sqrt{(\alpha - \alpha_{\mathrm{d}})^2 + r^2\,(\beta - \beta_{\mathrm{d}})^2}\;(\beta - \beta_{\mathrm{d}}) \; , \tag{6.11}$$

where M is the central body mass.

We can introduce new dimensionless variables r^*, t^*

$$r^* \;=\; \frac{r}{\Re} \; , \tag{6.12}$$

$$t^* \;=\; \frac{ct}{\Re} \; , \tag{6.13}$$

$$\Re \;=\; \frac{GM}{c^2} \tag{6.14}$$

(one can see that the gravitational radius of central mass is $R_{\mathrm{G}} = 2\Re$) and rewrite equations (6.8) $\div$ (6.11) to the dimensionless form

$$r^{*'} \;=\; \alpha^* \; , \tag{6.15}$$

$$\varphi' \;=\; \beta^* \; , \tag{6.16}$$

$$\alpha^{*'} \;=\; r^*\beta^{*2} - \frac{1}{r^{*2}} - \mathcal{K}^\star\,(\alpha^* - \alpha_{\mathrm{d}}^*) - \left.\frac{\partial V}{\partial r^*}\right|^* \; , \tag{6.17}$$

$$\beta^{*'} \;=\; -2\frac{\alpha^*\beta^*}{r^*} - \mathcal{K}^*\,(\beta^* - \beta_{\mathrm{d}}^*) \; , \tag{6.18}$$

where

$$
\begin{aligned}
\mathcal{K}^* &= \Im\,\sqrt{(\alpha^* - \alpha^*_{\rm d})^2 + r^{*\,2}(\beta^* - \beta^*_{\rm d})^2}\,, &(6.19)\\
\alpha^* &= \frac{\alpha}{c}\,,\\
\beta^* &= \frac{\Re}{c}\beta\,,\\
\Im &= \frac{\Gamma S \rho \Re}{M_*}\,.
\end{aligned}
$$

and

$$
{}' \equiv \frac{\rm d}{{\rm d}t^*}\,. \tag{6.20}
$$

For a numerical solution of (6.15) $\div$ (6.18) we can use standard methods (Runge-Kutta scheme; cf. [62]) and obtain r^*, φ, $r^{*'}$, $\varphi^{'}$. With these results, it is possible to define dimensionless energy E^* and angular momentum L^* as

$$
\begin{aligned}
E^* &= -\frac{1}{r^*} + \frac{1}{2}\left(r^{*'2} + r^{*2}\varphi'^2\right)\,, &(6.21)\\
L^* &= r^{*2}\varphi^{'}\,. &(6.22)
\end{aligned}
$$

Having [9]

$$
\begin{aligned}
E^* &= -\frac{1}{2\tilde{a}^*}\,, &(6.23)\\
L^{*2} &= \tilde{a}^*(1 - \tilde{e}^2)\,, &(6.24)
\end{aligned}
$$

(where $\tilde{a}^*$ is the dimensionless semimajor axis $\tilde{a}^* = \tilde{a}/\Re$ and $\tilde{e}$ is the eccentricity), we obtain

$$
\begin{aligned}
\tilde{e}^2 &= 1 + 2E^*L^{*2}\,, &(6.25)\\
\tilde{a}^* &= -\frac{1}{2E^*}\,. &(6.26)
\end{aligned}
$$

However, relations (6.25) and (6.26) defined in this way have their geometric meaning in the Newtonian potential only (see e.g. [6]). Here we consider also pseudo-Newtonian correction (see (6.33)) and the effect of hydrodynamical deceleration in the equations of motion. Thus eqs. (6.25)–(6.26) are not appropriate here, and we determine the orbital elements approximatively, using the approach of (osculating) elements instead. These stay almost constant during each single orbit around the central object, and therefore we can determine the maximum and minimum distances of the particle from the center ($r^*_{\rm max}$, $r^*_{\rm min}$) separately for each orbit; Here we defined $a^* = (r^*_{\rm max} + r^*_{\rm min})/2$, $e = (r^*_{\rm max} - r^*_{\rm min})/(r^*_{\rm max} + r^*_{\rm min})$. Thus a and e are determined independently on the form of potential. Differences between ($\tilde{a}^*$, $\tilde{e}$) and (a^*, e) are presented as an example in Fig. 7.19, where the evolution of eccentricities $\tilde{e}$ and e is shown. It is evident that e decreases (as expected) while $\tilde{e}$ oscillates and eventually even diverges. Thus the set of parameters $(\tilde{a}^*, \tilde{e})$ is not acceptable and it is convenient to use (a^*, e) instead of them.

Furthermore, one defines the Laplace vector

$$
\boldsymbol{K}^* \equiv \boldsymbol{r}^{*'} \times \boldsymbol{L}^* - \frac{\boldsymbol{r}^*}{r^*}\,. \tag{6.27}
$$

Since we deal with a two-dimensional problem, $\boldsymbol{L}^* = (0,\ 0,\ L^*_z)$, $\boldsymbol{r}^* = (r^*_x,\ r^*_y,\ 0)$, $\boldsymbol{r}^{*'} = (r^{*'}_x,\ r^{*'}_y,\ 0)$ and hence $\boldsymbol{K}^* = (K^*_x,\ K^*_y,\ 0)$. Two components of the Laplace vector are:

$$
\begin{aligned}
K^*_x &= r^{*'}_y L^*_z - \cos\varphi\,,\\
K^*_y &= -r^{*'}_x L^*_z - \sin\varphi\,.
\end{aligned}
$$

$\boldsymbol{K}^*$ is a constant vector which is always parallel to the semimajor axis. Therefore we can define the longitude of the pericenter[1] ω by

$$\omega = \arctan \frac{K_{\rm y}^*}{K_{\rm x}^*} \,. \tag{6.28}$$

Thus we obtain a procedure for computation of orbital elements

$$(r^*,\ \varphi,\ r^{*'},\ \varphi') \Rightarrow (a^*,\ e,\ \omega) \tag{6.29}$$

and we are able to plot them as functions of time,

$$a^* = a^*(t^*) \,, \tag{6.30}$$

$$e = e(t^*) \,, \tag{6.31}$$

$$\omega = \omega(t^*) \,. \tag{6.32}$$

Approximation of the central body potential

We have to remind that in some presented models we neglected two effects which can be important under some special conditions. At first we neglected any relativistic effects. It is acceptable approximation in a high radial distance but near to the inner edge of the disc this effect can has considerable influence on the evolution of orbital elements. At second we supposed somewhere that the effective cross section of the orbiting star is a constant although we know that it depends on its relative velocity. See, e.g. eqs. (3.6) $\div$ (3.9). As the first step to relativistic generalisation, one can adopt the pseudo-Newtonian approach [56]. We introduce potential $U(r)$ as

$$U(R) \equiv -\frac{GM}{R - R_{\rm G}} \,, \tag{6.33}$$

where $R_{\rm G} \equiv 2GM/c^2$ is the gravitational radius of the central mass. In our dimensionless units it has the form

$$U^*(r^*) = -\frac{1}{r^* - 2} \,. \tag{6.34}$$

We scale lengths with respect to $\Re$ which is $\Re = 1/2 \quad R_{\rm G}$.

In our scheme the radial and the transversal velocities in the disc depend on the Newtonian velocity (see (6.39) $\div$ (6.40)). It is useful to remind that while the classical Newtonian velocity is given as

$$v_\Omega(R) = \sqrt{\frac{GM}{R}} \,, \tag{6.35}$$

in the pseudo-Newtonian potential it is

$$v_\Omega(R) = \sqrt{GM}\frac{\sqrt{R}}{R - R_{\rm G}} \,, \tag{6.36}$$

which gives in our dimensionless units

$$v_\Omega^*(r^*) = \frac{\sqrt{r^*}}{r^* - 2} \,. \tag{6.37}$$

One can easily find that

$$\varphi\text{'} = \frac{1}{\sqrt{r^*}(r^* - 2)} \,. \tag{6.38}$$

[1]The problem is two-dimensional, and ω stands as a formal parameter only. It is however convenient to keep ω because we can use it to describe the time dependence of the orientation of the stellar orbit.

Models of the disc

The potential of the thin disc is defined by the surface density $\Sigma = \Sigma(R, \varphi)$, $R \in (\varepsilon, a)$ (supposing axially symmetric disc we neglect angular parameter φ and write always $\Sigma = \Sigma(R)$ only). In the first part of the thesis we asked for the potential of such disc and presented fully general solution $V(r)$ and $\partial V(r)/\partial r$ for an arbitrary Σ (see (2.30), (2.35) and (2.31)) in the integral form. The integral is solvable for some special models of $\Sigma = \Sigma(R)$ – see (2.51), (2.52), (2.68), (2.69) and (2.71). We adopt two possible models of the disc to the numerical solution of equations of motion: (2.68), describing the potential of the homogeneous disc, and (2.69) as a typical model of the inhomogeneous one. Moreover, the adopted models are readily integrable by the integrators mentioned above. In both of models we suppose the same total mass of the disc.

Another effect to be taken into account is the direct accretion inflow. The material acts on the orbiting star as resistive environment only. To find a solution we employed equations (6.15) ÷ (6.18). The material of the disc moves, in general, with a non-Keplerian velocity (see, e.g. [21, 22, 51]). We considered radial flow of material in the disc (in a way resembling the case of advection models) [22, 51]. A nice feature of this model is that there is a very simple relation between the transversal and the radial velocities of the material. Fukue & Ohna (also Narayan & Yi) [22, 51] set

$$v_{\mathrm{r}}(r) = -\alpha c_1 v_{\Omega}(r) \; , \tag{6.39}$$

$$v_{\varphi}(r) = c_2 v_{\Omega}(r) \; . \tag{6.40}$$

α denotes a dimensionless parameter used by Shakura in [70] to describe the viscosity:

$$\nu = \alpha c_{\mathrm{s}} H \; , \tag{6.41}$$

where c_{s} is the speed of sound and H is the semithickness of the disc. For more details see [21, 63]. Finally, Fukue & Ohna derive

$$\alpha c_1 = 0.4299 \; ,$$

$$c_2 = 0.4371 \, .$$

(see also [51]). For the consistence we admitted these values to the presented model.

Chapter 7

Results and discussion

7.1 Parameters of the model

In previous parts of the thesis we discussed different effects which affect the evolution of orbital parameters of the body infalling down to the disc center. First, it was the gravitational field of the disc (supposed to be much weaker than that of the central mass). Next, we considered the hydrodynamical drag, and, finally, we took gravitational friction into account. The latter processes are both influenced by expected variations of the effective cross-section of the body as a function of the relative velocity in the disc medium. The main aim of the discussion in this paragraph is to summarize mutual importance of these effects and to show the results from the numerical approach for a consistent set of parameters. In this respect, relevant parameters of accretion discs have been discussed in [21, 48, 54, 79, 85, 86], but one should remember that exact values are still unknown.

We assumed that the surface density of the disc was given, and we looked for the corresponding gravitational potential in the way discussed in Part I. (We noticed that relevant expressions can be substantially simplified under the assumption of the homogeneous disc but we did not impose this restriction in general.) The problem was to estimate the absolute value of the surface density or, in other words, to determine Σ_0 in physical units. The current status of the theory allows rather broad range of acceptable values. We decided to adopt those from [21, 48, 85] and we used a mean value of all ρ_0 and Σ_0 as a typical reference value of the required coefficients.

The coefficient $\Gamma S\ \rho\Re/M_*$, which governs the evolution (see eq. (6.19)), acquires a typical value of about 2.0×10^{-6} for the case of homogeneous discs, and it is 10^{-3} for an inhomogeneous disc. It is equivalent to the density of, typically, about $10^{-4} \div 10^{-5}$kg.m^{-3} for the homogeneous disc and to 10^{-2}kg.m^{-3} for the inhomogeneous disc near to its inner edge. The value of the coefficient $4G\Sigma_0$ in the expressions for gradients of discs (see Section 2.3 and equations (2.68), (2.69), (2.71)) is approximately 1.0×10^{-4}. It corresponds to the surface density of the order 10^6kg.m^{-2}. It is the typical value, widely quoted in literature – see, for example, [21, 51].

For the case of a *circular orbit*, the following parameters characterize our choice of parameters:

1. $r^*_{\rm init} = 1000$,
2. $r^{*,}_{\rm init} = 0$,
3. $\varphi_{\rm init} = 0$,
4. $\varphi^{,}_{\rm init} = \sqrt{10}/(10^5) = 3.17 \times 10^{-5}$,
5. $a^* = 1000$,
6. $\varepsilon^* = 8$.

In all simulations we started from initial radial distance $r^*_{\rm init} = 1000$ and we stopped at $r^*_{\rm final} = 10$ which is a bit higher then the inner edge of the disc ($\varepsilon^* = 8$).

The initial set of parameters for *elliptical orbits* have been chosen as

1. $r^*_{\rm init} = 1000$,
2. $r^{*,}_{\rm init} = 0$,
3. $\varphi_{\rm init} = 0$,
4. $\varphi^{,}_{\rm init} = 2.9 \times 10^{-5}$,
5. $\varepsilon^* = 8$,

which correspond to the initial eccentricity (selected initial parameter) $e = 0.19$. The initial semimajor axis is, naturally, different from the initial radial distance ($r^*_{\rm init} = 1000$): $a \doteq 840.3$. It can be seen from the relation

$$r_{\rm max} = (1+e)\, a \ . \tag{7.1}$$

7.2 Tests of the code

To solve eqs. (6.15) ÷ (6.18) we employed a Fortran code with RKF45 integration scheme. (To be specific, we refer to RKSUITE package containing the routines developed by Brankin, Gladwell & Shampine.) Furthermore, in order to check computations and to solve some specific problems we used also the Bulirsch-Stoer algorithm [62].

Analytical estimations

The resistive force of the gaseous environment is assumed in the form

$$F = \Gamma S \rho \, |v_* - v_{\rm d}| \, (\boldsymbol{v}_* - \boldsymbol{v}_{\rm d}) \ . \tag{7.2}$$

(see, e.g., eq. (6.1) or (6.6) ÷ (6.7)). For the case of motion of gas in the disc we assumed (cp. (6.39)÷(6.40))

$$\begin{aligned} v_{\rm rd} &= a\, v_\Omega \ , & (7.3)\\ v_{\rm td} &= b\, v_\Omega \ , & (7.4)\\ v_{\rm r\,*} &= 0 \ . & (7.5)\end{aligned}$$

Thus

$$|v_* - v_{\rm d}| = \sqrt{(v_* - v_{\rm d})^2_{\rm r} + (v_* - v_{\rm d})^2_{\rm t}} = v_\Omega \sqrt{(1-b)^2 + a^2} \ . \tag{7.6}$$

The variation of the energy transfer from the satellite body to the medium depends on the resistive force

$$\begin{aligned} \frac{{\rm d}E}{{\rm d}t} &= -\boldsymbol{F} \cdot \boldsymbol{v}_* & (7.7)\\ &= -\Gamma S \rho \, |v_* - v_{\rm d}| \, (\boldsymbol{v}_* - \boldsymbol{v}_{\rm d}) \cdot \boldsymbol{v}_* & (7.8)\\ &= -\Gamma S \rho \, |v_* - v_{\rm d}| \, (v_*^2 - \boldsymbol{v}_{\rm d} \cdot \boldsymbol{v}_*) & (7.9)\\ &= -\Gamma S \rho v_\Omega^3 (1-b) \sqrt{(1-b)^2 + a^2} & (7.10)\\ &= -\Gamma S \rho (1-b) \sqrt{(1-b)^2 + a^2} \left[\frac{GM}{r}\right]^{3/2} \ ; & (7.11)\\ \frac{{\rm d}E}{{\rm d}t} &= -\Gamma S \rho (1-b) \sqrt{(1-b)^2 + a^2} \left[\frac{GM}{r}\right]^{3/2} \ . & (7.12)\end{aligned}$$

Let us suppose, for the sake of an analytical estimation, the homogeneous density of gas in the disc, $\rho = {\rm const}$. Then one can write

$$\frac{{\rm d}E}{{\rm d}t} = \frac{{\rm d}E}{{\rm d}r} \dot{r} \ , \tag{7.13}$$

so

$$\frac{{\rm d}E}{{\rm d}t} = -\frac{GM}{r^2} \dot{r} \ ; \tag{7.14}$$

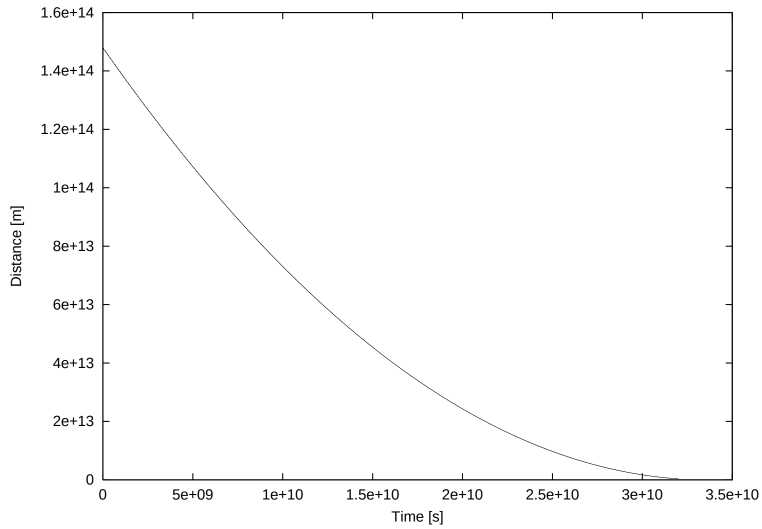

Figure 7.1: Analytical estimation of the infall of a test particle through a disc with non-negligible radial transport of matter.

$$
\begin{aligned}
-\frac{GMm}{r^2}\dot{r} &= \mathcal{K}\frac{1}{r^{3/2}} && (7.15)\\
\dot{r} &= -\mathcal{K}' r^{1/2} && (7.16)\\
\frac{\mathrm{d}r}{\sqrt{r}} &= -\mathcal{K}'\, dt && (7.17)\\
2\sqrt{r} + k &= -\mathcal{K}'\, t && (7.18)\\
\sqrt{r} &= \sqrt{r_0} - \mathcal{C}t && (7.19)\\
& && (7.20)
\end{aligned}
$$

Let us further assume

- The radius of the test particle $r_* = r_\odot = 7 \times 10^8$m;
- The mass ot the test particle $M_* = M_\odot = 2 \times 10^{30}$kg;
- The mass of the central body $M = 10^8 \times M_\odot = 2 \times 10^{38}$kg;
- The density of the disc $\rho = 10^{-5}$kg.m^{-3} = const;
- The transversal and radial components of velocity of the disc are $v_\mathrm{t} = 0.43 v_\Omega$ and $v_\mathrm{r} = 0.43 v_\Omega$;
- The initial distance of the test particle $r_\mathrm{init} = 5 \times 10^2 R_\mathrm{G} = 1.48 \times 10^{14}$m;
- Let the initial orbit of the test particle be circular.

Under the presented parameters, the analytical estimation gives the picture of infall as shown in Fig. 7.1.

The graph comes out different from those presented bellow in the next Chapter. It is due to the initial parameters: we suppose ρ = const while in the most of the numerical models we adopt either Σ = const or Σ is polynomial (in both assumptions it is not necessary to have ρ = const).

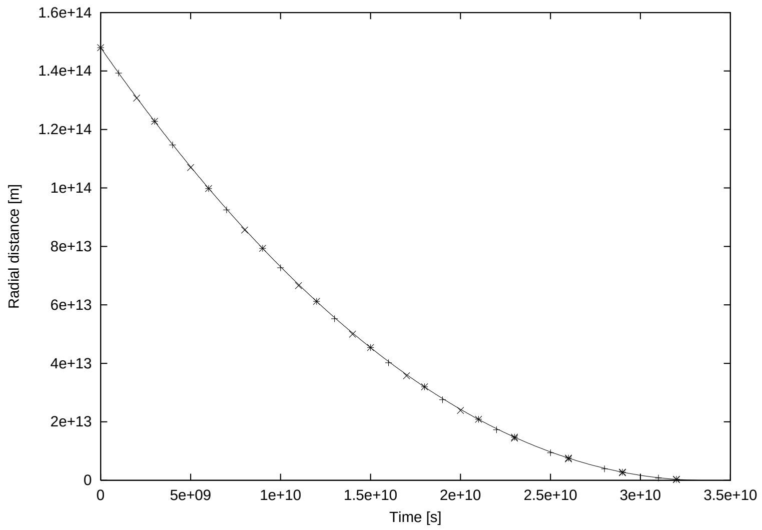

Figure 7.2: Comparison of the results regarding the infall process, as computed via different routines. The solid line denotes the analytical order-of-magnitude estimation (described in the text); stars $*$ denote the Runge-Kutta solution with a C++ code, $+$ crosses indicate the Runge-Kutta scheme in a Fortran code, while $\times$ crosses refer to the Bulirsch-Stoer scheme (also Fortran).

Comparisons of different numerical methods

As another test of accuracy of the numerical method (Runge-Kutta) we compared the solution of the considered differential equation within the framework of different computational schemes (see the list of parameters in the previous Section):

- The solution via Runge-Kutta (Fortran code);
- The solution via Runge-Kutta (code in C);
- The solution via Bulirsch-Stoer scheme.

In three independent codes we used as input the same initial parameters, and we compared the results. All the obtained results are in mutual agreement, as illustrated in Fig. 7.2, and they are also compatible with those presented in the above-given analytical estimation.

7.3 Numerical computations

Homogeneous and inhomogeneous discs

Here we discuss two inter-related effects which influence gradually decaying orbits: surface-density profile of the disc medium, and the initial shape (esp. eccentricity and semimajor axis) of the embedded trajectory of a satellite. We indicate that appropriate density profiles may tend to enhance initially small orbital eccentricity.

In Figure 7.3 we show the evolution of the semimajor axis for the case of a homogeneous disc with an initially *circular* orbit of the infalling star. For the better orientation we list relevant parameters of Fig. 7.3 in the table 7.1.

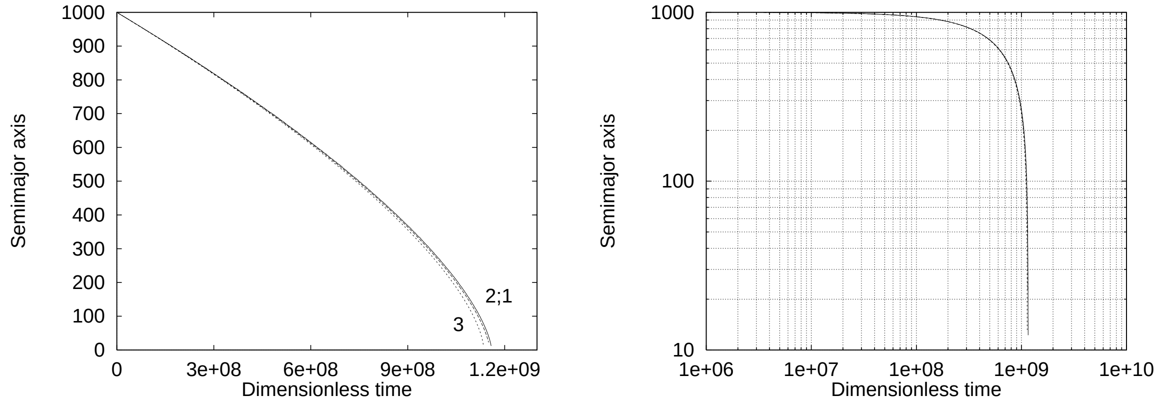

Figure 7.3: Radial distance (characterized in terms of semimajor axis) of the infalling star moving inside the homogeneous disc on an initially circular orbit. Left panel: a linear scale; right panel: a logarithmic scale (in the latter graph, a knee is clearly visible where rapid decay of the orbit starts). Constant and variable cross-section, and Newtonian/pseudo-Newtonian effects are accounted. Different cases are distinguished by different line styles in the plot (see further explanations in the text).

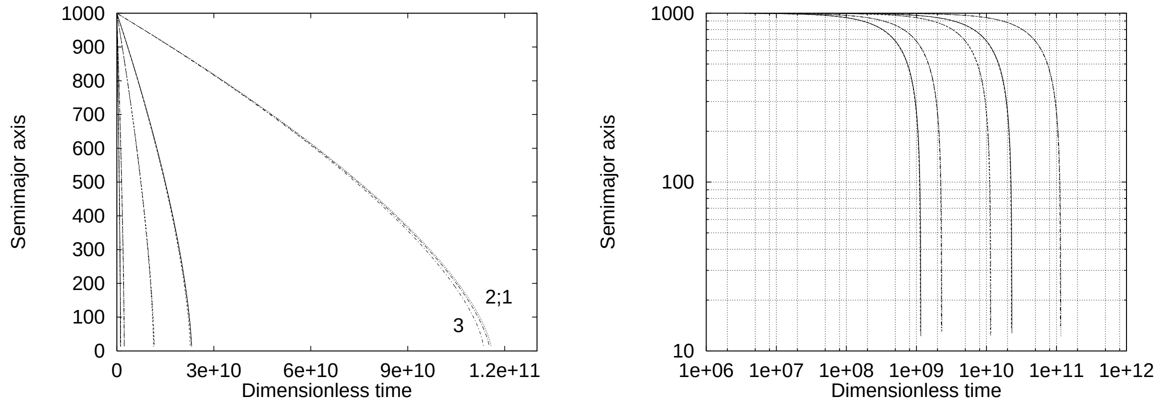

Figure 7.4: The same as in Fig. 7.3; five different values of surface density ($\Sigma = \text{const}$*) are taken into account in the range* $1 \div 100$.

Here the first column denotes the number of the corresponding curve in Figure $(1 \div 3)$; the second column indicates whether the effective cross-section of the star varies with the relative velocity of the star and the disc medium, or whether it is assumed constant; the third column concerns the form of potential of the central mass. Variations of the effective cross-section of the star are quite small and may be neglected in most of the adopted models.

Figure 7.4 compares the same models for five different surface density values, $\Sigma_0 = \text{const}$, which span over the range $10^2 : 1$. The infall times vary in the same proportion for all cases, and hence the infall time turns out to be indirectly proportional to Σ_0.

Figure 7.5, in correspondence with Fig. 7.3, shows the evolution of semimajor axis (of course, in the degenerate case of a circularized orbit, the graph of a comes out identical with the radial distance of the satellite). Here, the inhomogeneous disc model was adopted with $\Sigma \propto R^{-1}$. Numbers of curves are the same as in Fig. 7.3.

Similarly to Fig. 7.4, in Fig. 7.6 the graph is constructed for different values of the inner surface density Σ_0 (here we use three values in the range $10 : 1$), the inhomogeneous disc, and the initially circular orbit of the star. (The description of all curves is the same as in Fig. 7.3.)

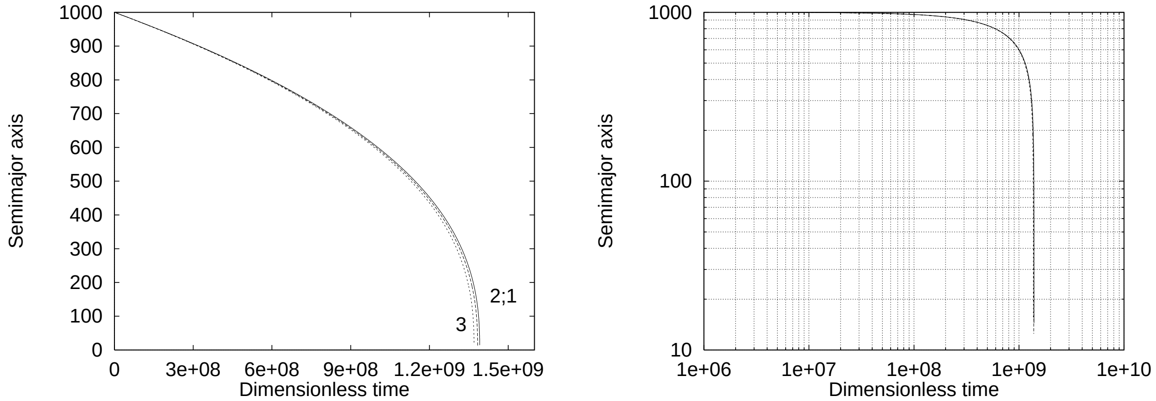

Figure 7.5: The orbital evolution of the star initially placed on a circular orbit, moving inside the inhomogeneous disc. Compare with Fig. 7.3 to reveal qualitatively similar though slightly different profile of the orbital evolution.

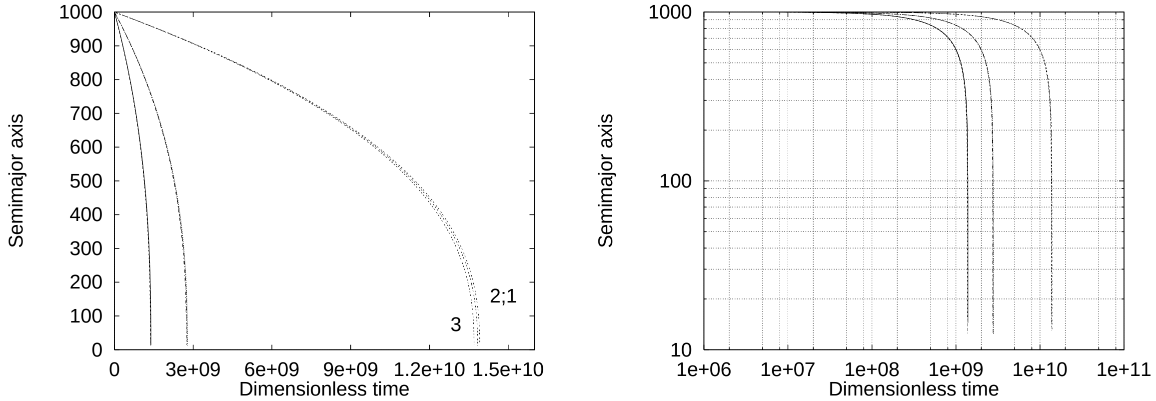

Figure 7.6: A similar model as in Fig. 7.5 is shown for several values of surface density Σ_0 near the inner edge.

Comparison of the homogeneous and inhomogeneous discs is provided in Figure 7.7, where the evolution of an initially circular orbit is shown with respect to the two disc models. As can be seen, the infall time is somewhat longer in the case of the inhomogeneous disc; the outer parts of the inhomogeneous disc have very low density and hence the infall velocity is small, however, the inner part of the disc acquires high density (in comparison with the homogeneous disc) and thus the radial component of velocity gets also sharply increased. Again, the description of individual curves remains similar as in Fig. 7.3 and it is supplemented by Tab. 7.2; Numbers $1 \div 3$ concern the homogeneous disc, $4 \div 6$ concern the inhomogeneous one.

Furthermore, the same comparison as in previous Figure is constructed also in Fig. 7.8, however, different values of the inner surface density Σ_0 have been adopted.

No.	$S \equiv S(v)$	$V(r)$
1	No	Newtonian
2	Yes	Newtonian
3	Yes	pseudo-Newtonian

Table 7.1: The case of the homogeneous disc. See Fig. 7.3.

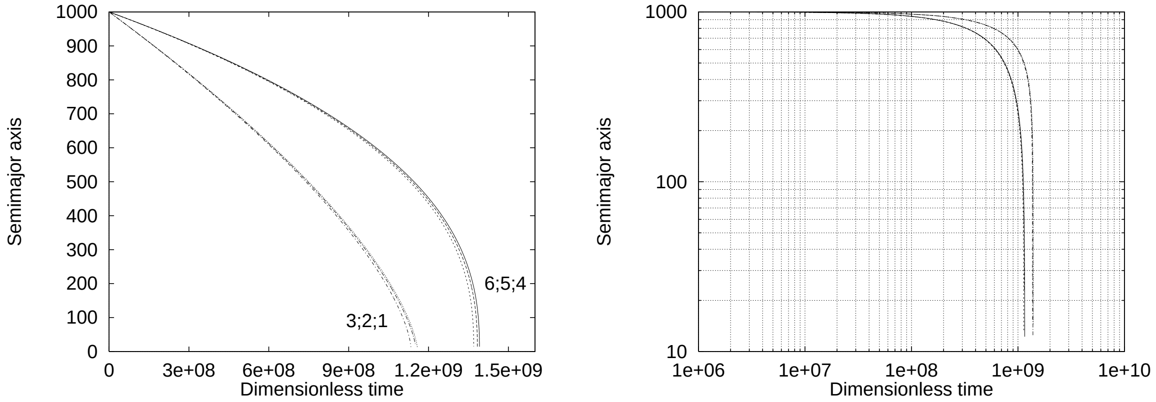

Figure 7.7: The evolution of circular orbits: a comparison between homogeneous and inhomogeneous discs.

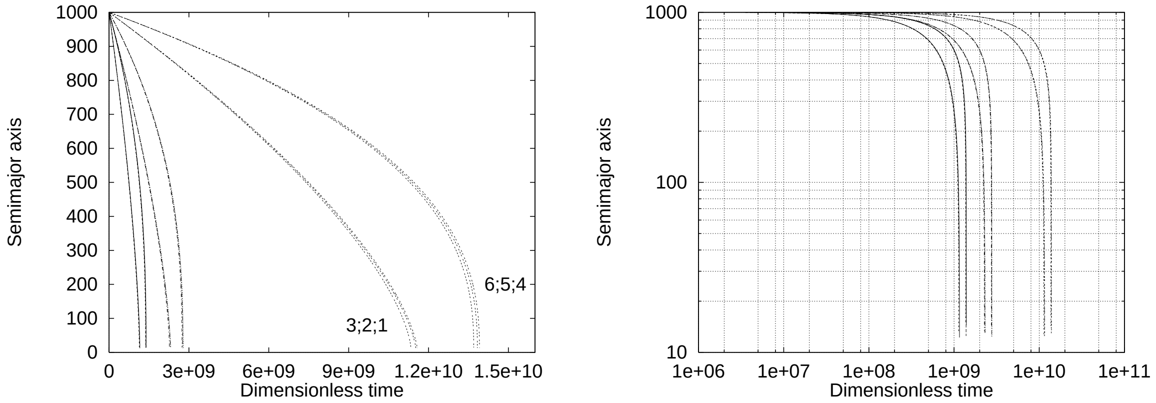

Figure 7.8: A similar model as in Fig. 7.7 for different values of inner surface density.

The evolution of the semimajor axis of the star moving through the homogeneous disc under initially *elliptical* orbit is shown in Fig. 7.9. The situation here is analogous to that in Fig. 7.3. For the explanation of the curves, see also Tab. 7.3.

The same situation as before (see 7.9) is treated also in 7.10 where three different surface densities are adopted. Similarly to the graph 7.9, the model is explored of the inhomogeneous disc in Figure 7.11, and three different surface densities are used in Figure 7.12. The inner surface densities are supposed to be in range 10 : 1 and the infall times appear to vary over the same range. These graphs are to be compared with corresponding Figures 7.4, 7.6, 7.8, and 7.10.

In Fig. 7.13, another comparison of the infall process is shown between the homogeneous and inhomogeneous models of the disc. As it is seen, there exists a difference between circular and elliptical initial orbits; cp. Fig. 7.7. In the model of the initially elliptical orbit, the infall

No.	$S = S(v)$	V
1; 4	No	Newtonian
2; 5	Yes	Newtonian
3; 6	Yes	pseudo-Newtonian

Table 7.2: Comparison of homogeneous and inhomogeneous discs – see Fig.7.7.

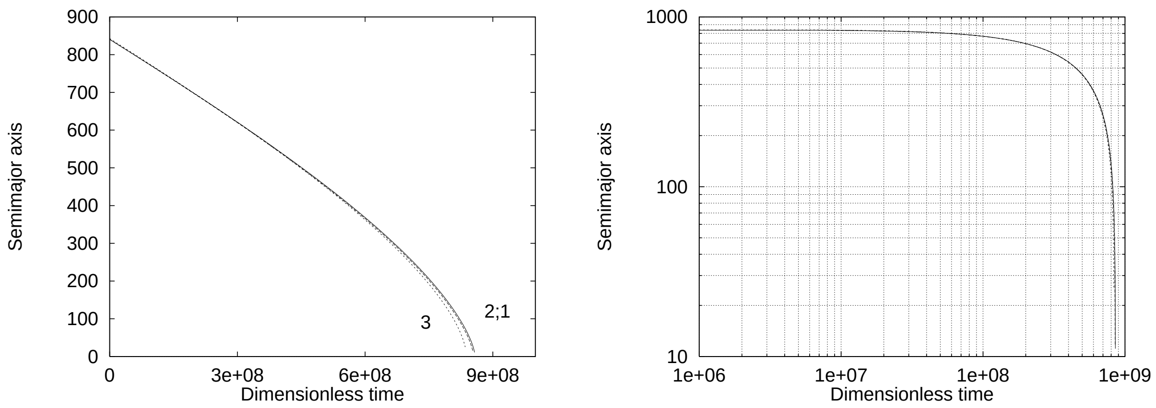

Figure 7.9: The evolution of the semimajor axis of an infalling body moving inside the homogeneous disc (initially elliptical orbit). The initial situation is similar to the one captured in Fig. 7.3. Again, the results are plotted in linear (left) and logarithmic (right) scales for comparison.

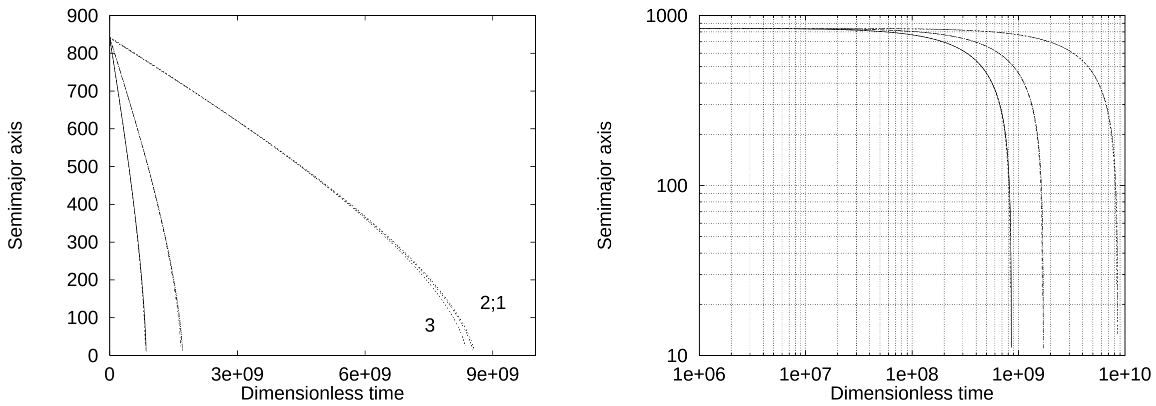

Figure 7.10: The evolution of the semimajor axis of the star moving through the homogeneous disc with several different surface densities. Similar description of curves as in Fig. 7.9 holds.

time of the inhomogeneous model is a bit shorter in comparison with the homogeneous disc case, while the shapes of all curves are quite similar. The root of these effects is in the difference of the decelerating force in apoastron *versus* periastron. While this behaviour can be understood in terms of relative velocities in a purely homogeneous disc, one has to consider also the effect of density variations in the model of the inhomogeneous disc. The two influences are inter-related with each other. (The net effect can be traced to an arbitrary value of the inner surface density.) This conclusion is rather transparent from Fig. 7.14.

No.	$S = S(v)$	V
1	No	Newtonian
2	Yes	Newtonian
3	Yes	pseudo-Newtonian

Table 7.3: The case of the initially elliptical orbit – see Fig. 7.9.

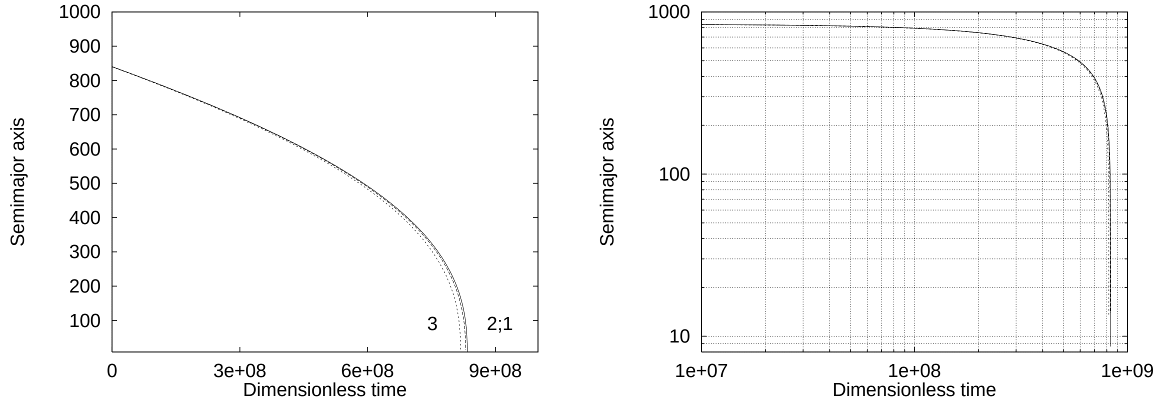

Figure 7.11: Similarly to Fig. 7.9, semimajor axis as a function of dimensionless time. However, the inhomogeneous disc is considered here.

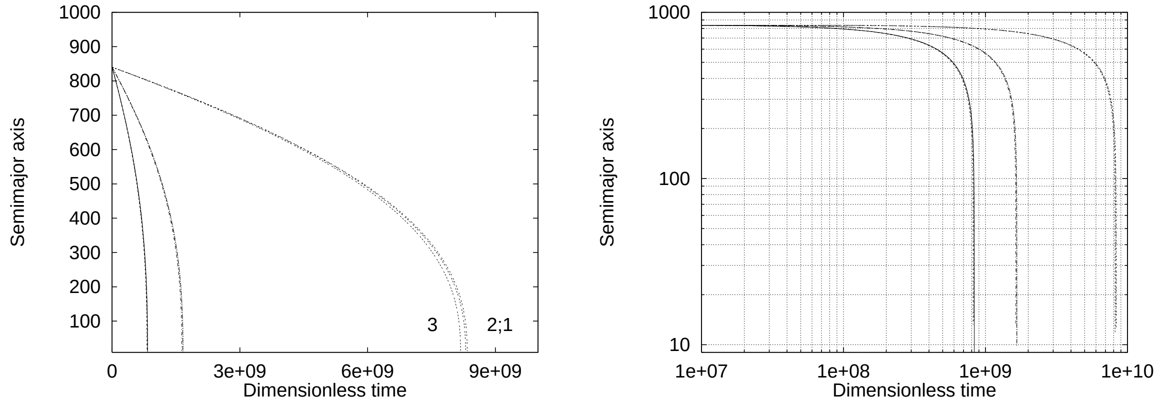

Figure 7.12: The corresponding model as in Fig. 7.11. Initially elliptical orbit of the star moving through an inhomogeneous disc. Different values of Σ_0 are shown.

Variations in the effective cross-section

Another question to be discussed is the problem of the effective cross-section. The rate of accretion depends on the relative velocity as in eqs. (3.7) $\div$ (3.9). From there, division by the term ρv gives immediately the *effective cross-section* depending on the relative velocity. The process of sinking of the satellite body with variable cross-section is explored in Figures 7.3 $\div$ 7.16.

We can see that varying effective cross-section leaves its imprints even at large radial distances (order of $10^2\ R_{\rm G}$). Both velocities (velocity of the star and velocity of the disc) are of the same order and hence the effective cross-section is large, and the resistive force as well. The curve of the radial distance comes out decaying more rapidly than in the case of constant $S_{\rm effective}$. As the relative velocity increases, the *effective* cross-section of the star runs over the corresponding *geometrical* cross-section (which is fixed, $S_{\rm geom}$ = constant) and hence both curves are similar to each other in their corresponding parts.

The relative difference between two presented models (S is constant or variable), as could be seen in the decay of the semimajor axis, is limited to $2 \div 3\%$ on large radial distances. Thus, in most of cases, one can assume $S = S(v) = \text{const}$ without any substantial loss of accuracy.

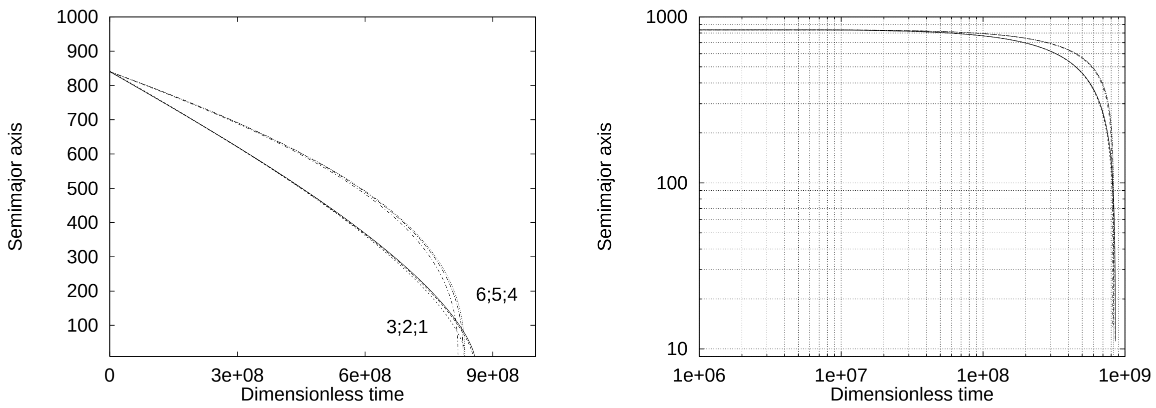

Figure 7.13: Comparison of the infall process for the homogeneous (curves 1 ÷ 3) and inhomogeneous (curves 4 ÷ 6) discs. Three curves in both models of the disc represent three discussed approximations, as described with Fig. 7.11.

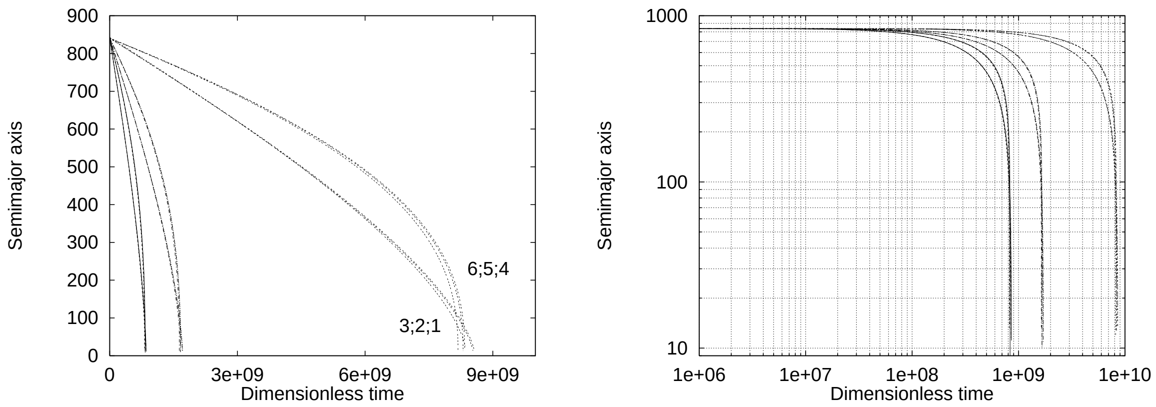

Figure 7.14: The influence of homogeneous vs. inhomogeneous surface density profiles on the evolution of semimajor axis.

Pseudo-Newtonian effects

Figures 7.17 ÷ 7.19 offer a comparison of the classical (Newtonian) and the pseudo-Newtonian effects acting orbital parameters. As expected, these effects are negligible on large radial distances and they are observable near to the central body only.

Indeed, very considerable effect can be seen in Fig. 7.19 (left panel) which is supposed to give an illustrative example of the effect by showing the evolution of eccentricity. The tendency to orbital circularisation decreases at high and mean radial distances (despite some oscillations) but at low radial distance one can observe a sharp divergence of the eccentricity for the pseudo-Newtonian model. The reason for this behaviour is that formulae (6.25) ÷ (6.27), used for the calculation of the orbital elements (eccentricity in particular), are suitable only in Newtonian potential, $\propto 1/R$. In the pseudo-Newtonian approximation we assume the potential proportional to the $1/(R - R_{\mathrm{G}})$ and hence we have to use a different approach in the calculation of eccentricity. To that purpose we we find the maximum and the minimum distances from the center during each revolution, and we express eccentricity as

$$e \approx \frac{r^*_{\max} - r^*_{\min}}{r^*_{\max} + r^*_{\min}} \, . \tag{7.21}$$

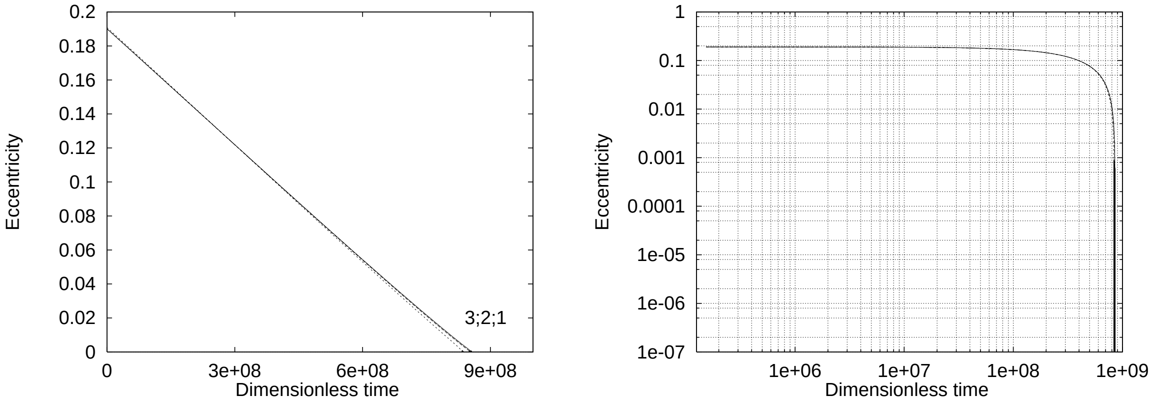

Figure 7.15: Eccentricity of the elliptical orbit in the homogeneous disc.

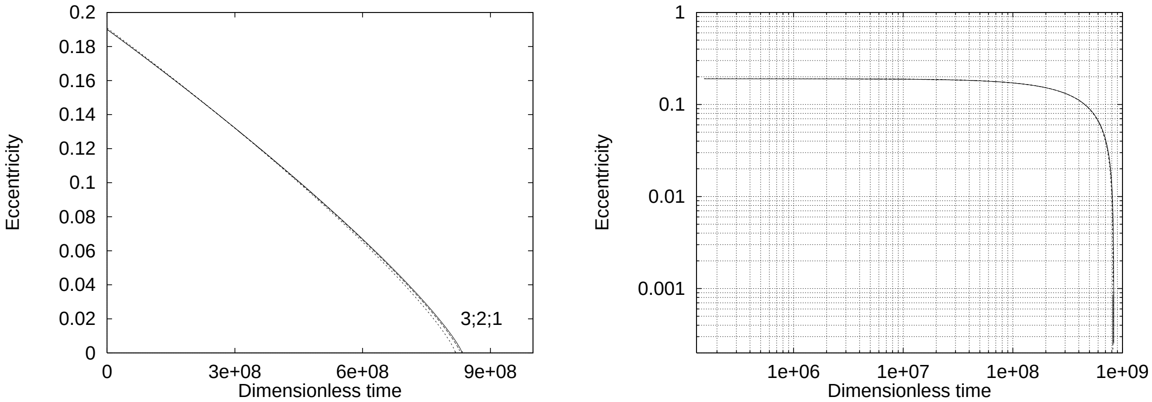

Figure 7.16: Eccentricity of the elliptical orbit in the inhomogeneous disc.

Effects of deceleration

It can be illustrative to find the influence of the disc potential on stellar orbits. Having

$$V = V_{\text{central mass}} + V_{\text{disc}} \ , \tag{7.22}$$

we expect that circular orbits in the potential of the central mass will be deformed under the influence of the potential of the disc. These effects are demonstrated in Figures 7.17 $\div$ 7.18.

Fig. 7.17 (left panel) can be considered as a typical illustrative case which we obtained numerically. We started with a circular orbit in the potential of the central body only, and we looked for its perturbed shape under the influence of the potential of the disc. We supposed that the disc acts with the gravitational force only (without any resistive deceleration). One can see the shape of the orbit in the case of the homogeneous disc with constant of proportionality $4G\Sigma_0 a$ (in our dimensionless units it is equal to 4.0×10^{-2}). This corresponds to high surface density but the value was chosen in order to be able to visualize the deformation of the orbit. In the right panel, a more realistic case is considered with the constant equal to 4.0×10^{-4}. Fig. 7.18 shows the equivalent situation in the case of the inhomogeneous disc.

We can introduce also the dragging of the longitude of the pericenter, ω, although the adopted definition is somewhat formal because it was derived for $1/R$ potential, while we consider a perturbed non-Newtonian potential here. Graphs of ω is shown in Figure 7.19 (right panel) where continuous dragging of the ellipse is clearly visible. One can also notice sudden dips which are typical for the motion in (slightly) non-spherical field.

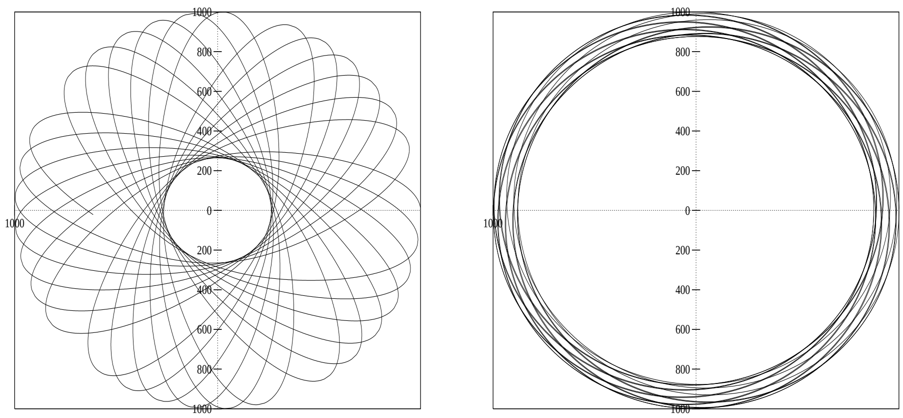

Figure 7.17: Left: An initially circular orbit in the potential of the central mass and the homogeneous disc. No deceleration force is accounted. Right: The same situation as in the left panel, but for the disc with low surface density.

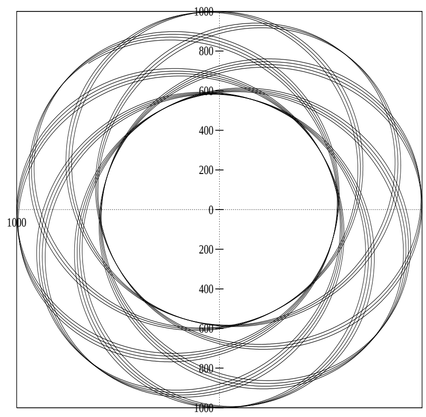

Figure 7.18: As in the previous Figure, but for the inhomogeneous disc.

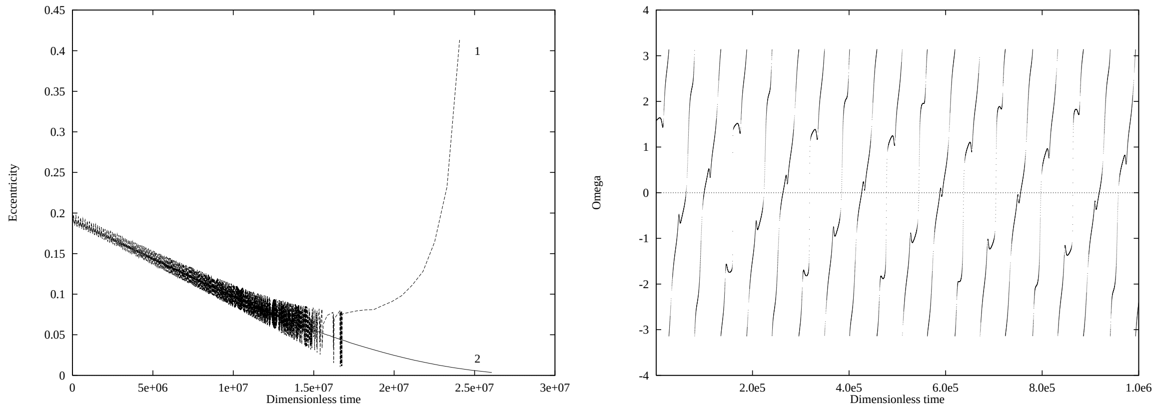

Figure 7.19: Left: An illustrative graph showing eccentricity of the initially elliptical orbit. Variables $\tilde{e}$ (1) and e (2) are plotted (cf. Section 6.2). A sharp increase of the curve 1 occurs at late stages when the satellite is very close to the center and the approximation of osculating elements becomes inaccurate. Right: Dragging of the longitude of the pericenter via resistive deceleration in the disc.

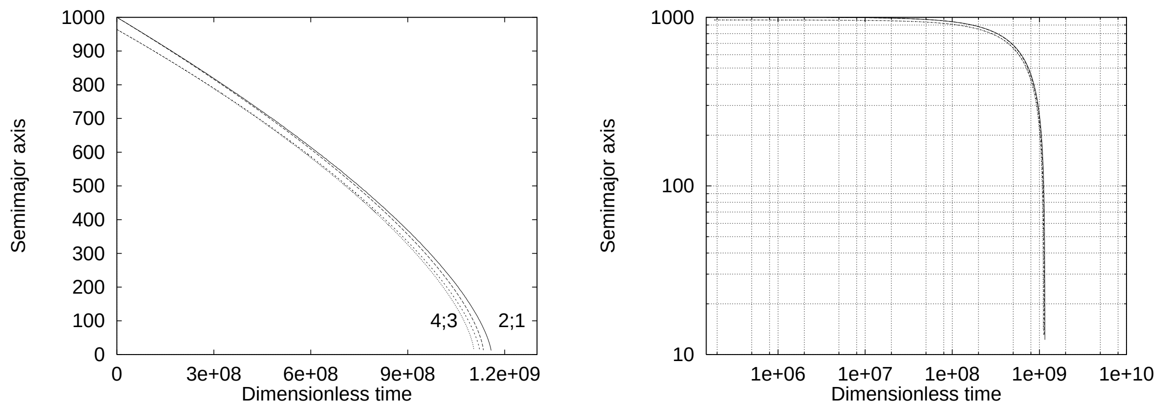

Figure 7.20: Radial distance of a sinking star inside the homogeneous disc. An initially circular (in terms of the gravitational field of the central mass) orbit was considered. The linear scale (left) and the log-log scale (right) are both shown for comparison. The gravitational influence of the disc is accounted, and the corresponding graph for the model without gravitation of the disc is also plotted.

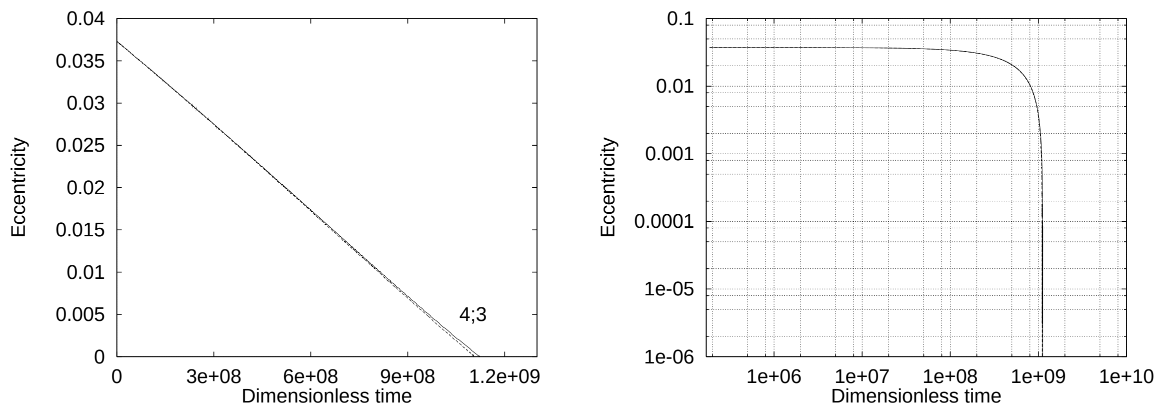

Figure 7.21: The evolution of eccentricity under the same conditions as in Fig. 7.20.

The case of a massive disc

In this paragraph we concentrate on the gravity of the disc as a special agent in the discussion of the stellar motion through the disc. Really, the gravitational field of the disc plays a role which should not be ignored when star migration is explored. We mention the models with and without the influence of gravitational field of the discs.

In Figures 7.20 and 7.21 we present the evolution of the semimajor axis and the eccentricity of the star moving through the homogeneous ($\Sigma = \text{const.}$) disc along the initially *circular* orbit. As expected, the disc deforms the curves of osculating elements of the body. The osculating circle is transformed to an ellipse with non-zero eccentricity (see 7.21), and the radial migration is more rapid. Similar model for the inhomogeneous disc is shown in Figures 7.22 $\div$ 7.23.

Correspondingly to the case of initially circular orbit, models with *elliptical* orbits are plotted in graphs 7.24 $\div$ 7.27. We give the evolution of semimajor axes and eccentricities for the motion through the homogeneous and inhomogeneous discs again. See the Tab 7.4.

Here the first column is the sequential number of the curve, the second column denotes whether the potential of the disc is accounted, and the third column specifies the form of the central mass potential.

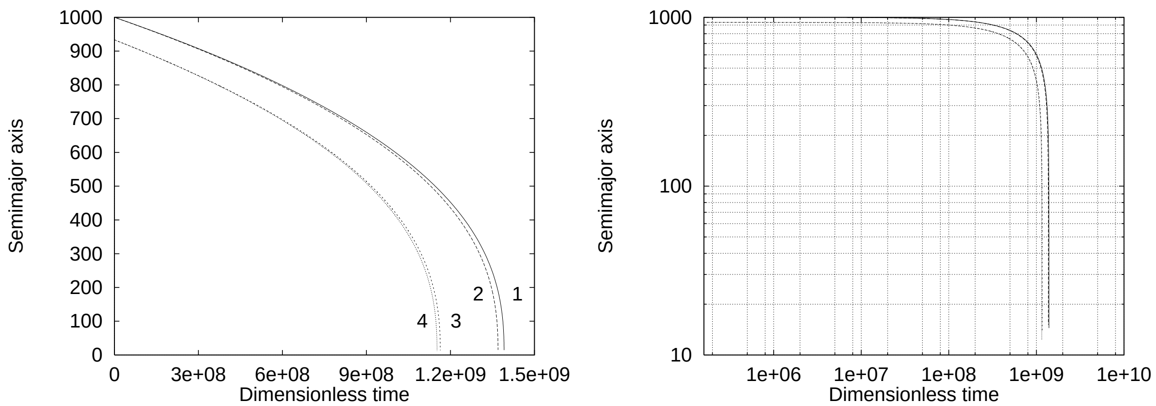

Figure 7.22: Radial distance of the satellite star infalling in the inhomogeneous disc. Cp. Fig. 7.20.

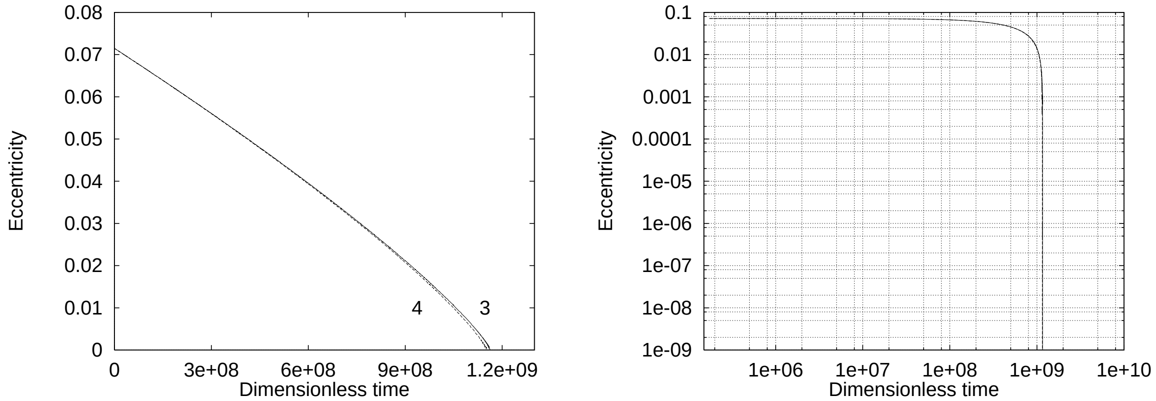

Figure 7.23: Eccentricity as a function of dimensionless time. The situation here is equivalent to that in Fig. 7.22.

One can see an interesting difference between circular and elliptical orbits. The perturbation driven by the disc on the elliptical orbit of a star is more considerable then that acting on a circular orbit. The gravitational perturbation at a given instant is dominated by the mass enclosed under the corresponding radius, and for that reason, supposing near-to-circular orbits, the perturbation is almost constant and the cumulative effect along the whole revolution is tiny. Moreover, the mass of the disc is much less than that of the central body, and hence the path of the star is only slightly perturbed. On the other hand, the elliptical orbit of the star evokes different perturbations near to the apocentra and pericentra of the path due to different masses enclosed bellow the star. Accumulation leads to presented graphs.

The gravitational potential of the disc, as an additional field to the potential of the central mass, leads to the distortion of osculating orbital parameters of the infalling body. This effect

No.	$V_{\rm disc}$	$V_{\rm central\ mass}$
1	No	Newtonian
2	No	pseudo-Newtonian
3	Yes	Newtonian
4	Yes	pseudo-Newtonian

Table 7.4: Effects of the gravity of discs – see Fig. 7.24.

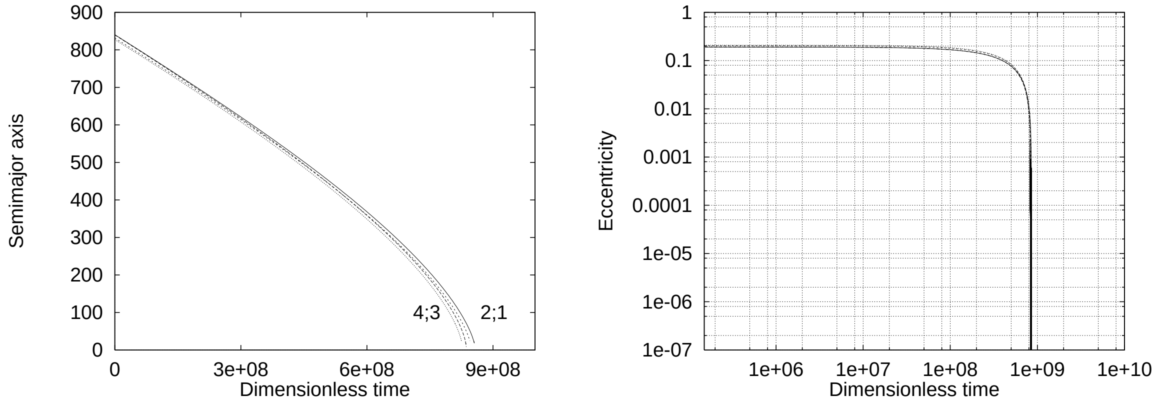

Figure 7.24: Semimajor axis of the star migrating through the homogeneous disc on an elliptical orbit. Comparison is shown for the model with and without gravitation of the disc.

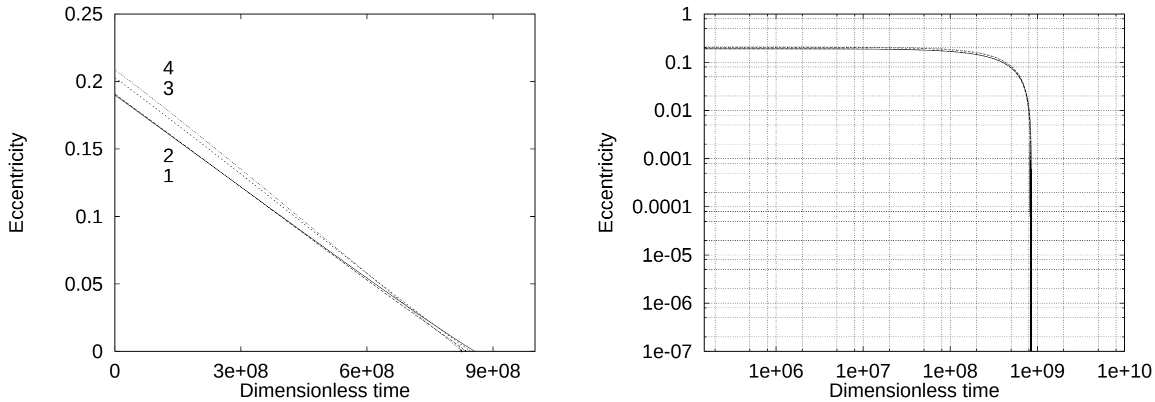

Figure 7.25: Eccentricity of the stellar orbit from Fig. 7.24

is seen both in semimajor axes and eccentricities (Figures 7.20 $\div$ 7.27). In our example, the circular orbit is distorted to an elliptical shape with the semimajor axis $a = 1000 \to a = 964.0$, resp. $a = 1000 \to a = 933.3$ for the homogeneous and inhomogeneous discs, respectively. The eccentricity of the orbit is modified from zero to 0.037, resp. 0.072. The orbital parameters of elliptical orbit are changed as follows:

1. homogeneous disc – $a = 840.3 \longrightarrow 831.3, \quad e = 0.19 \longrightarrow 0.203.$

2. inhomogeneous disc – $a = 840.3 \longrightarrow 807.7, \quad e = 0.19 \longrightarrow 0.238.$

It is possible to find new initial tangential velocity ${\varphi^*}'$, corresponding to the same initial semimajor axis as the one without gravitational field of the disc. The new tangential velocity has to be greater then the corresponding value with the disc neglected. It means that we can reconstruct circular and elliptical orbits with the same initial parameters a, e in the new non-Newtonian potential $V = V_{\text{central mass}} + V_{\text{disc}}$. These new graphs are shown in Figures 7.20 $\div$ 7.27. As can be seen, the infall time is longer for the model with the additional potential of the disc. The effect is stronger for the model of the homogeneous disc while the field of the inhomogeneous disc leads to a minimum difference of infall times; see, for comparison, Fig. 7.28 and 7.29, or 7.30 and 7.32. The curve No. 1 always denotes a model with gravitation of the disc accounted, while the curve No. 2 denotes a model without the disc gravity.

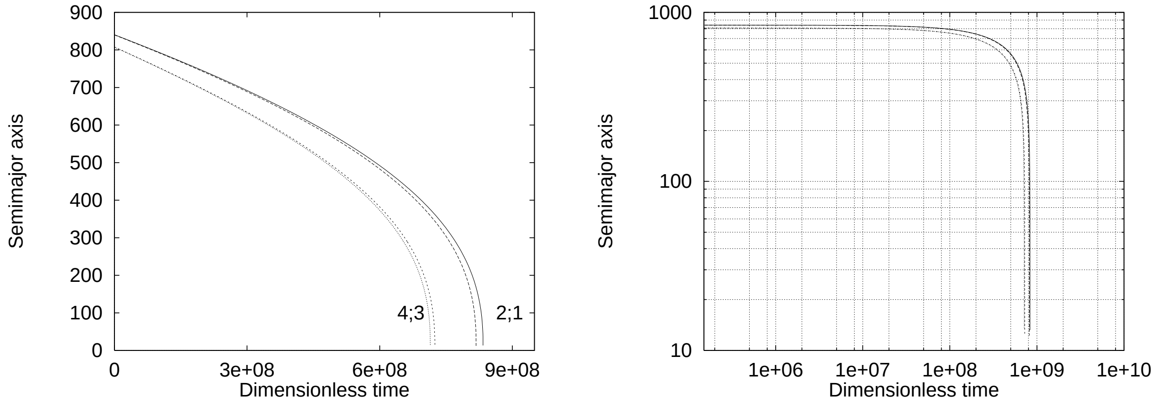

Figure 7.26: Semimajor axis of the star migrating through the inhomogeneous disc on the elliptical orbit. Comparison for the model with and without the gravitation of the disc is shown.

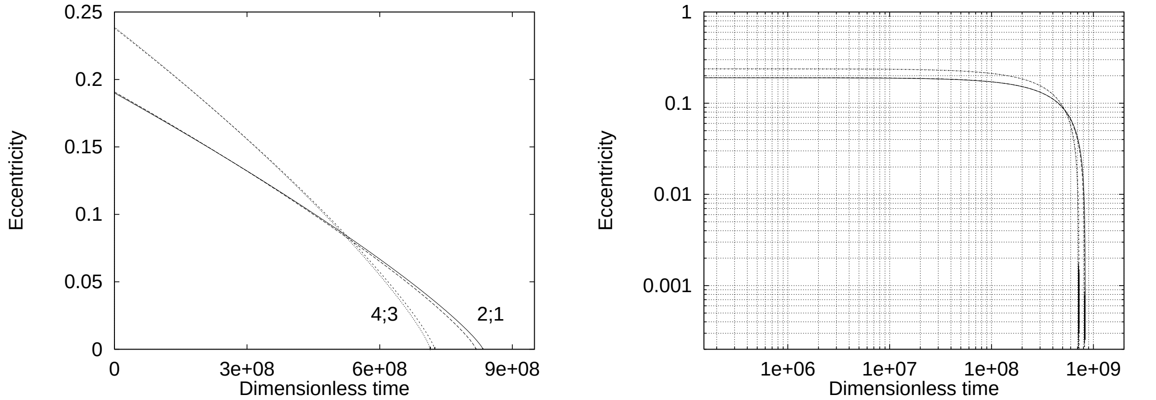

Figure 7.27: Eccentricity of the stellar orbit for the previous model.

Effects of gravitational friction

The gravitational drag is a specific effect which increases logarithmically with size of the system, and hence it is necessary to estimate an upper boundary for integrations. Supposing, for example, transit of a body through a stellar cluster, it appears natural to integrate up to characteristic radius of the cluster. Similarly, supposing the transit of a star inside the disc medium it should be quite natural to integrate over whole disc. Unfortunately, the boundary conditions do not allow such complex integration as the disc is too irregular object. It is neither isotropic nor homogeneous. Close to the moving body it is possible to assume the parallel velocity vectors of gas particles (representing the disc material), but far from the body this approximation breaks down as the curvature of orbits (star and particles – with respect to each other) increases. Thus it is necessary to find a compromise and integrate up to some reasonable upper bound.

We divided the contribution to gravitational friction in two modes. At first, in the close neighbourhood of the star we approximate the medium as homogeneous isotropic environment. Supposing the thin-disc mode of the accretion disc with typical semithickness of order $H/R \sim 10^{-2} \div 10^{-3}$, and integrating up to the H as an upper bound, it is possible to neglect inhomogeneities of the medium. One can find that typical value of the logarithm is

$$\ln\left(\frac{b_{\max}}{b_{\min}}\right) \leq 10 \ , \tag{7.23}$$

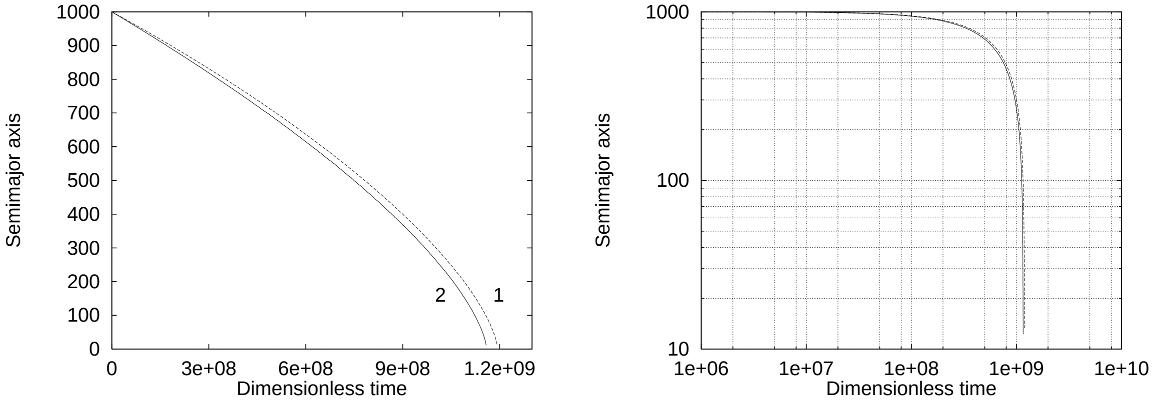

Figure 7.28: The evolution of semimajor axis of a circular orbit with [1] and without [2] the gravitation of the homogeneous disc.

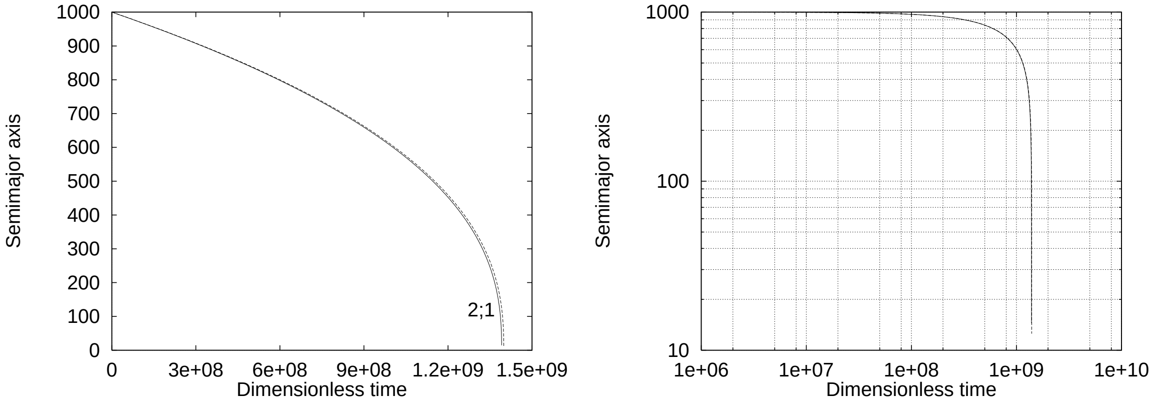

Figure 7.29: The evolution of semimajor axis of a circular orbit with [1] and without [2] the gravitation of the inhomogeneous disc.

where $b_{\min} \sim R_{\odot}$. At second, we integrate over the disc (which results in one-dimensional integration), supposing inhomogeneous surface density and parallel velocity vectors of test particles flowing at the migrating star. We suppose typical density of order 10^{-5} kg.m^{-3}, and other parameters of the disc and the star corresponding to those given in previous parts of this Chapter. We used relations

$$\frac{\mathrm{d}v^*}{\mathrm{d}t^*} = 8\pi 10^{-7} \frac{\xi}{v^{2\,*}} \ln\left(\frac{b_{\max}}{b_{\min}}\right) , \tag{7.24}$$

No.	V_{disc}	GF close	GF far
1	Yes	No	No
2	No	No	No
3	Yes	Yes	No
4	Yes	Yes	Yes

Table 7.5: Gravitational friction – see Fig. 7.34.

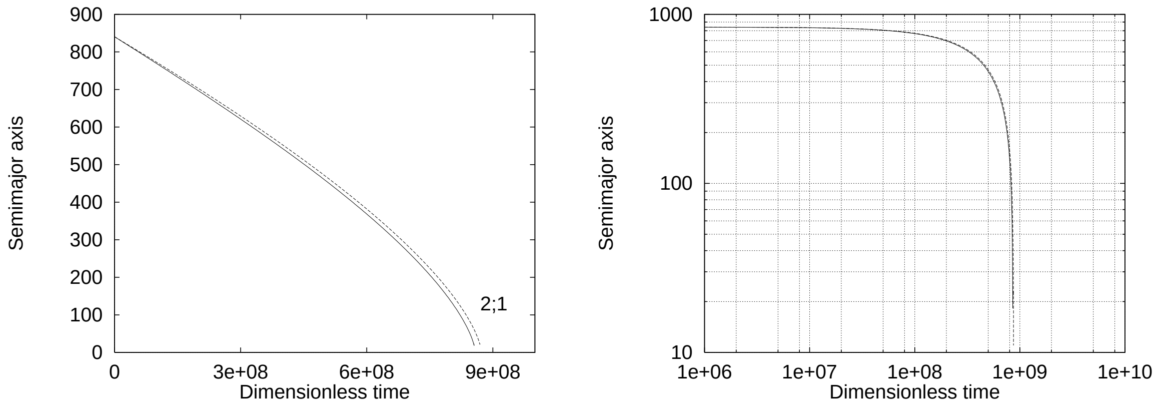

Figure 7.30: The evolution of semimajor axis of an elliptical orbit with [1] and without [2] the gravitation of the homogeneous disc.

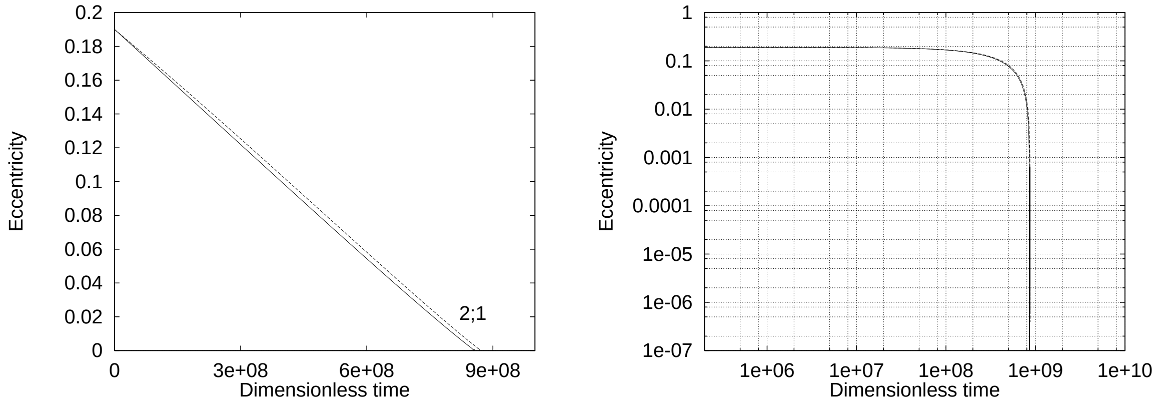

Figure 7.31: The evolution of the eccentricity of the elliptical orbit with [1] and without [2] the gravitation of the homogeneous disc.

$$\begin{matrix} \mathrm{d}v_{*\mathrm{t}}/\mathrm{d}t \\ \mathrm{d}v_{*\mathrm{r}}/\mathrm{d}t \end{matrix} = \int_{x_0-X}^{x_0+X} \frac{2m}{M} \frac{v_0(x)}{1+\left(\frac{bv_0^2}{GM}\right)^2} \begin{pmatrix} \sin\alpha - \frac{bv_0^2}{GM}\cos\alpha \\ \cos\alpha + \frac{bv_0^2}{GM}\sin\alpha \end{pmatrix} v_0(x)\sin\alpha\sigma(x)\mathrm{d}x \qquad (7.25)$$

(see relations (5.22) and (5.45) for the explanation of variables). The upper boundary of the integration (denoted by X) is defined as $1/15$ of the instantaneous distance from the center (denoted by x_0). The resulting effect of the gravitational drag is shown in Figures 7.34 ÷ 7.39 and the Tab 7.5.

Here "GF close" and "GF far" denote whether the gravitational friction was approximated by the relations (7.24) or (7.25), respectively. Of course, in eq. (7.25) one has to avoid the integration close to the migrating body.

Close to the body the gravitational friction is approximated by the relation 7.24. Also, very close to the massive body one would enter bellow the stellar surface (the distance to the massive center is smaller then the supposed radius of the body, depending on its compactness). Thus the integration region is limited to $(x_0 - X;\ x_0 + X) \cap (x_0 - R_*;\ x_0 + R_*)$, where R_* is the effective radius of the star.

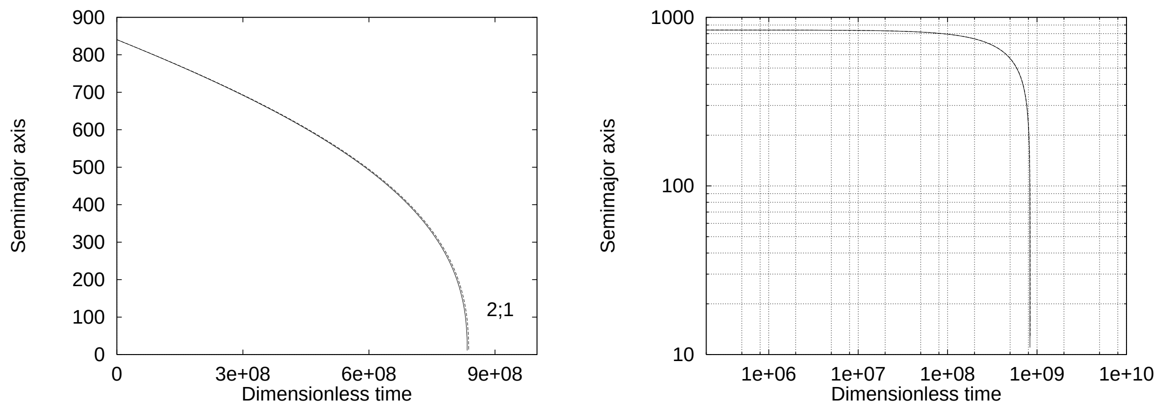

Figure 7.32: The evolution of semimajor axis of the elliptical orbit with [1] and without [2] the gravitation of the inhomogeneous disc.

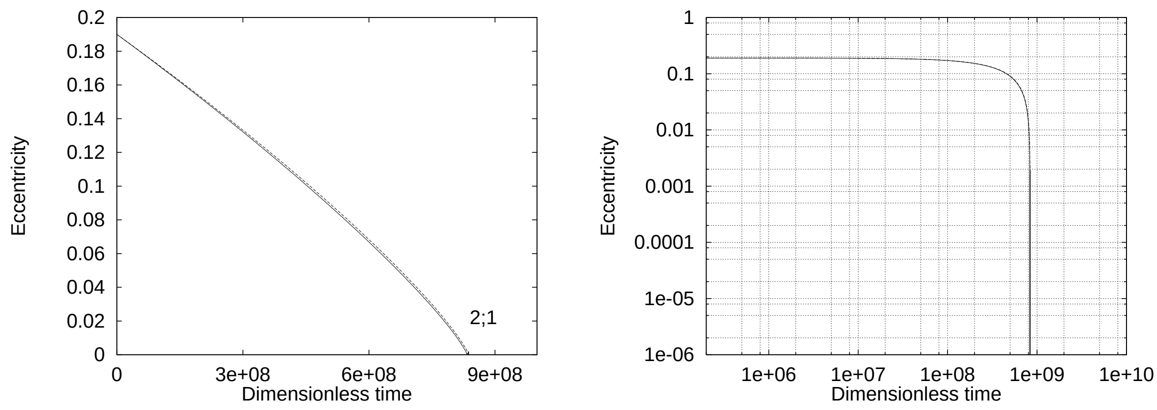

Figure 7.33: The evolution of eccentricity of the elliptical orbit with [1] and without [2] the gravitation of the inhomogeneous disc.

We can briefly summarize the most important information which is contained in the graphs presented above. There are two research areas where models similar to ours are relevant. First, they are calculations of the stellar distribution in galactic cores, which predict the presence of density cusps and corresponding integrated light profiles around the massive black hole. Stellar orbits and the overall form of the cusps must be modified by the presence of gas environment, and we demonstrated that time-scales on which the medium influences the orbits is one or two orders of magnitude less than the stellar life time. Its effect should be thus accounted. This is true especially for active galactic nuclei with non-negligible accretion rates, while in the center of Milky Way the gaseous environment is too rarefied to exert any substantial drag on the stars. Furthermore, sufficiently accurate knowledge of the long-term evolution of individual trajectories is necessary in computations of predicted light-curves and gravitational-wave forms produced just before the satellite capture. Both points are particularly relevant for the subsample of satellites which are aligned with the equatorial plane, because, as we indicated, hydrodynamical drag and gravitational friction act on these bodies most efficiently, resulting in relatively rapid orbital decay.

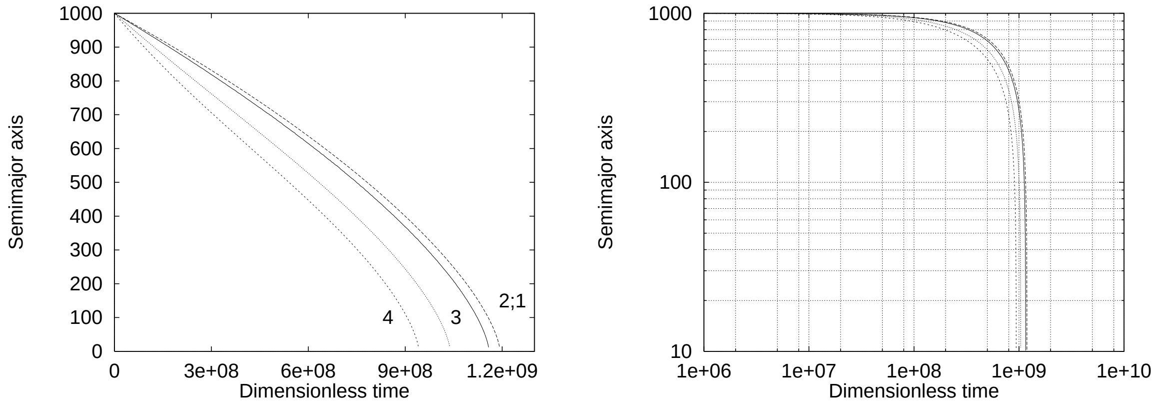

Figure 7.34: The evolution of semimajor axis of the circular orbit in the homogeneous disc with the gravitational drag accounted. For comparison, the cases with and without gravitational field of the disc are shown too.

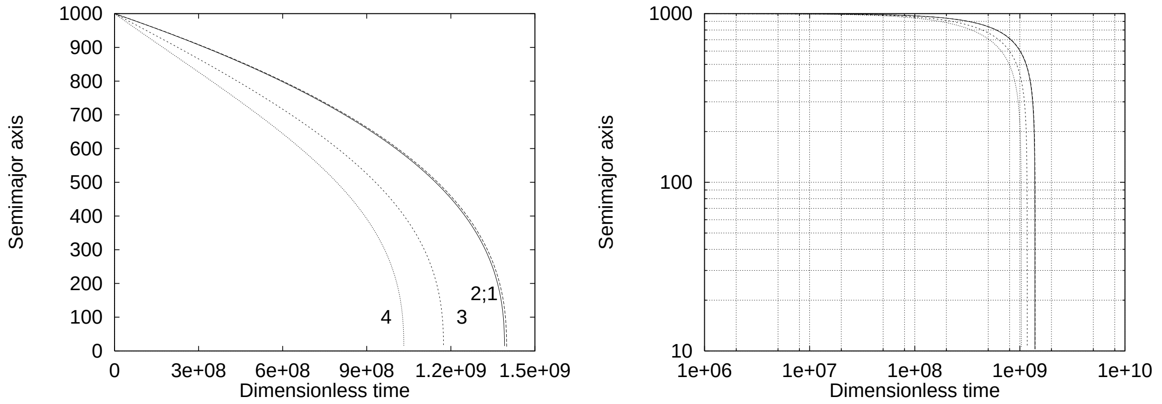

Figure 7.35: The evolution of semimajor axis of the circular orbit with and without gravitation of the inhomogeneous disc. Gravitational friction is now accounted. For the description of curves see text.

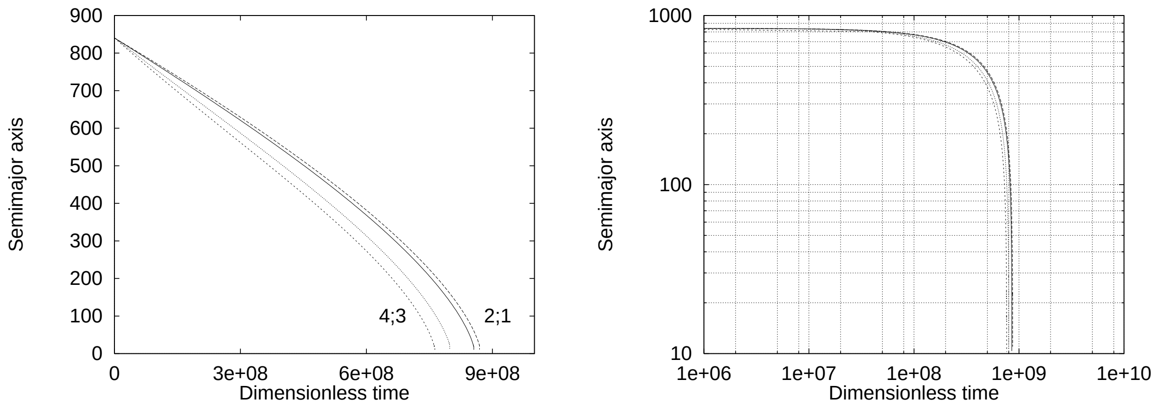

Figure 7.36: The evolution of semimajor axis of an elliptical orbit with gravitational friction accounted.

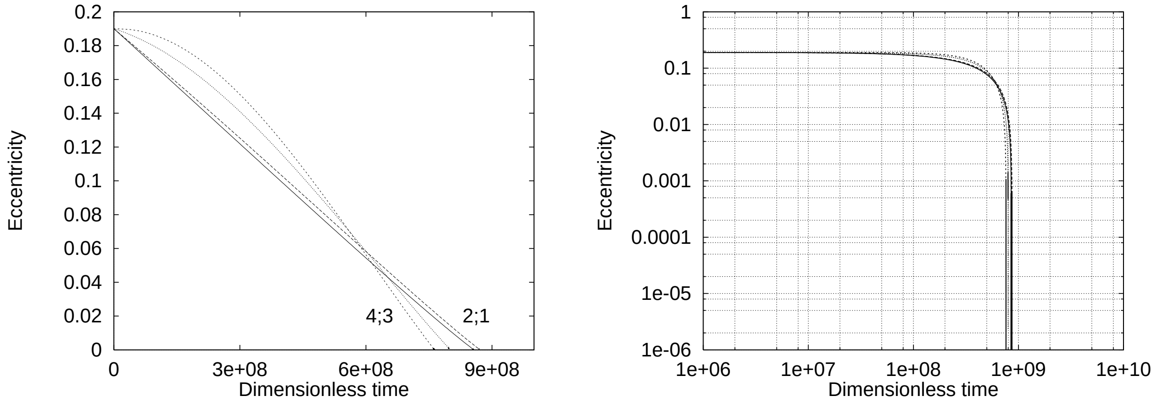

Figure 7.37: The evolution of eccentricity of the elliptical orbit with the gravitational friction accounted.

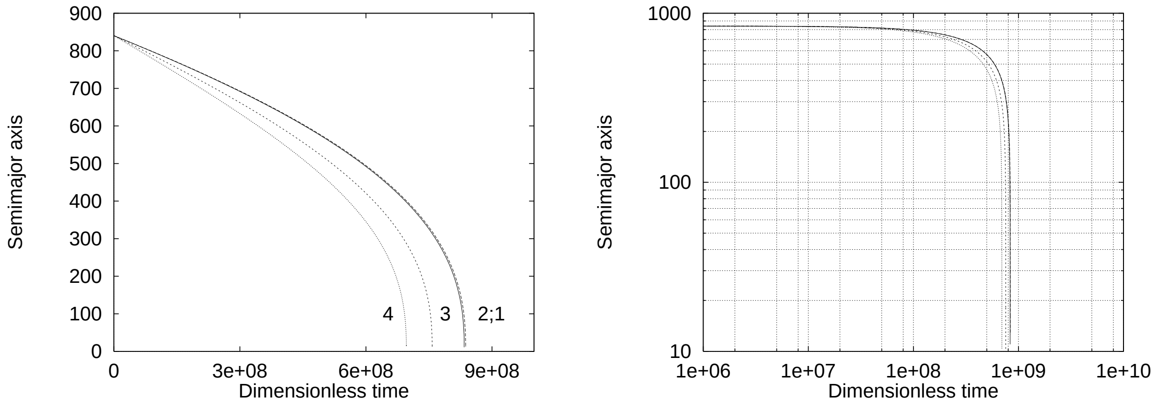

Figure 7.38: The evolution of semimajor axis of the elliptical orbit. The gravitational friction is accounted; the potential of the disc is accounted in curves [1], [3] and [4], while it is neglected in the case [2].

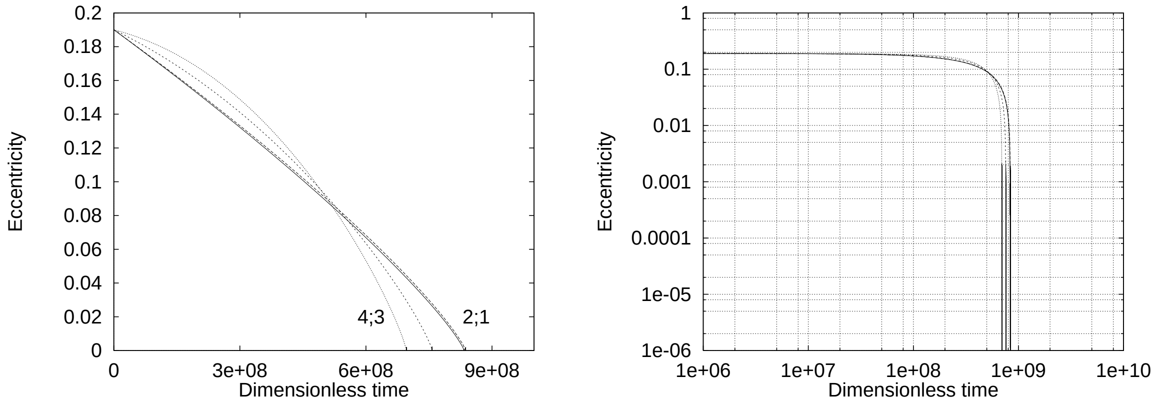

Figure 7.39: The evolution of eccentricity of the elliptical orbit.

Bibliography

[1] Artymowicz P., Lin D. N. C. & Wampler E. J. 1993, ApJ, 409, 592
[2] Artymowicz P. 1994, ApJ, 423, 581
[3] Aržanikov N. C. & Sadekova G. S. 1965, Aerodynamics of high velocities (Vysšaja škola, Moscow), in Russian (Aerodinamika bol'šich skorostěj)
[4] Bednarek W. & Protheroe R. J. 1998, MNRAS, 287, L9
[5] Bičák J. & Ledvinka T. 1993, Phys. Rev. Lett., 71, 1669
[6] Binney J. & Tremaine S. 1987, Galactic Dynamics (Princeton Univ. Press, Princeton)
[7] Bodenheimer P. & Pollack J. B. 1986, Icarus 67, 391
[8] Brada R. & Milgrom M. 1995, ApJ, 444, 71
[9] Brdička M. 1959, Mechanics of the Continuum (Academia, Prague), in Czech (Mechanika kontinua)
[10] Brdička M & Hladík J. Theoretical Mechanics (Academia, Prague), in Czech (Teoretická mechanika)
[11] Bromley B. C., Chen K., Miller W. A. 1997, ApJ, 475, 57
[12] Bronšten A. P. 1983, Physics of Meteoritical Phenomena (Nauka, Moscow), in Russian (Fizika metĕornych javlenij)
[13] Byrd P. F. & Friedmann M. D. 1971, Handbook of Elliptic Integrals for Engineers and Sciencists (Springer Verlag, Berlin)
[14] Carlson B. C. 1979, Num. Math, 33, 1
[15] Collin S. & Zahn J.-P. 1999, A&A, 344, 433
[16] Danby J. M. A. 1992, Fundamentals of Celestial Mechanics (Willman-Bell Inc., Richmond)
[17] Dejonghe H. & de Zeeuw P. T. 1998, ApJ, 333, 90
[18] de Zeeuw P. T. 1985, MNRAS, 216, 273
[19] Evans C. R. & Kochanek C. S. 1989, ApJ, 346, L13
[20] Evans N. W. & de Zeeuw P. T. 1992, MNRAS, 257, 152
[21] Frank J., King A. R. & Raine D. J. 1992, Accretion Power in Astrophysics (Cambridge Univ. Press), second edition 1998
[22] Fukue J. & Ohna E. 1997, PASJ, 49, 315
[23] Giraud J.-P. 1963, Topics in hypersonic flow theory, (Dept. of Aeronautics and Astronautics Stanford Univ., Stanford, California)
[24] Goldreich P. & Tremaine S. 1978, Icarus, 34, 227
[25] Harmanec P., Habuda P., Štefl S., Hadrava P., Korčákiová D., Koubský P., Krtička J., Kubát J., Škoda P., Šlechta M. & Wolf M. 2000, A&A Lett, 364, L85
[26] Hoffer J. B. 1985, ApJ, 289, 193
[27] Jaroszyński M., Abramowicz M. A. & Paczyński B. 1980, Acta Astronomica, 30, 1
[28] Karas V. 1994, in Contr. of XI. Congresso Nazionale di Relativita Generale a Fisica della Gravitazione (Trieste)
[29] Karas V., Lanza A. & Vokrouhlický D. 1995, ApJ, 440, 108
[30] Karas V. & Vokrouhlický D. 1994, ApJ, 208, 218

[31] Karas V. 1998, Astrophysical Analogies: From Quasars to Pulsars (students textbook)
[32] Kato S., Fukue J. & Mineshige S. 1998, Black-hole Accretion Disks (Kyoto University Press)
[33] Kippenhahn R. & Weigert A. 1991, Stellar Structure and Evolution (Springer-Verlag)
[34] Kley W. 2000, MNRAS, 313, L47
[35] Kormendy J., Richstone D. 1995, ARAA, 33, 581
[36] Krolik J. H. 1999, Active Galactic Nuclei (Princeton University Press, Princeton)
[37] Landau L. D. & Lifšic E. 1985, Hydrodynamics (Nauka, Moscow), in Russian (Gidrodinamika)
[38] Lanza, A. 1992, ApJ, 389, 141
[39] Lass H. & Blitzer L. 1983 Cel. Mech., 30, 225
[40] Leech J. W. 1958, Classical Mechanics (Butler & Tanner Ltd., London)
[41] Lehmann H., Harmanec P., Aerts C., Božič H., Eenens P., Hildebrandt G., Holmgren D., Mathias P., Scholtz G., Šlechta M. & Yang S. 2001, A&A, 367, 236
[42] Lemaitre A. & Dubru P. 1991 Cel. Mech., 52, 57
[43] Lin D. N. C. & Papaloizou J. C. B. 1993, in Protostars and Planets III, eds. E. H. Levy, J. I. Lunine (Univ. of Arizona, Tucson), 749
[44] Lin D. N. C., Papaloizou J. C. B., Bryden G., Ida S. & Terquem C. 2000, in Protostars and Planets IV, eds. Boss A., Mannings V. & Russel S. (Univ of Arizona Press, Tucson), 1111
[45] Livio M. , Soker N., de Kool M. & Savonije G. J. 1986, MNRAS, 218, 593
[46] Luminet J.-P. & Marck J.-A. 1985, MNRAS, 212, 57
[47] Lynden-Bell D. 1969, Nature, 223, 690
[48] Madau P. 1988, ApJ, 327, 116
[49] Marconi A., Axon D. J., Macchetto F. D., Capetti A., Soarks W. B. & Crane P. 1997, MNRAS, 289, L21
[50] Nandra K., George I. M., Mushotzky R. F., Turner T. J., Yaqoob T. 1997, ApJ, 476, 70; ibid. 1997, ApJ, 477, 602
[51] Narayan R. & Yi I. 1994, ApJ, 428, L13
[52] Narayan R., Mahadevan R. & Quataert E. 1999, in The Theory of Black Hole Accretion Disc, eds. Abramowicz M. A., Bjornsson G. & Pringle J. E. (Cambridge Univ. Press), 148
[53] Norman C., Silk J. 1983, ApJ, 266, 502
[54] Olivier S. 1991, MNRAS, 252, 102
[55] Ostriker E. C. 1999, ApJ, 513, 252
[56] Paczyński B. & Wiita P. J. 1980, A&A, 88, 23
[57] Perry J. & Williams R. 1993, MNRAS, 260, 437
[58] Peterson B. M. 1997, An Introduction to Active Galactic Nuclei (Cambridge University Press, Cambridge)
[59] Petrich L. I., Shapiro S. L., Stark R. F. & Teukolsky S. A. 1989, ApJ, 336, 313
[60] Pineault S. & Landry S. 1994, MNRAS, 265, 557
[61] Pringle J. E. & Rees M. J. 1972, A&A, 21, 1
[62] Press W. H., Teukolsky S. A., Vettering W. T. & Flannery B. P. 1992, Numerical Recipes in Fortran (Cambridge Univ. Press, Cambridge)
[63] Pringle, J. E. 1981, ARAA, 19, 137
[64] Rees M. 1984, ARAA, 22, 471
[65] Rees M. 1988, Nature, 333, 523
[66] Rees M. 1998, in Black Holes and Relativistic Stars, ed. R. M. Wald (Univ. Chicago Press, Chicago), 79
[67] Rektorys K. 1981, Review of Applied Mathematics (SNTL, Prague), in Czech (Přehled

užité matematiky)
[68] Rephaeli Y. & Salpeter E. E. 1980, ApJ, 240, 20
[69] Semerák O., Karas V., de Felice F. 1999, PASJ, 51, 571
[70] Shakura N. I. & Sunyaev R. A. 1973, A&A, 24, 337
[71] Syer D. & Clarke C. J. 1995, MNRAS, 277, 758
[72] Syer D., Clarke C. J. & Rees M. 1991, MNRAS, 250, 505
[73] Šlechta M. 1998, in Proc. of the 20th Stellar Conf., eds. J. Dušek & M. Zejda (Copernicus Observatory, Brno), p. 109
[74] Šlechta M. & Mészáros A. 1997, A&Sp.Sci. 249, 1
[75] Šubr L. 2001, Thesis (Charles University, Prague), in preparation
[76] Šubr L. & Karas V. 1999, A&A, 352, 452
[77] Takeda H., Matsuda T., Sawada K. & Hayashi Ch. 1985, Progress of Theor. Phys., 74, 272
[78] Townsend, A. A. 1956, The Structure of Turbulent Shear Flows (Cambridge Univ. Press, Cambridge)
[79] Treves A., Maraschi L. & Abramowicz M. 1988, PASP, 100, 427
[80] Urry C. M., Padovani P. 1995, PASP, 107, 803
[81] Vokrouhlický D. & Karas V. 1993, MNRAS, 265, 365
[82] Vokrouhlický D. & Karas V. 1998, MNRAS, 293, L1
[83] Vokrouhlický D. & Karas V. 1998, MNRAS, 298, 53
[84] Wolfson R. 1977, ApJ, 213, 200
[85] Zentsova A. 1983, A&Sp.Sci., 95, 11
[86] Zurek W. H., Siemiginowska A. & Colgate S. A. 1994, ApJ, 434, 46; ibid. 1996, ApJ, 470, 652

Part III

Appendices

Appendix A

Comments on basic accretion modes

The aim of this Appendix is to give a broader discussion of some elementary topics regarding the accretion process, and to summarize basic equations which have been used in the main text.

Steady spherically symmetric accretion

In this section we give a short review of perhaps the simplest model of accretion, namely, we will discuss steady, spherically symmetric accretion onto a central object. These topics have been described even on a textbook level [21].

Let us consider continuity equation, Euler's equation, and energy equation for perfect gas,

$$\begin{aligned} \frac{\partial \rho}{\partial t} + \nabla \cdot (\rho \boldsymbol{v}) &= 0 \,, && \text{(A.1)} \\ p &= \frac{\rho K T}{\mu m_{\mathrm{H}}} \,, && \text{(A.2)} \\ \rho \frac{\partial \boldsymbol{v}}{\partial t} + \rho \boldsymbol{v} \cdot \nabla \boldsymbol{v} &= -\nabla p + \boldsymbol{f} \,, && \text{(A.3)} \\ \frac{\partial}{\partial t}\left(\frac{1}{2}\rho v^2 + \rho\epsilon\right) + \nabla \cdot \left[\left(\frac{1}{2}\rho v^2 + \rho\epsilon + p\right)\boldsymbol{v}\right] &= \boldsymbol{f} \cdot \boldsymbol{v} && \text{(A.4)} \end{aligned}$$

where $m_{\mathrm{H}} \approx m_{\mathrm{p}}$ is the mass of the hydrogen atom, μ is the mean molecular weight which is the mean mass per particle of gas measured in units of m_{H}; ϵ is the energy density which can be expressed also as

$$\epsilon = \frac{3}{2}\frac{KT}{\mu m_{\mathrm{H}}} \,, \tag{A.5}$$

and (yet unspecified) force density acting on the gas, $\boldsymbol{f}$. Since we suppose the steady model, we can set

$$\frac{\partial}{\partial t} \equiv 0 \,. \tag{A.6}$$

In spherical coordinates the continuity equation is

$$\frac{1}{r^2}\frac{\mathrm{d}}{\mathrm{d}r}\left(r^2\rho v\right) = 0 \;\Rightarrow\; r^2\rho v = \mathrm{const}\ . \tag{A.7}$$

With this we can define the rate of the accretion $\dot{M}$ like

$$\dot{M} = 4\pi r^2\rho(-v)\ . \tag{A.8}$$

We use $(-v)$ because the accretion is an inflow of the gas onto the central mass. Since in our case the unspecified $\boldsymbol{f}$ is the gravitational force, we obtain Euler's equation in form

$$\rho v\frac{\mathrm{d}v}{\mathrm{d}r} + \frac{\mathrm{d}p}{\mathrm{d}r} + \frac{GM\rho}{r^2} = 0\ . \tag{A.9}$$

Since the continuity equation (A.7) leads to

$$\frac{1}{\rho}\frac{\mathrm{d}\rho}{\mathrm{d}r} = -\frac{1}{r^2 v}\frac{\mathrm{d}}{\mathrm{d}r}r^2 v\ , \tag{A.10}$$

we can rewrite it into form

$$v\frac{\mathrm{d}v}{\mathrm{d}r} - \frac{c_{\mathrm{s}}^2}{r^2 v}\frac{\mathrm{d}}{\mathrm{d}r}r^2 v + \frac{GM}{r^2} = 0\ . \tag{A.11}$$

It can be rewritten again

$$\begin{aligned}
\frac{1}{2}\frac{\mathrm{d}}{\mathrm{d}r}\left(v^2\right) - \frac{1}{2}\frac{c_{\mathrm{s}}^2}{v^2}\frac{\mathrm{d}}{\mathrm{d}r}(v^2) - \frac{2}{r}c_{\mathrm{s}}^2 &= -\frac{GM}{r^2} \\
\frac{1}{2}\left(1 - \frac{c_{\mathrm{s}}^2}{v^2}\right)\frac{\mathrm{d}}{\mathrm{d}r}v^2 &= -\frac{GM}{r^2}\left(1 - \frac{2}{r}\frac{r^2 c_{\mathrm{s}}^2}{GM}\right) \\
\frac{1}{2}\left(1 - \frac{c_{\mathrm{s}}^2}{v^2}\right)\frac{\mathrm{d}}{\mathrm{d}r}v^2 &= -\frac{GM}{r^2}\left(1 - \frac{2rc_{\mathrm{s}}^2}{GM}\right)\ .
\end{aligned} \tag{A.12}$$

We can find on which r the v is equal to the sound speed. It is on

$$r_{\mathrm{s}} = \frac{GM}{2c_{\mathrm{s}}^2}\ . \tag{A.13}$$

Now we will study (A.12) in more details. It is reasonable to suppose

$$\lim_{r\to\infty} c_{\mathrm{s}}(r) = c_{\mathrm{s}}(\infty) \tag{A.14}$$

and hence for large r

$$-\frac{GM}{r^2}\left(1 - \frac{2rc_{\mathrm{s}}^2}{GM}\right) > 0\ . \tag{A.15}$$

In the case of an inflow it is necessary to suppose

$$\frac{\mathrm{d}}{\mathrm{d}r}v^2 < 0 \tag{A.16}$$

and hence

$$v(r) < c_{\mathrm{s}}(r)\ \forall\, r > r_{\mathrm{s}}\ . \tag{A.17}$$

By the similar way we obtain

$$v(r) > c_{\mathrm{s}}\ \forall\, r < r_{\mathrm{s}}\ . \tag{A.18}$$

To be fully correct we have to admit also the second possible solution of (A.12). For

$$1 - \frac{2rc_{\rm s}^2}{GM} = 0 \tag{A.19}$$

we can also admit

$$\frac{\rm d}{{\rm d}r}v^2 = 0\ . \tag{A.20}$$

Hence we have two solutions valid at $r = r_{\rm s}$ – these are $v = c_{\rm s}$ and (A.20), and two possible types of behaviour at large r – these are (A.17), (A.18). Hence we obtain

1. $v^2(r_{\rm s}) = c_{\rm s}^2(r_{\rm s}),\ v^2 \to 0$ as $r \to \infty$; $v^2 < c_{\rm s}^2\ \forall\, r > r_{\rm s}$, $v^2 > c_{\rm s}^2\ \forall\, r < r_{\rm s}$.
2. $v^2(r_{\rm s}) = c_{\rm s}^2(r_{\rm s}),\ v^2 \to 0$ as $r \to 0$; $v^2 > c_{\rm s}^2\ \forall\, r > r_{\rm s}$, $v^2 < c_{\rm s}^2\ \forall\, r < r_{\rm s}$.
3. $v^2 < c_{\rm s}^2$ everywhere, $\frac{\rm d}{{\rm d}r}v^2 = 0$ for $r = r_{\rm s}$.
4. $v^2 > c_{\rm s}^2$ everywhere, $\frac{\rm d}{{\rm d}r}v^2 = 0$ for $r = r_{\rm s}$.
5. $\frac{\rm d}{{\rm d}r}v^2 = \infty \Leftrightarrow v^2 = c_{\rm s}^2$; $r > r_{\rm s}$ always.
6. $\frac{\rm d}{{\rm d}r}v^2 = \infty \Leftrightarrow v^2 = c_{\rm s}^2$; $r < r_{\rm s}$ always.

For graphical representation of solutions, see [21]. It is easily seen that only the first row above is consistent with our assumptions. Hence there is a unique solution of our problem which we will find right now. We obtain equations

$$\begin{aligned} v\frac{{\rm d}v}{{\rm d}r} + \frac{1}{\rho}\frac{{\rm d}p}{{\rm d}r} + \frac{GM}{r^2} &= 0\ , \\ p &= \mathcal{K}\rho^\gamma \end{aligned}$$

(see (A.9)) which lead to

$$\begin{aligned} v\frac{{\rm d}v}{{\rm d}r} + \frac{1}{\rho}\frac{{\rm d}p}{{\rm d}r} + \frac{GM}{r^2} &= 0\ , \\ \frac{v^2}{2} + \int \frac{1}{\rho}{\rm d}p - \frac{GM}{r} &= {\rm const}\ , \\ \frac{v^2}{2} + \int \mathcal{K}\gamma\rho^{\gamma-2}{\rm d}\rho &= {\rm const}\ , \qquad (A.21) \\ \frac{v^2}{2} + \frac{\gamma\mathcal{K}}{\gamma-1}\rho^{\gamma-1} - \frac{GM}{r} &= {\rm const}\ , \\ \frac{v^2}{2} + \frac{1}{\gamma-1}c_{\rm s}^2 - \frac{GM}{r} &= {\rm const}\ . \qquad (A.22) \end{aligned}$$

We note that the special case $\gamma = 1$ equation (A.21) leads to the logarithmic solution. Now, we have to solve equation (A.22). Assuming that

$$\begin{aligned} \lim_{r\to\infty} v^2(r) &= 0\ , \\ \lim_{r\to\infty} \frac{GM}{r} &= 0\ , \end{aligned}$$

we can find the unknown constant in the form

$$\frac{v^2}{2} + \frac{c_{\rm s}^2(r)}{\gamma-1} - \frac{GM}{r} = \frac{c_{\rm s}^2(\infty)}{\gamma-1}\ . \tag{A.23}$$

Now we can set $v = c_\mathrm{s} \bigcup r = r_\mathrm{s}$ and obtain

$$\begin{aligned} \frac{c_\mathrm{s}^2}{2} + \frac{c_\mathrm{s}^2}{\gamma-1} - 2c_\mathrm{s}^2 &= \frac{c_\mathrm{s}^2(\infty)}{\gamma-1} , \\ \frac{5-3\gamma}{2(\gamma-1)} c_\mathrm{s}^2(r_\mathrm{s}) &= \frac{c_\mathrm{s}^2(\infty)}{\gamma-1} , \\ c_\mathrm{s}^2(r_\mathrm{s}) &= c_\mathrm{s}^2(\infty)\frac{2}{5-3\gamma} . \end{aligned} \tag{A.24}$$

We obtain

$$c_\mathrm{s}^2 = \mathcal{K}\gamma\rho^{\gamma-1} \tag{A.25}$$

and hence we can easily obtain

$$\rho(r_\mathrm{s}) = \rho(\infty)\left[\frac{2}{5-3\gamma}\right]^{\frac{1}{\gamma-1}} . \tag{A.26}$$

It is reasonable to suppose that, in the case of the steady accretion, the rate of the accretion $\dot{M}$ must be independent of r. The same amount of material flows across each sphere, independently of its radius. Without any loss of generality we can set $r = r_\mathrm{s}$.

$$|\dot{M}| = 4\pi r^2 \rho v = 4\pi r_\mathrm{s}^2 \rho(r_\mathrm{s}) c_\mathrm{s}(r_\mathrm{s}) \tag{A.27}$$

and hence

$$\begin{aligned} |\dot{M}| &= 4\pi r_\mathrm{s}^2 \rho(r_\mathrm{s}) c_\mathrm{s}(r_\mathrm{s}) \\ &= 4\pi \frac{(GM)^2}{4c_\mathrm{s}^3}\rho(r_\mathrm{s}) = \pi (GM)^2 \frac{\rho(\infty)}{c_\mathrm{s}^3(\infty)}\left[\frac{2}{5-3\gamma}\right]^{\frac{1}{\gamma-1}-\frac{3}{2}} , \\ |\dot{M}| &= \pi (GM)^2 \frac{\rho(\infty)}{c_\mathrm{s}^3(\infty)}\left[\frac{2}{5-3\gamma}\right]^{\frac{5-3\gamma}{2(\gamma-1)}} . \end{aligned} \tag{A.28}$$

Equation (A.28) gives the rate of steady spherically symmetric accretion [21].

Axially symmetric accretion discs

The previous section dealt with perhaps the most trivial mode of accretion. In this section we describe the axially symmetric mode. The accretion via an axially symmetric discs has been summarized, for example, in refs. [21, 56, 63, 71, 84]. In view of large complexity of this subject, we will give only a brief summary of the problem.

Diffusion equation

At first we will derive *the continuity equation* and *the equation of angular momentum.* Then we will use them to obtain *the diffusion equation* which describes $\partial\Sigma/\partial r$.

Let us consider a thin ring in the disc. Its thickness is Δr and surface $2\pi r\Delta r$. The difference between the amount of matter which inflows and which outflows per unit of time is equal to $(2\pi r\Delta r\Sigma)^{\cdot}$. Hence

$$\begin{aligned} \frac{\partial}{\partial t}(2\pi r\Delta r\Sigma) &= v_\mathrm{r}(r,t)2\pi r\Sigma(r,t) \\ &\quad -v_\mathrm{r}(r+\Delta r)2\pi(r+\Delta r)\Sigma(r+\Delta r,t) \\ &\approx -2\pi\Delta r\frac{\partial}{\partial r}(rv_\mathrm{r}\Sigma) . \end{aligned}$$

For $\Delta r \to 0$ we suppose that we can set both r and Δr in front of time derivative:

$$r\frac{\partial \Sigma}{\partial t} + \frac{\partial}{\partial r}\left(r v_{\rm r} \Sigma\right) = 0 \, , \tag{A.29}$$

which is the continuity equation we looked for. Now we derive *equation for angular momentum*. The method will be analogous to previous discussion of the continuity equation. We can write:

$$\begin{aligned}
&\frac{\partial}{\partial t}\left(2\pi r \Delta r \Sigma r^2 \Omega\right) = 2\pi r v_{\rm r}(r,t)\Sigma(r,t) r^2 \Omega(r,t) - \\
&2\pi(r+\Delta r) v_{\rm r}(r+\Delta r,t)(r+\Delta r)^2 \Omega(r+\Delta r,t) + \frac{\partial G}{\partial r}\Delta r \\
&\approx -2\pi \Delta r \frac{\partial}{\partial r}\left(r v_{\rm r} \Sigma r^2 \Omega\right) + \frac{\partial G}{\partial r}\Delta r
\end{aligned}$$

Here G is *the viscous torque*, defined by

$$G \equiv 2\pi r \nu \Sigma r^2 \frac{\partial \Omega}{\partial r} \, . \tag{A.30}$$

ν is a viscous coefficient. Finally, the angular-momentum equation reads

$$r\frac{\partial}{\partial t}\left(\Sigma r^2 \Omega\right) + \frac{\partial}{\partial r}\left(r v_{\rm r} \Sigma r^2 \Omega\right) = \frac{1}{2\pi}\frac{\partial G}{\partial r} \, . \tag{A.31}$$

Thus we obtained three equations which we will use to obtain the diffusion equation. The fourth equation follows from the expression for Keplerian velocity which stands in the definition of viscous torques,

$$\Omega \equiv \Omega_\Omega \equiv \left(\frac{GM}{r^3}\right)^{\frac{1}{2}} \, . \tag{A.32}$$

Hence we have these equations:

$$r\frac{\partial \Sigma}{\partial t} + \frac{\partial}{\partial r}\left(r v_{\rm r} \Sigma\right) = 0 \, , \tag{A.33}$$

$$r\frac{\partial}{\partial t}\left(\Sigma r^2 \Omega\right) + \frac{\partial}{\partial r}\left(r v_{\rm r} \Sigma r^2 \Omega\right) = \frac{1}{2\pi}\frac{\partial G}{\partial r} \, , \tag{A.34}$$

$$G \equiv 2\pi \nu \Sigma r^2 \frac{\partial \Omega}{\partial r} \, , \tag{A.35}$$

$$\Omega \equiv \Omega_\Omega \equiv \left(\frac{GM}{r^3}\right)^{\frac{1}{2}} \, . \tag{A.36}$$

At first we will set (A.33) to (A.34). To be able to do it, we will adapt some expressions in (A.34) by this way:

$$\begin{aligned}
(I) \quad : \quad & r\frac{\partial}{\partial t}(\Sigma r^2 \Omega) = r\frac{\partial \Sigma}{\partial t} r^2 \Omega + r\Sigma \frac{\partial}{\partial t}(r^2 \Omega) = \\
& -r^2 \Omega \frac{\partial}{\partial r}(r v_{\rm r} \Sigma) + r\Sigma \frac{\partial}{\partial t}(r^2 \Omega) = \\
& -r^2 \Omega \frac{\partial}{\partial r}(r v_{\rm r} \Sigma) \, .
\end{aligned}$$

Here we used $r^2\Omega$ is a constant and we also set the continuity equation.

$$(II) : \frac{\partial}{\partial r}(r v_{\rm r} \Sigma r^2 \Omega) = r v_{\rm r} \Sigma \frac{\partial}{\partial r}(r^2 \Omega) + r^2 \Omega \frac{\partial}{\partial r}(r v_{\rm r} \Sigma). \tag{A.37}$$

Thus we have:

$$\begin{aligned}
-r^2\Omega\frac{\partial}{\partial r}(rv_{\rm r}\Sigma)+rv_{\rm r}\Sigma\frac{\partial}{\partial r}(rv_{\rm r}\Sigma)+\Sigma rv_{\rm r}\frac{\partial}{\partial r}(r^2\Omega) &= \frac{1}{2\pi}\frac{\partial G}{\partial r}\\
\Sigma rv_{\rm r}\frac{\partial}{\partial r}(r^2\Omega) &= \frac{1}{2\pi}\frac{\partial G}{\partial r}
\end{aligned}$$

In this equation we will use the continuity equation again:

$$\begin{aligned}
r\frac{\partial\Sigma}{\partial r} &= -\frac{\partial}{\partial r}(rv_{\rm r}\Sigma)=-\frac{\partial}{\partial r}\left[\frac{1}{2\pi}\frac{\partial G}{\partial r}\frac{1}{\frac{\partial}{\partial r}(r^2\Omega)}\right]\\
r\frac{\partial\Sigma}{\partial r} &= -\frac{\partial}{\partial r}\left[\frac{1}{2\pi}\frac{\partial G}{\partial r}\frac{1}{\frac{\partial}{\partial r}(r^2\Omega)}\right]
\end{aligned}$$

For the Keplerian orbit:

$$\Omega=\left(\frac{GM}{r^3}\right)^{\frac{1}{2}} \tag{A.38}$$

(see (A.36)) and at last we will use (A.35)

$$G\equiv 2\pi r\nu r^2\Sigma\frac{\partial\Omega}{\partial r}\ . \tag{A.39}$$

$r^2\Omega$ is equal to:

$$r^2\Omega=r^2\left(\frac{GM}{r^3}\right)^{\frac{1}{2}}=(GMr)^{\frac{1}{2}}\ , \tag{A.40}$$

hence:

$$\frac{\partial}{\partial r}(r^2\Omega)=\frac{1}{2}\left(\frac{GM}{r}\right)^{\frac{1}{2}}\ . \tag{A.41}$$

Together with the upper expression it gives:

$$-\frac{\partial}{\partial r}\left[\frac{1}{2\pi}\frac{1}{\frac{\partial}{\partial r}(r^2\Omega)}\frac{\partial G}{\partial r}\right]=-\frac{\partial}{\partial r}\left[\frac{1}{\pi}\frac{r^{\frac{1}{2}}}{(GM)^{\frac{1}{2}}}\frac{\partial G}{\partial r}\right]\ . \tag{A.42}$$

Since

$$\Omega=\sqrt{\frac{GM}{r}}\ \Rightarrow\ \frac{\partial\Omega}{\partial r}=-\frac{3}{2}\frac{(GM)^{\frac{1}{2}}}{r^{\frac{5}{2}}}\ , \tag{A.43}$$

we have trivially:

$$G=2\pi\nu\Sigma r^3\left(-\frac{3}{2}\right)\frac{(GM)^{\frac{1}{2}}}{r^{\frac{5}{2}}}=-3\pi\nu\Sigma(GMr)^{\frac{1}{2}}\ , \tag{A.44}$$

and the derivative with respect to r:

$$\frac{\partial G}{\partial r}=-3\pi(GM)^{\frac{1}{2}}\frac{\partial}{\partial r}\left(\nu\Sigma r^{\frac{1}{2}}\right)\ . \tag{A.45}$$

It leads to

$$\begin{aligned}
r\frac{\partial\Sigma}{\partial r} &= -\frac{\partial}{\partial r}\left[\frac{1}{\pi}\frac{r^{\frac{1}{2}}}{(GM)^{\frac{1}{2}}}(-3\pi)(GM)^{\frac{1}{2}}\frac{\partial}{\partial r}(\nu\Sigma r^{\frac{1}{2}})\right]=\\
&= 3\frac{\partial}{\partial r}\left[r^{\frac{1}{2}}\frac{\partial}{\partial r}(\nu\Sigma r^{\frac{1}{2}})\right]\\
\frac{\partial\Sigma}{\partial r} &= \frac{3}{r}\frac{\partial}{\partial r}\left[r^{\frac{1}{2}}\frac{\partial}{\partial r}(\nu\Sigma r^{\frac{1}{2}})\right]\ ,
\end{aligned}$$

which is asked *diffusion equation*. Now we will look for the rate of the accretion. Let us define

$$f \equiv \nu\Sigma \tag{A.46}$$

(see [71]). Then

$$v = -\frac{3}{\Sigma r^{1/2}}\frac{\partial}{\partial r}\left(r^{1/2}f\right) \ . \tag{A.47}$$

Multiplication by $2\pi r\Sigma$ leads to:

$$2\pi r\Sigma v \ = -6\pi r^{1/2}\frac{\partial}{\partial r}\left(r^{1/2}f\right) \ . \tag{A.48}$$

Rate of the accretion is defined by:

$$\dot{M} \equiv 2\pi r\Sigma v \tag{A.49}$$

which is

$$\dot{M} = -6\pi r^{1/2}\frac{\partial}{\partial r}\left(r^{1/2}f\right) \ , \tag{A.50}$$

and

$$\frac{\dot{M}}{3\pi} = -2r^{1/2}\frac{\partial}{\partial r}\left(r^{1/2}f\right) \ . \tag{A.51}$$

It is asked equation for the rate of accretion as it is discussed in [71]. Now we will look for the radial velocity. We have these expressions:

$$\begin{aligned}
\frac{\partial}{\partial r}\left(r^2\Omega\right) &= \frac{1}{2}\left(\frac{GM}{r}\right)^{\frac{1}{2}} \ , \\
\frac{\partial\Omega}{\partial r} &= -\frac{3}{2}\left(\frac{GM}{r^5}\right)^{\frac{1}{2}} \ , \\
\frac{\partial G}{\partial r} &= -3\pi(GM)^{\frac{1}{2}}\frac{\partial}{\partial r}\left(\nu\Sigma r^{\frac{1}{2}}\right) \ ,
\end{aligned}$$

All this we set to

$$r\Sigma v_{\mathrm{r}}\frac{\partial}{\partial r}\left(r^2\Omega\right) = \frac{1}{2\pi}\frac{\partial G}{\partial r} \tag{A.52}$$

and obtain:

$$\begin{aligned}
r\Sigma v_{\mathrm{r}}\frac{1}{2}\left(\frac{GM}{r}\right)^{\frac{1}{2}} &= -\frac{3\pi}{2\pi}(GM)^{\frac{1}{2}}\frac{\partial}{\partial r}\left(\nu\Sigma r^{\frac{1}{2}}\right) \\
\frac{1}{2}\Sigma v_r(GM)^{\frac{1}{2}}r^{\frac{1}{2}} &= -\frac{3}{2}(GM)^{\frac{1}{2}}\frac{\partial}{\partial r}\left(\nu\Sigma r^{\frac{1}{2}}\right) \ .
\end{aligned}$$

It leads to the expression of the radial velocity

$$v_{\mathrm{r}} = -\frac{3}{\Sigma r^{\frac{1}{2}}}\frac{\partial}{\partial r}\left(\nu\Sigma r^{\frac{1}{2}}\right) \ . \tag{A.53}$$

In the case of a steady disc we can obtain expressions for the transversal velocity [63].

Stationarity – a steady disc

Momentum equation

$$\rho\frac{\mathrm{d}\boldsymbol{v}}{\mathrm{d}t} + \rho(\bigtriangledown\boldsymbol{v}).\boldsymbol{v} = -\bigtriangledown p + \boldsymbol{f} \tag{A.54}$$

in the steady case in which time derivative is explicitly zero has shape in radial coordinates:

$$v_{\mathrm{r}}\frac{\mathrm{d}v_{\mathrm{r}}}{\mathrm{d}r} - \frac{v_{\Phi}^2}{r} = -\frac{1}{\rho}\frac{\mathrm{d}p}{\mathrm{d}r} - \frac{GM}{r^2}\ . \tag{A.55}$$

If the radial velocity is small in comparison with the transversal one, we can neglect it and obtain

$$\begin{aligned}
\frac{v_{\Phi}^2}{r} &= \frac{1}{\rho}\frac{\mathrm{d}p}{\mathrm{d}r} + \frac{GM}{r^2} \\
v_{\Phi}^2 &= \frac{c_{\mathrm{s}}^2}{\rho} r \frac{\mathrm{d}\rho}{\mathrm{d}r} + \frac{GM}{r} \\
v_{\Phi}^2 &= \frac{GM}{r}\left(1 + \frac{r^2}{\rho}\frac{c_{\mathrm{s}}^2}{GM}\frac{\mathrm{d}\rho}{\mathrm{d}r}\right) \\
\mathcal{M} \equiv \frac{v}{c_{\mathrm{s}}} &\Rightarrow\ c_{\mathrm{s}}^2 = \frac{v^2}{\mathcal{M}} \\
v_{\Phi}^2 &= \frac{GM}{r}\left(1 + \frac{r^2}{GM\rho}\frac{v^2}{\mathcal{M}^2}\frac{\mathrm{d}\rho}{\mathrm{d}r}\right) \Rightarrow \\
v_{\Phi} &= \left(\frac{GM}{r}\right)^{\frac{1}{2}}\left(1 + \mathcal{O}(\mathcal{M}^{-2})\right)\ .
\end{aligned} \tag{A.56}$$

You can see that in this model the transversal velocity is very similar to the Keplerian orbital velocity.

Equation of the hydrostatic equilibrium

$$\frac{1}{\rho}\frac{\partial p}{\partial z} = \frac{\partial}{\partial z}\left[\frac{GM}{(r^2+z^2)^{\frac{1}{2}}}\right] \tag{A.57}$$

can be rewritten for small z (i. e. in a thin disc) with using of

$$\frac{1}{(r^2+z^2)^{\frac{1}{2}}} = \frac{1}{r\left(1+\frac{z^2}{r^2}\right)} = \frac{1}{r}\left(1 - \frac{1}{2}\frac{z^2}{r^2}\right) \tag{A.58}$$

to form:

$$\begin{aligned}
\frac{1}{\rho}\frac{\partial p}{\partial z} &= \frac{\partial}{\partial z}\left[\frac{GM}{r}\left(1 - \frac{1}{2}\frac{z^2}{r^2}\right)\right] = -\frac{GM}{r^3}z \\
\frac{1}{\rho}\frac{\partial p}{\partial z} &= -\frac{GM}{r^3}z
\end{aligned}$$

This equation can be integrated:

$$\begin{aligned}
\frac{1}{\rho}\frac{\partial p}{\partial z} &= -\frac{GM}{r^3}z \\
\frac{c_{\mathrm{s}}^2}{\rho}\frac{\partial \rho}{\partial z} &= -\frac{GM}{r^3}z \\
\frac{1}{\rho}\mathrm{d}\rho &= -\frac{GM}{r^3 c_{\mathrm{s}}^2}z\mathrm{d}z \\
\ln\rho &= -\frac{GM}{r^3 c_{\mathrm{s}}^2}\frac{z^2}{2} \\
\rho &= \rho_0 e^{-\left(\frac{GM}{r^3 c_{\mathrm{s}}^2}\frac{z^2}{2}\right)} \quad \Big| \quad H^2 \equiv \frac{r^3 c_{\mathrm{s}}^2}{GM} \\
\rho &= \rho_0 e^{-\frac{z^2}{2H^2}}
\end{aligned} \tag{A.59}$$

Since

$$\frac{v_\Phi^2}{r} = \frac{GM}{r^2} \Rightarrow v_\Phi^2 = \frac{GM}{r} , \tag{A.60}$$

we can rewrite H to form:

$$H^2 = r^2 c_\mathrm{s}^2 \frac{r}{GM} = r^2 \frac{c_\mathrm{s}^2}{v_\Phi^2} . \tag{A.61}$$

Viscosity

In order to describe viscosity, we introduce α-parameter. Effective kinematic viscosity is defined by:

$$\varsigma \equiv l \cdot v , \tag{A.62}$$

where l is the scale and v circular velocity of the largest eddies. In accretion discs we can assume these whirls (or vortices) to be smaller then the semithickness of the disc H [63]. Introducing the above-mentioned α-parameter yields

$$\varsigma \equiv \alpha c_\mathrm{s} H . \tag{A.63}$$

We can see that H is restricted by the relation for l and $v \to c_\mathrm{s}$. From these limits it is easily seen that

$$\alpha < 1 . \tag{A.64}$$

Pringle in [63] reminds that (see [70]):

$$\alpha \propto \left(\frac{v_\mathrm{A}}{c_\mathrm{s}}\right)^2 , \tag{A.65}$$

where v_A is the Alfvén's speed – in this case we have to suppose a magnetic field.

Local structure of the disc

We have solution A.59

$$\rho = \rho_0 e^{-\frac{z^2}{2H^2}} . \tag{A.66}$$

Let us denote the dissipation in the disc per unit of surface and unit of time as $D(r)$. The structure of the disc in z-direction on given r is similar to one–dimensional model of a star and it is given by the equilibrium between the inflowing heat (per unit of surface)

$$Q_+ = \frac{1}{2} D(r) \tag{A.67}$$

and the outflowing heat (per unit of surface). This heat is given by the radiative transport equation approximatively like [63]

$$Q_- = acT_\mathrm{c}^4 \frac{1}{\tau} , \tag{A.68}$$

where a is Stefan constant and τ is optical depth: $\tau \equiv \rho H \kappa(\rho, T_\mathrm{c})$, κ is an opacity.

Emitted spectrum

We have to find emitted spectrum from any part of the disc and then from these parts obtain emitted spectrum of the whole disc. If the disc is optically thick (and any element can be modelled as black body with temperature $T_{\rm s}$), then

$$Q_{-} = \sigma T_{\rm s}^4 \; , \tag{A.69}$$

where σ is Stefan-Boltzmann constant. Supposing

$$Q_{-} = Q_{+} \; , \tag{A.70}$$

we have

$$\frac{1}{2}D(r) = \sigma T_{\rm s}^4 \Rightarrow T_{\rm s} = \left[\frac{1}{2\sigma}D(r)\right]^{\frac{1}{4}} \; . \tag{A.71}$$

Since:

$$D(r) = \frac{3GM\dot{M}}{4\pi r^3}\left[1 - \left(\frac{r_*}{r}\right)^{\frac{1}{2}}\right] \; , \tag{A.72}$$

we have immediately:

$$T_{\rm s} = \left[\frac{3GM\dot{M}}{8\pi\sigma r^3}\left[1 - \left(\frac{r_*}{r}\right)^{\frac{1}{2}}\right]\right]^{\frac{1}{4}} \; . \tag{A.73}$$

Total disc luminosity is given by:

$$\begin{aligned}
L_{\rm disc} &= \int_{r_*}^{\infty} 2\pi r D(r) {\rm d}r = \\
&= \int_{r_*}^{\infty} 2\pi r \frac{3GM\dot{M}}{4\pi r^3}\left[1 - \left(\frac{r_*}{r}\right)^{\frac{1}{2}}\right] {\rm d}r = \\
&= \frac{3GM\dot{M}}{2}\int_{r_*}^{\infty}\left(\frac{1}{r^2} - \frac{r_*^{\frac{1}{2}}}{r^{\frac{5}{2}}}\right){\rm d}r = \\
&= \frac{3GM\dot{M}}{2}\left(\frac{1}{r_*} - \frac{2}{3}\frac{r_*^{\frac{1}{2}}}{r_*^{\frac{3}{2}}}\right) = \\
L_{\rm disc} &= \frac{1}{2}\frac{GM\dot{M}}{r_*}
\end{aligned} \tag{A.74}$$

since

$$\begin{aligned}
\int_{r_*}^{\infty} \frac{1}{r^2}{\rm d}r &= -\left[\frac{1}{r}\right]_{r_*}^{\infty} = -0 + \frac{1}{r_*} = \frac{1}{r_*} \\
\int_{r_*}^{\infty} \frac{1}{r^{\frac{5}{2}}}{\rm d}r &= \frac{2}{3}\frac{1}{r_*^{\frac{3}{2}}}
\end{aligned}$$

Upper we set the equivalent temperature of black body – see (A.73). Black body approximation leads to the assumption that the spectrum of whole disc is

$$S_\nu \propto \int_{r_*}^{r_{\rm out}} B_\nu(T_{\rm s}(r)) \, . \, 2\pi r {\rm d}r \; . \tag{A.75}$$

B_ν is Planck function.

For $r \gg r_*$ we can rewrite expression (A.73)

$$T_\mathrm{s} = \left[\frac{3GM\dot{M}}{8\pi\sigma r^3}\left[1 - \left(\frac{r_*}{r}\right)^{\frac{1}{2}}\right]\right]^{\frac{1}{4}} \tag{A.76}$$

to form

$$T_\mathrm{s} = T_* \left(\frac{r_*}{r}\right)^{\frac{3}{4}} \quad ; \quad T_*^4 = \frac{3GM\dot{M}}{8\pi\sigma r^3} \ , \tag{A.77}$$

i. e.

$$T_\mathrm{s} \propto r^{-\frac{3}{4}} \ . \tag{A.78}$$

From the part of the disc where $r \gg r_*$ the incoming emission has $\nu \ll \frac{kT_*}{h}$. Then we can rewrite expression for S_ν to form:

$$S_\nu \propto \nu^{\frac{1}{3}} \int\limits_0^{x_\mathrm{out}} \frac{x^{\frac{5}{3}}}{e^x - 1}\mathrm{d}x \ , \ x = \frac{h\nu}{kT_s(r)} \ . \tag{A.79}$$

Here $T_\mathrm{out} = T_\mathrm{s}(r_\mathrm{out})$ where r_out is the outer radius of the disc. Finally, let us a solution for an infinite disc (which has $x_\mathrm{out} = \infty$):

$$\int\limits_0^{\infty} \frac{x^{\frac{5}{3}}}{e^x - 1}\mathrm{d}x = \frac{10}{9}\Gamma\left(\frac{2}{3}\right)\zeta\left(\frac{8}{3}\right) \ . \tag{A.80}$$

$\zeta(\xi)$ is a Riemann zeta-function defined by

$$\zeta(\xi) \equiv \sum_{i=1}^{\infty} \frac{1}{i^\xi} \ . \tag{A.81}$$

Fully general solution for any $x_\mathrm{out} < \infty$ does not exist because the integral of the upper type has not analytical solution for an arbitrary x_out. For frequencies $kT_\mathrm{out} \ll \nu \ll kT_*/h$ we can admit $x_\mathrm{out} \gg 1$ and hence $S_\nu \propto \nu^{1/3}$. For $\nu \ll kT_\mathrm{out}/h$ we obtain $S_\nu \propto \nu^2$.

Appendix B

Approximations valid near rotation axis

In the previous section we dealt with the description of thin (accretion) discs near to the disc plane, $z = 0$. On the other hand it can be interesting to study the accretion process also near to the axis. Description of such process is widely discussed in, for example, [84]. We will review the approximation.

Let us introduce spherical coordinates (r, ϑ, φ). Due to symmetry we can neglect dependence on φ and study dependence on (r, ϑ) only. We consider equations of the radial momentum conservation (B.1), the transversal momentum conservation (B.2), the continuity equation (B.3), and the entropy conservation (B.4):

$$V_{\mathrm{r}}\frac{\partial V_{\mathrm{r}}}{\partial r} + \frac{V_\vartheta}{r}\frac{\partial V_{\mathrm{r}}}{\partial \vartheta} - \frac{V_\vartheta^2}{r} = -\frac{1}{\rho}\frac{\partial P}{\partial r} - \frac{GM}{r^2} \quad , \tag{B.1}$$

$$V_{\mathrm{r}}\frac{\partial V_\vartheta}{\partial r} + \frac{V_\vartheta}{r}\frac{\partial V_\vartheta}{\partial \vartheta} + \frac{V_{\mathrm{r}} V_\vartheta}{r} = -\frac{1}{\rho r}\frac{\partial P}{\partial \vartheta} \quad , \tag{B.2}$$

$$\rho\left(\frac{\partial V_{\mathrm{r}}}{\partial r} + \frac{2V_{\mathrm{r}}}{r} + \frac{1}{r}\frac{\partial V_\vartheta}{\partial \vartheta} + \frac{V_\vartheta}{r}\cot\vartheta\right) + \left(V_{\mathrm{r}}\frac{\partial \rho}{\partial r} + \frac{V_\vartheta}{r}\frac{\partial \rho}{\partial \vartheta}\right) = 0 \quad , \tag{B.3}$$

$$V_{\mathrm{r}}\frac{\partial P}{\partial r} + \frac{V_\vartheta}{r}\frac{\partial P}{\partial \vartheta} - \gamma\frac{P}{\rho}\left(V_{\mathrm{r}}\frac{\partial \rho}{\partial r} + \frac{V_\vartheta}{r}\frac{\partial \rho}{\partial \vartheta}\right) = 0 \quad . \tag{B.4}$$

In all above-given equations we supposed $\partial/\partial t \equiv 0$. V_{r} and V_ϑ are radial and transversal velocities, respectively.

Rewriting of equations into new variables

We suppose that the region of interest is much lesser than an accretion radius from which matter inflows. It means that we can neglect V_∞^2 in compare with the specific infall energy GM/r. Hence the flow velocity should behave like $r^{-1/2}$. For the density we suppose a power-law dependence $\rho \propto r^{-m}$. Thus the assumed solution is:

$$V_{\mathrm{r}} = \beta r^{-\frac{1}{2}} x(\vartheta) \ , \tag{B.5}$$

$$V_\vartheta = \beta r^{-\frac{1}{2}} y(\vartheta) \ , \tag{B.6}$$

$$\rho = \alpha r^{-m} f(\vartheta) \ , \tag{B.7}$$

$$P = \alpha\beta^2 r^{-(m+1)} g(\vartheta) \ , \tag{B.8}$$

where

$$\beta \equiv \left(\frac{\gamma-1}{\gamma+1}\right)(2GM)^{\frac{1}{2}} \Rightarrow GM = \frac{1}{2}\beta^2\left(\frac{\gamma+1}{\gamma-1}\right)^2 \tag{B.9}$$

and α is a constant defined, except for others, by the specific heat ratio. Functions $x,\ y,\ f,\ g$ are unknown quantities. Let us introduce them into hydrodynamic equations, at first into (B.1):

$$\begin{aligned}
V_{\mathrm{r}}\frac{\partial V_{\mathrm{r}}}{\partial r} + \frac{V_\vartheta}{r}\frac{\partial V_{\mathrm{r}}}{\partial \vartheta} - \frac{V_\vartheta^2}{r} &= -\frac{1}{\rho}\frac{\partial P}{\partial r} - \frac{GM}{r^2} \\
\beta r^{-\frac{1}{2}} x(\vartheta)\frac{\partial}{\partial r}\left(\beta r^{-\frac{1}{2}} x(\vartheta)\right) + & \\
\frac{1}{r}\beta r^{-\frac{1}{2}} y(\vartheta)\frac{\partial}{\partial \vartheta}\left(\beta r^{-\frac{1}{2}} x(\vartheta)\right) - & \\
\frac{1}{r}\left(\beta r^{-\frac{1}{2}} y(\vartheta)\right)^2 &= -\frac{1}{\alpha r^{-m} f(\vartheta)}\frac{\partial}{\partial r}\left(\alpha\beta^2 r^{-(m+1)} g(\vartheta)\right) \\
& \quad -\frac{GM}{r^2}
\end{aligned}$$

$$\begin{aligned}
\beta^2 x^2(\vartheta)\left(-\frac{1}{2}\right) r^{-2}+ & \\
\beta^2 y(\vartheta) r^{-2} x'(\vartheta) - \beta^2 r^{-2} y^2(\vartheta) &= \beta^2 \frac{g(\vartheta)}{f(\vartheta)} r^m(-m-1) r^{-(m+2)} - \frac{GM}{r^2} \\
GM &= \frac{1}{2}\beta^2 \left(\frac{\gamma+1}{\gamma-1}\right)^2 \text{ (see (B.9))} \\
-\frac{1}{2}\beta^2 x^2(\vartheta) r^{-2}+ & \\
\beta^2 x'(\vartheta) y(\vartheta) r^{-2} - \beta^2 y^2(\vartheta) r^{-2} &= \beta^2 \frac{g(\vartheta)}{f(\vartheta)} r^{-2}(-m-1) - \frac{1}{2} r^{-2}\beta^2 \left(\frac{\gamma+1}{\gamma-1}\right)^2 \\
-\frac{1}{2} x^2(\vartheta) + x'(\vartheta) y(\vartheta) - y^2(\vartheta) &= -\frac{g(\vartheta)}{f(\vartheta)}(m+1) - \frac{1}{2}\left(\frac{\gamma+1}{\gamma-1}\right)^2 . \qquad \text{(B.10)}
\end{aligned}$$

By the same way we can rewrite (B.2):

$$\begin{aligned}
V_{\mathrm{r}} \frac{\partial V_\vartheta}{\partial r} + \frac{V_\vartheta}{r}\frac{\partial V_\vartheta}{\partial \vartheta} + \frac{V_{\mathrm{r}} V_\vartheta}{r} &= -\frac{1}{\rho r}\frac{\partial P}{\partial \vartheta} \\
V_{\mathrm{r}} &= \beta r^{-\frac{1}{2}} x(\vartheta) \\
V_\vartheta &= \beta r^{-\frac{1}{2}} y(\vartheta) \\
\rho &= \alpha r^{-m} f(\vartheta) \\
P &= \alpha\beta^2 r^{-(m+1)} g(\vartheta) \text{ (see (B.5) } \div \text{ (B.8))} , \\
\beta r^{-\frac{1}{2}} x(\vartheta) \frac{\partial}{\partial r}\left(\beta r^{-\frac{1}{2}} y(\vartheta)\right) + & \\
\frac{\beta r^{-\frac{1}{2}} y(\vartheta)}{r}\frac{\partial}{\partial \vartheta}\left(\beta r^{-\frac{1}{2}} y(\vartheta)\right) + & \\
\frac{\beta r^{-\frac{1}{2}} x(\vartheta) \beta r^{-\frac{1}{2}} y(\vartheta)}{r} &= -\frac{1}{\alpha r^{-m} r f(\vartheta)}\frac{\partial}{\partial \vartheta}\left(\alpha\beta^2 \boldsymbol{r}^{-(m+1)} g(\vartheta)\right) \\
\beta^2 x(\vartheta) y(\vartheta) r^{-\frac{1}{2}}\left(-\frac{1}{2}\right) r^{-\frac{3}{2}}+ & \\
\beta^2 r^{-2} y(\vartheta) y'(\vartheta) + \beta^2 r^{-2} x(\vartheta) y(\vartheta) &= -\frac{1}{\alpha} r^m \frac{1}{r^m}\frac{1}{f(\vartheta)}\alpha\beta^2 \frac{1}{r^{m+1}} g'(\vartheta) \\
-\frac{1}{2} x(\vartheta) y(\vartheta) + y(\vartheta) y'(\vartheta) + x(\vartheta) y(\vartheta) &= -\frac{g'(\vartheta)}{f(\vartheta)} \\
\frac{1}{2} x(\vartheta) y(\vartheta) + y(\vartheta) y'(\vartheta) &= -\frac{g'(\vartheta)}{f(\vartheta)} . \qquad \text{(B.11)}
\end{aligned}$$

It is (B.2) rewritten into quantities x, y, f, g. Equation (B.3):

$$\begin{aligned}
\rho\left(\frac{\partial V_{\mathrm{r}}}{\partial r} + \frac{2V_{\mathrm{r}}}{r} + \frac{1}{r}\frac{\partial V_\vartheta}{\partial \vartheta} + \frac{V_\vartheta}{r}\cot\vartheta\right) + \left(V_{\mathrm{r}}\frac{\partial \rho}{\partial r} + \frac{V_\vartheta}{r}\frac{\partial \rho}{\partial \vartheta}\right) &= 0 \\
\alpha r^{-m} f(\vartheta)\left[\frac{\partial}{\partial r}\left(\beta r^{-\frac{1}{2}} x(\vartheta)\right) + \frac{2}{r}\left(\beta r^{-\frac{1}{2}} x(\vartheta)\right) + \right. & \\
\left. \frac{1}{r}\frac{\partial}{\partial \vartheta}\left(\beta r^{-\frac{1}{2}} y(\vartheta)\right) + \frac{1}{r}\beta r^{-\frac{1}{2}} y(\vartheta)\cot\vartheta\right] + & \\
\left[\beta r^{-\frac{1}{2}} x(\vartheta)\frac{\partial}{\partial r}\left(\alpha r^{-m} f(\vartheta)\right) + \frac{1}{r}\beta r^{-\frac{1}{2}} y(\vartheta)\frac{\partial}{\partial \vartheta}\left(\alpha r^{-m} f(\vartheta)\right)\right] &= 0 \\
\alpha r^{-\frac{1}{2}} f(\vartheta)\left[-\frac{1}{2} r^{-\frac{3}{2}}\beta x(\vartheta) + 2r^{-\frac{3}{2}}\beta x(\vartheta) + \beta r^{-\frac{3}{2}} y'(\vartheta) + r^{-\frac{3}{2}}\beta y(\vartheta) cot\vartheta\right] + &
\end{aligned}$$

$$
\begin{aligned}
\left[\alpha\beta x(\vartheta)f(\vartheta)(-m)r^{-m}r^{-\frac{3}{2}} + r^{-m}r^{-\frac{3}{2}}\alpha\beta y(\vartheta)f'(\vartheta)\right] &= 0 \\
-\frac{1}{2}x(\vartheta) + 2x(\vartheta) + y'(\vartheta) + y(\vartheta)\cot\vartheta - mx(\vartheta) + y(\vartheta)\frac{f'(\vartheta)}{f(\vartheta)} &= 0 \\
\left(\frac{3}{2} - m\right)x(\vartheta) + y'(\vartheta) + y(\vartheta)\cot\vartheta + y(\vartheta)\frac{f'(\vartheta)}{f(\vartheta)} = 0\ . &
\end{aligned}
\tag{B.12}
$$

It is the third equation. And the last one (B.4):

$$
\begin{aligned}
V_{\mathrm{r}}\frac{\partial P}{\partial r} + \frac{V_\vartheta}{r}\frac{\partial P}{\partial \vartheta} - \gamma\frac{P}{\rho}\left(V_{\mathrm{r}}\frac{\partial \rho}{\partial r} + \frac{V_\vartheta}{r}\frac{\partial \rho}{\partial \vartheta}\right) &= 0 \\
\left[\beta r^{-\frac{1}{2}}x(\vartheta)\frac{\partial}{\partial r}\left(\alpha\beta^2 r^{-(m+1)}g(\vartheta)\right) + \right.& \\
\left.\frac{1}{r}\beta r^{-\frac{1}{2}}y(\vartheta)\frac{\partial}{\partial \vartheta}\left(\alpha\beta^2 r^{-(m+1)}g(\vartheta)\right)\right] - & \\
\left[\beta r^{-\frac{1}{2}}x(\vartheta)\frac{\partial}{\partial r}\left(\alpha r^{-m}f(\vartheta)\right) + \right.& \\
\left.\frac{1}{r}\beta r^{-\frac{1}{2}}y(\vartheta)\frac{\partial}{\partial \vartheta}\left(\alpha r^{-m}f(\vartheta)\right)\right]\gamma\frac{\alpha\beta^2 r^{-(m+1)}g(\vartheta)}{\alpha r^{-m}f(\vartheta)} &= 0 \\
-\alpha\beta^3 r^{-\frac{3}{2}}r^{-(m+1)}x(\vartheta)g(\vartheta)(m+1) + \alpha\beta^3 r^{-\frac{3}{2}}y(\vartheta)g'(\vartheta) - & \\
\left[-\alpha\beta r^{-\frac{3}{2}}r^{-m}mx(\vartheta)f(\vartheta) + \alpha\beta r^{-\frac{3}{2}}y(\vartheta)r^{-m}f'(\vartheta)\right]\gamma\frac{\alpha\beta^2}{\alpha}r\frac{g(\vartheta)}{f(\vartheta)} &= 0 \\
-(m+1)x(\vartheta)g(\vartheta) + y(\vartheta)g'(\vartheta) + m\gamma x(\vartheta)f(\vartheta)\frac{g(\vartheta)}{f(\vartheta)} + \gamma y(\vartheta)g(\vartheta)\frac{f'(\vartheta)}{f(\vartheta)} &= 0 \\
-(m+1-\gamma m)x(\vartheta)g(\vartheta) + y(\vartheta)g'(\vartheta) + \gamma y(\vartheta)g(\vartheta)\frac{f'(\vartheta)}{f(\vartheta)} &= 0 \\
-\left[m(1-\gamma)+1\right]x(\vartheta)g(\vartheta) + y(\vartheta)g'(\vartheta) + \gamma y(\vartheta)g(\vartheta)\frac{f'(\vartheta)}{f(\vartheta)} = 0\ . &
\end{aligned}
\tag{B.13}
$$

It is the last equation (B.4) rewritten into quantities x, y, f, g. Hence we have these equations (B.10) $\div$ (B.13):

$$
\begin{aligned}
-\frac{1}{2}x^2(\vartheta) + x'(\vartheta)y(\vartheta) - y^2(\vartheta) = -\frac{g(\vartheta)}{f(\vartheta)}(m+1) - \frac{1}{2}\left(\frac{\gamma+1}{\gamma-1}\right)^2\ , \\
\frac{1}{2}x(\vartheta)y(\vartheta) + y(\vartheta)y'(\vartheta) = \frac{g'(\vartheta)}{f(\vartheta)}\ , \\
\left(\frac{3}{2} - m\right)x(\vartheta) + y'(\vartheta) + y(\vartheta)\cot\vartheta + y(\vartheta)\frac{f'(\vartheta)}{f(\vartheta)} = 0\ , \\
-\left[m(1-\gamma)+1\right]x(\vartheta)g(\vartheta) + y(\vartheta)g'(\vartheta) + \gamma y(\vartheta)g(\vartheta)\frac{f'(\vartheta)}{f(\vartheta)} = 0\ .
\end{aligned}
$$

Boundary conditions

We suppose that the transversal velocity $y(\vartheta)$ is zero for $\vartheta = 0$. It means that we do not assume any accretion flows across axis of the flow. Of course, we describe the process of an accretion and hence we have to suppose that central body acquires a matter. In mathematical symbols it means negative radial velocities. On the accretion axis therefore

$$
x \to x_0 = \text{constant}\ . \tag{B.14}
$$

From (B.10) one can verify, if we suppose this condition together with $y(0) = 0$, that gravitational force has to overcome the outward pressure gradient and pressure of radiation. It also leads to limitation of

$$\frac{g(\vartheta)}{f(\vartheta)} \ . \tag{B.15}$$

Since $\frac{g(\vartheta)}{f(\vartheta)}$ is essentially temperature, the axis temperature remains finite in an accretion solution.

Hence we have these boundary conditions:

$$\frac{g(\vartheta)}{f(\vartheta)} < \infty \ , \ y(0) = 0 \ , \ V_\vartheta(0) < 0 \ . \tag{B.16}$$

With these condition we can look for asymptotic solutions for $\vartheta \to 0$.

Asymptotic solution

It is possible to show that the asymptotic solution adopts a form $y(\vartheta) = a\vartheta$, where a is a negative constant. This solution is not valid in $m = \frac{3}{2} \cap \gamma = \frac{5}{3}$. See [84]. Hence we have three possible ways: $m < \frac{3}{2}$, $m = \frac{3}{2}$, $m > \frac{3}{2}$.

- $m = \frac{3}{2}$

1. We can integrate (B.12) and obtain:

$$f(\vartheta)y(\vartheta)\sin\vartheta = -A \ , \tag{B.17}$$

where A is a positive constant. We can easily find that this expression is really a solution of (B.12). Since $y(\vartheta) = a\vartheta$ for $\vartheta \ll 1$, the asymptotic form of this equation is:

$$f(\vartheta) = -\frac{A}{a\vartheta^2} \ . \tag{B.18}$$

In this expression the density $f(\vartheta)$ diverges in $\vartheta \to 0$.

2. (B.11) gives for the asymptotic case $x \to x_0$, $y(\vartheta) = a\vartheta$ expression:

$$\frac{1}{2}x_0 a\vartheta + a\vartheta a = +g'(\vartheta)\frac{a\vartheta^2}{A} \ . \tag{B.19}$$

Hence

$$\frac{1}{2}x_0 + a = g'(\vartheta)\frac{\vartheta}{A} \ . \tag{B.20}$$

It is very easy to integrate it and obtain:

$$\begin{aligned} \frac{1}{2}x_0 + a &= \frac{\mathrm{d}g(\vartheta)}{\mathrm{d}\vartheta}\frac{\vartheta}{A} \\ \frac{\mathrm{d}\vartheta}{\vartheta} &= \frac{\mathrm{d}g(\vartheta)}{A(\frac{1}{2}x_0 + a)} \\ A\left(\frac{1}{2}x_0 + a\right)\frac{\mathrm{d}\vartheta}{\vartheta} &= \mathrm{d}g(\vartheta) \\ g(\vartheta) &= A\left(\frac{1}{2}x_0 + a\right)\ln\vartheta \end{aligned}$$

Hence we have the asymptotic solution:

$$\begin{aligned} x &\to x_0 \,, && \text{(B.21)} \\ y(\vartheta) &= a\vartheta \,, && \text{(B.22)} \\ f(\vartheta) &= -\frac{A}{a\vartheta^2} \,, && \text{(B.23)} \\ g(\vartheta) &= A\,\left(\frac{1}{2}x_0 + a\right)\ln\vartheta \,. && \text{(B.24)} \end{aligned}$$

We can rewrite equation (B.13), supposing $m = \frac{3}{2}$:

$$\begin{aligned} \left[m(\gamma-1)-1\right]g(\vartheta)x(\vartheta) + y(\vartheta)g'(\vartheta) - \gamma y(\vartheta)g(\vartheta)\frac{f'(\vartheta)}{f(\vartheta)} &= 0 \\ \left[\frac{3}{2}\gamma - \frac{3}{2} - 1\right]x_0 A\,\left(\frac{1}{2}x_0 + a\right)\ln\vartheta + & \\ a\vartheta A\,\left(\frac{1}{2}x_0 + a\right)\frac{1}{\vartheta} - \gamma a\vartheta A\,\left(\frac{1}{2}x_0 + a\right)\ln\vartheta\frac{2\frac{A}{a\vartheta^3}}{-\frac{A}{a\vartheta^2}} &= 0 \\ \left[\frac{3}{2}\gamma - \frac{5}{2}\right]x_0\ln\vartheta + a + 2a\gamma\ln\vartheta &= 0 \\ (3\gamma-5)\,x_0 + \frac{2a}{\ln\vartheta} + 4a\gamma &= 0 \end{aligned}$$

If we consider $2a/\ln\vartheta$ as negligible, then the result has a form:

$$(3\gamma-5)\,x_0 + 4a\gamma = 0 \,. \qquad \text{(B.25)}$$

In this equation we ask for $x_0 < 0$, $a < 0$ (we require $x_0 < 0$, in order that $V_\mathrm{r} < 0$ because this case corresponds to the accretion). We can satisfy the last condition if $3\gamma - 5 < 0$ because under this assumption $(3\gamma-5)x_0 > 0$ and it overcomes the negative expression $4a\gamma$. Finally, from $3\gamma - 5 < 0 \Rightarrow \gamma < \frac{5}{3}$.

- $m < \frac{3}{2} \bigcup m > \frac{3}{2}$.

The same condition as in the previous item holds also for $m < \frac{3}{2}$. For $m > \frac{3}{2}$ it is more complicated and it is valid (see [84]): $\gamma < 1 + \frac{1}{m}$.

In all these cases the accretion process exists with $\gamma < \frac{5}{3}$ only, except for $m = \frac{3}{2}$, $\gamma = \frac{5}{3}$. However, the flow must be radial and conical shock waves are not possible. See [84] for more details.

Appendix C

Star trapping in accretion discs

Some portion of stars moving within central parts of galaxies can be captured in the disc. See, for example, [81, 82, 83]. This thesis deals with stellar motion (of captured stars) inside the disc only. In this section we will give a brief review of the process of star trapping in an accretion disc as it is discussed in literature or, by the other words, we will summarize our knowledge of processes which occur before capture. Detailed discussion of these effects are given in, for example, [1, 83]. The mass of the disc is

$$m(R) = \int_0^R 2\pi r \Sigma(r) \mathrm{d}r \ . \tag{C.1}$$

M is a mass inside of radius r including central body. M_{h} is mass of central body. For $M \approx M_{\mathrm{h}}$ we have light disc and the motion inside it is almost Newtonian. Let us denote κ orbital frequency of the star. Newtonian motion gives $\kappa = \Omega$. Useful parameter quantifying surface density is the axisymmetric gravitational-stability parameter:

$$Q \equiv \frac{c_{\mathrm{s}}\kappa}{\pi G \Sigma} \ . \tag{C.2}$$

If the semithickness of the disc H is $H \approx \frac{c_{\mathrm{s}}}{\Omega}$, then $\kappa \approx \Omega$, $c_{\mathrm{s}} \approx H\Omega$ and hence:

$$Q = \frac{H\Omega\Omega}{\pi G \Sigma} = \frac{H}{\pi G \Sigma}\Omega^2 \ . \tag{C.3}$$

Let us find expression for Ω^2. Since

$$\frac{GM}{r^2} = \frac{v^2}{r} = \frac{r^2\Omega^2}{r} = r\Omega^2 \Rightarrow \Omega^2 = \frac{GM}{r^3} \ . \tag{C.4}$$

By this way we obtain

$$Q = \frac{M}{\pi \Sigma r^2}\,\frac{H}{r} \ . \tag{C.5}$$

For *non-selfgravitating discs* or *slightly self-gravitating discs*, $Q > 1$, since we suppose $\frac{H}{r} \ll 1$, we obtain condition

$$M \gg \pi \Sigma R^2 \ . \tag{C.6}$$

Hence it is necessary to suppose a very massive central body. As a counter-example, let us take a relatively heavy disc whose mass is comparable with the mass of the central body. Here $Q < 1$. In this case we cannot ignore axially symmetric perturbations (gravitational instabilities of the disc with axial symmetry). It induces a rapid transport of the mass and angular momentum. Thus to catch a stable disc we indeed have to suppose a light accretion disc in our calculation. See also [1].

Numerical estimations:

$$\begin{aligned} R &\leq 1\ \mathrm{pc} \\ \frac{H}{r} &\approx 10^{-2} \\ T &\approx 10^4\ \mathrm{K} \\ \Sigma &\leq 10^2\ \mathrm{g\ cm^{-2}} \end{aligned}$$

Star trapping

Let us consider transit of a star with mass m through the disc with density $\rho = \frac{\Sigma}{H}$. For the thin disc $\frac{H}{r} \ll 1$ we can suppose Newtonian motion. We introduce co-rotating coordinates (with the disc material). Velocity of a star is v and its z-component is v_z. These quantities are small in comparison with the Newtonian velocity v_Ω because we suppose that the star orbits in the same direction as the disc. If the stellar orbit does not coincide with the disc plane, it is

$$v_z > H\Omega \approx c_s ; \tag{C.7}$$

the transit through the disc leads to shock waves with effective radius

$$r_a = \frac{2GM}{v^2} . \tag{C.8}$$

Decelerating force acting on the star is

$$\begin{aligned} F_d &= 4\pi G^2 m^2 \rho C_d \frac{1}{v^2} \qquad v < v_c , \\ F_d &= 4\pi G^2 m^2 \rho C_d \frac{v^2}{v_c^4} \qquad v > v_c , \end{aligned}$$

where C_d is a dimensionless decelerating coefficient and v_c is the critical velocity having the same order as escape velocity:

$$v_c = C_d^{\frac{1}{4}} v_{esc} . \tag{C.9}$$

In fact, this critical velocity divides the transit of a star into two categories, a slow transit which is slower than escape velocity from the surface of the star (this process considerably increases the effective gravitational cross-section of the transiting star), and on a rapid transit (which decreases the effective gravitational cross-section, in limit of high velocity, to the geometrical cross-section of the body). "Hyper-rapid" transit involves shock waves with small radius, typically about

$$r_a < r_* . \tag{C.10}$$

Dimensionless deceleration coefficient can be divided into two parts:

$$C_d = C_d^{gas} + C_d^{wave} , \tag{C.11}$$

where

$$C_d^{gas} = \ln\Lambda = \ln\left(\frac{b_{max}}{r_*}\right) . \tag{C.12}$$

Here b_{max} is a maximal effective impact parameter, or, eventually, length of an accretion column. See [1]. We can easily find that time interval when the star resides inside the disc (we suppose sloping transit) is

$$\frac{H}{v_z}\frac{2}{P} . \tag{C.13}$$

Then the rate of change of specific kinetic energy of epicyclic motion

$$\dot{E} = \frac{d}{dt}\left(\frac{1}{2}v^2\right) = 2\frac{F_d}{m}\frac{H}{v_z}\frac{v}{P} . \tag{C.14}$$

Remind that

- in time interval $\Delta T = \frac{v^2}{4\dot{E}}$ the star with sloping initial orbit with $v < v_c$ is captured if

$$u_z u^3 \le \zeta^4 , \tag{C.15}$$

where

$$\begin{aligned}
\zeta^4(\Delta T) &= 32 C_{\rm d}\mu_* \left(\frac{\pi\Sigma R^2}{M}\right)\frac{\Delta T}{P} \, , \\
u &= \frac{v}{v_\Omega} \, , \\
u_{\rm z} &= \frac{v_{\rm z}}{v_\Omega} \, , \\
\mu_* &= \frac{m}{M} \, .
\end{aligned}$$

- for stars with $v > v_{\rm c}$:

$$\frac{u_{\rm z}}{u}\, u_{\rm cr}^4 \left(1 + 4\ln\frac{u}{u_{\rm cr}}\right) \le \zeta^4 \, ,$$
$$u_{\rm cr} = \frac{v_{\rm c}}{v_\Omega} \, .$$

Following cases have been considered:

- $C_{\rm d}^{\rm gas}$ acts considerably in the gaseous disc only;
- $C_{\rm d}^{\rm wave}$ acts in both gaseous and dust disc;
- When in the disc act both of them, then we can estimate $C_{\rm d}^{\rm gas} \approx C_{\rm d}^{\rm wave}$.
- Artymowicz et. al. use model in which:

$$\begin{aligned}
\pi R^2\Sigma &= \frac{H}{R}\frac{M}{Q} = 10^{-2} \, , \\
P &= 10^4\left(\frac{R}{\rm pc}\right)^{\frac{3}{2}} \, .
\end{aligned}$$

- For the estimation of $\Delta T \approx 10^8$yr and $\mu_* = 10^{-8}$ we obtain:

$$\zeta \ge 0.1 \, . \tag{C.16}$$

Stellar spheroids

It can be found that the central body increases its mass on time scale $\gg$ *crossing time* and, from another viewpoint, on the time scale $\ll$ *relaxation time of stellar spheroid*. If the radius of the galactic nuclei r_0 is of the order of parsec and the stellar density in the nucleus $\nu_0 \approx 10^6\ {\rm pc}^{-3}$, then the relaxation time scale is about $t_{\rm relax} \approx 10^9$yr. Let $\sigma_0 \approx 200\ {\rm km\ s}^{-1}$ is the initial velocity dispersion of an isothermal spheroid. Within a radius

$$r_{\rm h} = \frac{GM_{\rm h}}{\sigma_0^2} = 10.6\left(\frac{\sigma_0}{200}\ {\rm km\ s}^1\right)^{-2}\left(\frac{M_{\rm h}}{10^8}M_\odot\right)\ {\rm pc} \tag{C.17}$$

the growth of the central body induces the dispersion of velocities to increase from σ_0

$$\sigma = \left(\sigma_0^2 + \frac{GM_{\rm h}}{r}\right)^{\frac{1}{2}} \, . \tag{C.18}$$

For a typical value r_0 of the order of a parsec, the gravitational potential is dominated by the central body and velocity dispersion is:

$$\sigma \simeq v_\Omega = 660 \left(\frac{M}{10^8 M_\odot}\right)^{\frac{1}{2}} \left(\frac{r}{\mathrm{pc}}\right)^{-\frac{1}{2}} \ \mathrm{km\ s}^{-1} \ . \tag{C.19}$$

Adiabatic peak rotates with mean angular velocity V:

$$\frac{V}{\sigma} \sim 0.77 \pm 0.18 \ . \tag{C.20}$$

In the first estimation the peak density in the phase diagram (phase space):

$$\mathrm{d}N_* = \nu_* \ e^{-\frac{1}{2\sigma^2}\left[v_\mathrm{r}^2+(v_\phi-V)^2+v_\mathrm{z}^2\right]} \ \frac{\mathrm{d}^3 r \ \mathrm{d}^3 v}{(2\pi\sigma^2)^{\frac{3}{2}}} \tag{C.21}$$

Here the v_ϕ is determined in the inertial coordinate system and

$$\nu_* = \frac{4\nu_0}{3\sqrt{\pi}} \left(\frac{r_\mathrm{h}}{r}\right)^{\frac{3}{2}} \ . \tag{C.22}$$

It describes the radial profile of the density of stars in the peak. For disc-like orbits we have

$$v_\phi = v_\Omega + v_\vartheta \ \ ; \ \ v_\vartheta \ll v_\Omega \ . \tag{C.23}$$

Number of captured stars

In this section we suppose $v < v_\mathrm{c} \sim 10^3$ km s^{-1} . Number of stars captured during time ΔT in an interval of radii $[r, r+\mathrm{d}r]$ in the disc surrounded by a stellar cluster with stellar density ν_* is a fraction of q (total number of stars in a sphere with radius r and semithickness dr)

$$\mathrm{d}N = q \ \mathrm{d}N_* = q\nu_* 4\pi r^2 \mathrm{d}r \ , \tag{C.24}$$

where

$$q(\zeta) = \left(\frac{\sigma}{v_\Omega}\right)^3 \int\limits_{u_z u^3 \le \zeta^4} e^{-(E_\mathrm{x}+E_\mathrm{z})} \ \frac{\mathrm{d}^2 u \ \mathrm{d}^2\zeta}{(2\pi)^2} \ , \tag{C.25}$$

$$\begin{aligned} \zeta_\mathrm{z} &= \frac{z}{r} \ , \\ \zeta_\mathrm{r} &= \frac{R-r}{r} \ , \\ E_\mathrm{i} &= \frac{\zeta_\mathrm{i}^2 + u_\mathrm{i}^2}{2} \ , \end{aligned}$$

where $i = (r, z)$.
We can estimate

$$q \simeq 2^{-3}\zeta^4 \ . \tag{C.26}$$

For the total number of captured star we obtain formula (see [1]):

$$\mathrm{d}N = 2^{-3}\zeta^4 \nu_* 4\pi r^2 \mathrm{d}r = 2^{-2}\zeta^4 \nu_* \pi r^2 \mathrm{d}r \ . \tag{C.27}$$

Remind that:

$$\zeta^4(\Delta T) = 32 C_\mathrm{d} \mu_* \left(\frac{\pi\Sigma R^2}{M}\right) \frac{\Delta T}{P} \ . \tag{C.28}$$

Amount of the captured matter is given by:

$$\mathrm{d}\dot{M} = m\,\frac{\mathrm{d}N}{\Delta T} = \frac{3\;2^3 C_\mathrm{d}}{\sqrt{\pi}}\,\frac{Gm}{\sigma_0 r_0^2}\Sigma r \mathrm{d}r\;. \tag{C.29}$$

Here

$$\begin{aligned} M_\mathrm{c} &= \frac{4\pi}{9} m \nu_0 r_0^3\;, \\ \sigma_0^2 &= \frac{GM_\mathrm{c}}{r_0}\;, \\ \frac{r_0}{\sigma_0} &= \frac{3}{2\sqrt{\pi G m \nu_0}}\;. \end{aligned}$$

The initial stellar spheroid has a characteristic core mass M_c and σ_0^2 initial disperse velocity. Hence we obtain amount of captured matter. It is clear that the number of captured stars is

$$\mathrm{d}\dot{N} = \frac{\mathrm{d}\dot{M}}{m} \tag{C.30}$$

while amount of intercepting matter in the disc is

$$\mathrm{d}M_\mathrm{d} = 2\pi r \Sigma \mathrm{d}r\;, \tag{C.31}$$

which leads to the rate

$$\frac{\mathrm{d}\dot{N}}{\mathrm{d}M_\mathrm{d}} = \frac{12\;C_\mathrm{d}}{\pi^{\frac{3}{2}}}\,\frac{G}{r_0^2\sigma_0}\;. \tag{C.32}$$

It can be interesting to estimate the time scale of refuelling (or reproduction) of the disc with material of captured stars (or clouds):

$$\tau_\mathrm{rep} = \frac{\mathrm{d}M_\mathrm{d}}{\mathrm{d}\dot{M}}\;; \tag{C.33}$$

for $C_\mathrm{d} \sim 6$ is

$$\tau_\mathrm{rep} = 2\times 10^{10}\left(\frac{m}{M_\odot}\right)^{-1}\left(\frac{\sigma_0}{300\ \mathrm{km\ s^{-1}}}\right)\left(\frac{r_0}{2\ \mathrm{pc}}\right)^2\ \mathrm{yr}\;. \tag{C.34}$$

See [1].

Rapid migration through the disc

This section deals with the case of the rapid transition of a star through the disc. In this case stars have a lower effective cross-section which is given essentially by their geometrical cross-section only (see the corresponding section in this thesis). It is also the limit in which impact velocity of a star overcomes escape velocity: $v_\mathrm{c} \sim v_\mathrm{esc}$. We can introduce the critical radius: it is defined as a radius $r = r_\mathrm{c}$ on which stars captured in time T have maximum impact velocity $\zeta(\Delta T)v_\Omega$ equal to critical velocity $v_\mathrm{c} = C_\mathrm{d}^{1/4}\,v_\mathrm{esc}$.

Numerical estimations:

$$v_{\odot\,\mathrm{esc}} = 620\ \mathrm{km\ s^{-1}} \Rightarrow v_\mathrm{c} = 960\ \mathrm{km\ s^{-1}}\;; \tag{C.35}$$

We take escape velocity from the solar surface as typical reference value. Estimation of zeta-function $\zeta(\Delta T)$ then yields:

$$\zeta(\Delta T) \sim 1.5\left(\frac{r_\mathrm{c}}{\mathrm{pc}}\right)^{\frac{1}{2}} \tag{C.36}$$

and we can estimate

$$r_\mathrm{c} \sim 0.027\ \mathrm{pc}\;. \tag{C.37}$$

Rate of accretion

During the transit of a star through the disc we can suppose accretion of matter in a typical rate

$$
\begin{aligned}
\dot{m} &= 4\lambda\pi G^2 m^2 \rho \left(c_{\mathrm{s}}^2 + v^2\right)^{-\frac{3}{2}} \quad , \quad v < v_{\mathrm{esc}} \ , \\
\dot{m} &= 4\lambda\pi G^2 m^2 \rho \frac{1}{v_{\mathrm{esc}}^3} \quad , \quad v \geq v_{\mathrm{esc}} \ .
\end{aligned}
$$

Here $\lambda \in (\frac{1}{2}, 1)$ is parameter of efficiency.

The inclination of stellar orbits decreases to zero on time scale typically about ΔT. It can be estimated that the relative mass increases $\frac{\lambda}{C_{\mathrm{d}}} \sim 0.1$ times slower then the relative (dimensionless) momentum increases. It means that the mass of the star does not considerably change until the inclination of the stellar orbit is very small.